

PALAEOCLIMATE SIMULATION STUDIES OF THE INDIAN MONSOON

**Ph. D. Thesis
MARCH 2000**

Deveerappa Jagadheesha

**PHYSICAL RESEARCH LABORATORY
NAVRANGPURA
AHMEDABAD 380 009 INDIA**

PALAEOCLIMATE SIMULATION STUDIES OF THE INDIAN MONSOON

**A Thesis submitted to
Devi Ahilya Vishwa Vidhyalaya, Indore**

**for
THE DEGREE OF DOCTOR OF PHILOSOPHY
in PHYSICS**


**by
DEVEERAPPA JAGADHEESHA
PHYSICAL RESEARCH LABORATORY
NAVRANGPURA
AHMEDABAD 380 009 INDIA**

MARCH 2000

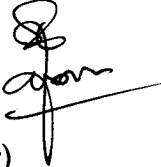
*To the fond memories
of my father*

CERTIFICATE

I hereby declare that to the best of my knowledge this thesis does not contain any part of any work which has been submitted for the award of any degree or diploma either in this university or in any other university or institution.


Deveerappa Jagadheesha
(Author)

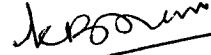
Certified by:


(Supervisor)

Dr. R. Ramesh

Physical Research Laboratory

Ahmedabad 380 009


22-3-2020

Prof. Head,
School of Physics
Davi Ahilya Vishwavidyalaya,
Khadwa Road, Indore-452-001



(Co-supervisor)

Dr. A. Mishra

School of Physics

Davi Ahilya Vishwa Vidyalaya

Indore (M.P.)

List of Publications

1. "Orbital forcing of monsoonal climates in NCAR CCM2 with two horizontal resolutions", **Jagadheesha D.**, R. S. Nanjundiah, and R. Ramesh, 1999, *Palaeoclimates: Data and Modelling*, Vol. 3, No. 4, pp 279-301.
2. "Past monsoons: A review of proxy data and modelling", **Jagadheesha D.** and R. Ramesh, (in press), *Mausam*.
3. "Sensitivity of an AGCM to 6 ka orbital parameters: Impact of model dependent factors" (paper under preparation).

Contents

Acknowledgements	iii
1 Introduction	1
1.1 Climate modelling	1
1.2 Aim and scope of the thesis	3
1.3 Plan of the thesis	5
2 The model and the simulation of the present day monsoon	9
2.1 A brief description of CCM2 AGCM	9
2.2 The Present Indian monsoon	11
2.2.1 Summer mean precipitation and circulation	11
2.2.2 Monsoon Variability	14
2.2.3 Monsoon Indices	16
2.3 Simulation of the present day monsoon using CCM2	18
3 Sensitivity Experiments I	23
3.1 Insolation changes during 6 and 115 ka	23
3.2 Inferences from palaeoclimate reconstructions	25
3.3 Modelling studies of the past monsoons	28
3.4 Sensitivity experiments	33
3.5 6 ka results	34
3.5.1 Summer mean precipitation and circulation	34
3.5.2 Anomalies in monsoon indices	38
3.5.3 Seasonal transitions	39
3.6 115 ka results	50
3.6.1 Seasonal mean precipitation and circulation	50
3.6.2 Anomalies in monsoon indices	54

3.6.3	Seasonal transitions	55
3.7	Comparison with palaeo-data	56
3.8	Concluding remarks	58
4	Sensitivity Experiments II	60
4.1	Introduction	60
4.2	Simulation of the present day monsoon	62
4.2.1	Geographical pattern	62
4.2.2	Monsoonal indices	65
4.3	6 ka results	68
4.3.1	Geographical features	68
4.3.2	Anomalies in monsoonal indices	72
4.3.3	Seasonal transitions	74
4.4	115 ka results	81
4.4.1	Geographical features	81
4.4.2	Anomalies in monsoonal indices	84
4.4.3	Seasonal transitions	85
4.5	Concluding Remarks	86
5	Summary, conclusions and future directions	89
5.1	Summary and conclusions	89
5.2	Future directions	96
	Bibliography	98

Acknowledgments

I express my sincere gratitude to my thesis supervisor Dr. R. Ramesh for all the help, encouragement, and valuable guidance. Apart from thesis matters his interests in leading a healthy and disciplined life also influenced me. I am highly indebted to him for his generous help. I am grateful to Dr. Ravi S Nanjundiah of Center for Atmospheric and Oceanic Sciences, IISc, Bangalore for critically going through the manuscript and giving useful suggestions. His help in matters of getting the computational work done for my thesis work in a short span of time is unforgettable. Besides he has taught me to look at the positive side of things, to be patient, and cool minded which are essential for a researcher. I am highly indebted to Prof. J. Srinivasan, and Chairman, SERC, IISc for providing me the computational facility.

I sincerely thank my thesis co-supervisor, Dr. A. Mishra, School of Physics, Devi Ahilya Vishwa Vidhyalaya (DAVV), Indore, for his kind help. Many thanks to Professors K. P. Joshi, and K. P. Maheshwari of DAVV, for their help and encouragement.

I am grateful to Professors Krishnaswami, Somayajulu, Bhattacharya, Singhvi, Goswami, Sheorey and academic committee members for their concern and suggestions. Many thanks to Drs. Sarin, Gupta, and Shukla for their concern and interest.

I am grateful to Drs. Pranav Desai and Vijay Agarwal of Space Applications Center, Ahmedabad for their critical comments.

I sincerely thank staff members of PRL computer center and library for providing excellent facilities.

Many thanks to Dr. Anne de Vernal of University of Quebec, Canada, and Dr. Pascale Braconnote of CNRS, France for providing me travel assistance to attend 3rd PMIP workshop held at Quebec, Canada.

I am grateful to Rajendran, Manik Bali, Natraj and Semeena of CAOS, IISc, for their help in getting the computational work done.

Research scholars and PDFs of PRL helped me generously. I am highly indebted to all of them. They were like family members and made me feel at home. It is always nice to remember many of my colleagues, Anirban, Agnihotri, Dalai, Rajesh, Rajneesh, Anil, Shubrangshu, Tarak, Jayendra, Sudeshna, Sarika, Kuljeet, Shikha, Vinay, Bala, Aital, Nandakumar, Anandmayee, Siva, Tarun, Ramachandran, Biju, Jyoti, Watson, Paulose, Gautam, Santanam, Prabir, Manish, Debu, Ban, Ghosh, Prashant, Dinanath, Supriyo,... to name a few.

I am grateful to Prof. G. S. Agarwal, Director, PRL for the continued financial support and encouragement. I thank all PRL staff members, who directly or indirectly helped me.

Last but not least, I thank my family members and relatives, especially my mother, brothers, uncles, and aunts, for always being kind and generous to me.

Introduction

1.1 Climate modelling

Earth comprises of lithosphere, atmosphere, ocean, cryosphere and biosphere, whose interactions on various time scales determine the state of the earth's climate system. The time scales of interaction and physics of the components vary from days to thousands of years. In spite of the fact that the climate system is complex, many features of the climate can be explained based on the knowledge of the forces and processes that drive this system. A hierarchy of models from simple energy balance models to complex general circulation models have been used to model the climate system to varying degrees of detail (Crowley and North 1991). For instance many of the features of the present day climate on interannual time scales can be modelled with the help of atmospheric general circulation models (AGCMs). A typical AGCM solves equations governing the atmospheric dynamics, forced by seasonally varying insolation and sea surface temperatures (SSTs). The forcing is not uniform over the globe primarily because of the spherical shape of the earth and its orbital parameters. In addition the geographically varying surface characteristics such as albedo, land-sea distribution etc add to further spatial inhomogeneities in the absorption of solar radiation. Though the equations governing the atmospheric dynamics have a strong physical basis, the factors that determine the forces driving the dynamics such as cloud formation, turbulent exchange of heat and moisture, convection etc, have to be parameterized in terms of large scale dynamical quantities in AGCMs. These parameterizations thus being semi-empirical

in nature are uncertain to some extent. Moreover, there is no guarantee that the parameterizations that are tuned to simulate the present day climate work under different scenarios such as doubling of CO₂ concentration in the atmosphere. Some features of the present day climate such as El Niño Southern Oscillation (ENSO) occur on interannual time scales. Such events can be used to test the AGCMs and coupled ocean atmosphere general circulation models (COAGCMs). It has been shown that the atmospheric circulation in the tropics responds to changes at the surface such as sea surface temperatures (SSTs) and modelling studies have shown in seasonal mean state of the tropical climate is predictable to a large extent, depending on the accuracy with which surface conditions are prescribed (Shukla 1998).

In addition to the present day interannual variability in the climate system, past climatic changes recorded in oceanic and continental sediments may also be modelled in detail with the help of climate models. As a first step AGCMs can be used for periods wherein required boundary conditions and climatic state are known fairly well. Late Quaternary is one such period wherein palaeoclimate data with considerably extensive spatial coverage and temporal resolution exists. Analysis of palaeoclimate data together with the insolation variation due to earth's orbital parameter changes have indicated that the insolation variations are the pace makers of past climatic changes. Earth's orbital parameters namely, eccentricity, axial tilt, and precession of longitude of perihelion undergo quasi-periodic variations with periodicities of ~ 100 , 41, and 23 kilo years (kyrs) respectively (Berger and Loutre 1991). Oxygen isotope ratios ($\delta^{18}\text{O}$) of foraminiferal shells preserved in deep sea sediments reveal that the earth has undergone several glaciations with build up of cold conditions lasting ~ 100 kyrs and warm interval of ~ 20 kyrs. For instance high latitude palaeoclimate records have shown variations with a periodicity of 100, 40, and 23 kyrs corresponding to earth's orbital parameters (Hays et al 1976, Imbrie et al 1984). In the tropical regions dominated by monsoon climate, the palaeoclimate records show variability predominantly with a periodicity

of ~ 23 kyrs corresponding to the precession cycle (Pokras and Mix 1985, McIntyre et al 1989, Clemens et al 1991). Precession cycle mainly controls the seasonal amount of solar radiation while the tilt controls the latitudinal gradient of insolation and hence high latitude insolation receipt. Once in $\sim 23,000$ years longitude of perihelion occurs during boreal summer. Presently it is during winter. During ~ 6000 years ago, it was near northern summer and hence the summer insolation received by the northern hemisphere was higher than that of the present day by $\sim 5\%$. Due to the high thermal inertia of the oceans, tropical SSTs may be expected to remain more or less similar to that of the present day which is also supported by palaeo-SST indicators to a certain extent (Ruddiman and Mix 1993). Hence the land-sea thermal contrast during summer increased relative to the present day during 6000 years ago. It is a well known fact that the monsoon circulation is primarily driven by land-ocean thermal contrast. Thus it is expected that the monsoon circulation also enhanced relative to the present during 6000 years ago. Similarly during 115,000 years ago, changes in eccentricity and tilt favoured $\sim 8\%$ less summer insolation relative to the present day. This facilitated decrease in land-sea thermal contrast, and hence decrease of monsoon strength. This period is also the beginning of last glaciation which culminated with maximum arid and cold conditions $\sim 21,000$ years ago. Periods like these wherein there is a strong contrast in seasonal insolation and other boundary conditions relative to the present day may be modelled with the help of AGCMs.

1.2 Aim and scope of the thesis

AGCMs continually improve in their simulation of the present day climate. What impact do the improvements have on their climate sensitivity to changes in forcing factors? For instance Kothavala et al (1999) reports that the sensitivity of the National Center for Atmospheric Research (NCAR) community climate model version 3 (CCM3) to changing CO_2 concentrations is significantly less compared to

previous NCAR AGCM CCM1. The factors that lead to reduced sensitivity are improved radiation, cloud, and convection parameterizations which lead to improvements in the simulation of the present day climate in many respects. What is the impact of such changes on palaeomonsoon sensitivity of the model? A recent comparison of Palaeoclimate Modelling Intercomparison Project (PMIP) AGCM simulations for 6 ka (Yu and Harrison 1996) shows that the sensitivity over the north African monsoon region is relatively reduced compared to the previous models CCM0 and CCM1 and some AGCMs with low horizontal resolutions are relatively more sensitive than the other AGCMs. However, it is difficult to conclude whether the intermodel differences in the sensitivities are due to horizontal resolution, or due to physical parameterizations. Hence intramodel sensitivity studies may give some hints in explaining the differences in the intermodel sensitivities. Also it is important to know the AGCM related factors as AGCMs form a major component of more complete climate system models and any biases in AGCMs are likely to be accentuated in climate system models also (Gates 1992). In order to know the the impact of these factors we use CCM2 AGCM to simulate the response of atmospheric circulation changes to 6 and 115 ka orbital parameters relative to the present day. For this purpose, we use CCM2 AGCM at two horizontal resolutions, namely T42 (triangular truncation at 42 waves, transform grid $\sim 2.8^\circ$ longitude by 2.8° latitude) and T21(transform grid $\sim 5.6^\circ$ longitude by 5.6° latitude) in order to infer any differences in model sensitivities that can be due to changes in horizontal resolution in one set of simulations. As convective latent heat release in the atmosphere forms a major heat source that drives the monsoon circulation, we do simulations with CCM2 at T21 horizontal resolution with moist convective adjustment (MCA) parameterization of Manabe (1969) and a simple mass flux scheme of Hack (1994) for the present day, 6 ka and 115 ka orbital parameters in order to determine whether the changes in current AGCM sensitivities are a result of changing convection parameterizations. *Thus this thesis aims towards understanding the impact of these aspects of AGCM formulation on model sensitivities rather than attempting a complete simulation including all the realistic boundary boundary conditions such*

as vegetation, regional SSTs etc., for these periods. Palaeoclimate modelling studies is a continuing exercise as the models improve in their ability to simulate the present day climate and should not be taken as successful simulation of the past climatic changes. Rather, the modelling studies should be viewed as an attempt to explain the palaeoclimate changes inferred from reconstructions, in terms of physical processes taking place in the climate system. As the model formulations change, the details of the climatic changes simulated by the model also change. An examination of the effect of changes in model formulation on changes in model sensitivity may bring additional facts and new perspectives for the mechanism behind the monsoonal changes. Thus thesis is limited to examining the model monsoon sensitivities to changes in some aspects of the AGCM formulations without invoking all the boundary conditions such as vegetation and SSTs relevant to 6 and 115 ka.

1.3 Plan of the thesis

This thesis is divided into five chapters including this introductory chapter. A brief summary of the subsequent chapters is given below.

Chapter 2: Simulation of the present day monsoon using a version of NCAR AGCM CCM2 and its comparison with observations is given in this chapter. A brief description of the model formulation is given. CCM2 AGCM uses the spectral transform method for solving the primitive equations describing the dynamics of the atmosphere. The model physical parameterizations include delta-Eddington approximation for solar radiation transfer, a simple mass flux scheme for convection, and a non-local atmospheric boundary layer (ABL) parameterization. Monthly mean SSTs, atmospheric ozone concentration, and sea ice extent are specified in the model as time varying boundary conditions. Atmospheric CO₂ concentration is also prescribed. Surface albedo, surface roughness, surface vegetation type, are time invariant boundary conditions specified in the model. The model is used at two horizontal resolutions i.e., T42L18 and T21L18 to simulate the present day

climate and response to 6 and 115 ka orbital parameters.

A brief overview of the Indian summer monsoon and its variability is given. Indian monsoon is unique among regions of the globe which experience monsoon climate, because of the presence of Tibetan plateau, shape of the continent, and vast Asian land mass to the north, all contributing to the strongest monsoon circulation over this region. Indian monsoon exhibits interannual variability which is linked to ENSO, Eurasian snow cover, coupled land-ocean-atmosphere hydrological processes, chaotic intraseasonal oscillations, and is complex. Due to its complex nature, modelling of the climatological mean monsoon as well as its variability still remain active areas of research. There are many attempts to quantify the Indian monsoon using a single index. Seasonal mean precipitation averaged over the Indian region is a natural choice in quantifying the monsoon strength. However, due to its high spatio-temporal variability, it is difficult to rely on this quantity alone as a measure of monsoon strength. From the circulation perspective, monsoon is baroclinic, driven by convective latent heat release at the mid-troposphere and hence there will be a strong vertical wind shear. Examining the geographical pattern of monsoon wind at upper and lower levels, many regions are identified whose circulation features are unique and characteristic to the Indian monsoon and hence zonal and meridional wind shears averaged over these regions are also used to quantify the monsoon strength and are shown to represent its interannual variability fairly well. We describe the simulation of the present day monsoon using the model, calculate various monsoon indices, and compare it with the observational reanalysis so as to assess the model's ability to simulate the present day monsoon.

Chapter 3: Simulation of 6 and 115 ka monsoons and their sensitivities relative to the present day using CCM2 at two horizontal resolutions (T42 and T21) are described in this chapter. A brief account of seasonal insolation changes during 6 and 115 ka relative to the present day calculated using orbital parameters are given.

Palaeomonsoon proxy data with high temporal resolution and a fairly good spatial coverage are available for the past many thousand years and are examined in conjunction with the northern summer insolation variations. The analyses have shown that the Indian monsoon is sensitive to insolation as well as glacial events in the northern hemisphere. At any particular period, the competing effects of insolation and glaciation appear to determine the Indian monsoon strength relative to the present day. A brief survey of inferences on Indian monsoon strength obtained from marine and continental palaeomonsoon proxy records is given.

A number of modelling studies have been carried out to understand monsoon changes induced by due to orbital parameter and glacial cover variations. Many of these studies focussed on 6 (mid-Holocene) and 21 ka (Last Glacial Maximum). AGCMs alone do not simulate moisture balance conditions over northern Africa. Inclusion of inferred vegetation and wetlands in AGCMs also appear to be not sufficient to explain the palaeomonsoon over northern Africa. It appears that the biogeophysical feedbacks are necessary to model the moisture conditions over northern Africa to a certain extent. Over the Indian region, the AGCMs appear to simulate mid-Holocene moisture changes fairly well. The inference from palaeomonsoon proxies in conjunction with coupled ocean atmosphere general circulation model experiments suggest that the permanent El Niño like situations as suggested by some palaeoclimatic and archaeological records is unlikely. A brief account of these modelling studies is given.

CCM2 experiments at T42 and T21 prescribing orbital parameters of 6 and 115 ka are described. Geographic pattern of seasonal mean anomalies are compared with the lake level data for 6 ka at the two resolutions. Anomalies in monsoon indices are also compared at the two resolutions. Subseasonal evolution of Indian monsoon is examined using average summer time series of precipitation(P), precipitation-evaporation(P-E), latent heat flux, sensible heat flux and atmospheric kinetic energy at 850 and 200 hPa and compared at the two resolutions. Role of soil moisture feedbacks in determining the Indian monsoon strength is illustrated. On

the contrary the north African monsoon does not show any significant changes. Similarly sensitivity of the model for 115 ka experiments is discussed and role of interactive hydrology in determining the model monsoon sensitivity over India is discussed. The impact of horizontal resolution in determining the model monsoon sensitivity is discussed.

Chapter 4: It is shown that the simulation of many of the features of the monsoon circulation depends on how moist convection is parameterized in an AGCM. In this chapter we do similar experiments for the present, 6 and 115 ka periods as described in chapter 3 except that we use CCM2 at T21 horizontal resolution with moist convective adjustment (MCA) scheme of Manabe (1969). The main objective was to infer the effect of this parameterization change on model monsoon sensitivity.

A brief account of the importance of convection on the simulation of the Indian monsoon is given. We describe the major changes in the simulation of the present day climate by changing the moist convection parameterization from mass flux scheme to MCA scheme, with the help of geographical pattern of circulation, and precipitation and also monsoon indices so as to assess the ability of the two approaches in simulating the present day monsoon. Model sensitivities to 6 and 115 ka are described and compared with those discussed in chapter 3 so as to assess the impact of changing convection parameterization on the model sensitivities.

The model and the simulation of the present day monsoon

2.1 A brief description of CCM2 AGCM

CCM2 AGCM solves the so called primitive equations describing the atmospheric general circulation. Spectral transform and finite difference methods are used for approximating the dry dynamics in the horizontal and vertical directions respectively. Water vapour transport is calculated using a 3-dimensional semi-Lagrangian transport method (Williamson and Rasch, 1994). The model can be used at various horizontal and vertical resolutions. Here we use the model at two horizontal resolutions namely T42 (approximately $2.8^\circ \times 2.8^\circ$ transform grid) and T21 (approximately $5.6^\circ \times 5.6^\circ$ transform grid) keeping the number of vertical levels 18 as in the standard version of CCM2 released by NCAR. Terrain following hybrid coordinates (a combination of sigma and pressure coordinates) are used as vertical coordinates with model top-of-the-atmosphere at 2.917 hPa (Simmons and Strüfing 1981). A ∇^4 order diffusion term is used to approximate subgrid scale exchanges of dynamic variables in the horizontal direction.

Monthly mean climatological sea surface temperatures (SSTs), sea ice extent from the analysis of Shea et al (1990), and ozone volume mixing ratios (Dutsch 1978, Chervin 1986) are prescribed in the model as time varying boundary conditions. SSTs and sea ice distribution are assigned the mid-month date and updated every time step at each grid point using linear interpolation. In a similar way ozone

mixing ratios which are prescribed as a function of latitude and vertical level are updated every 12 hours for radiative heating rate calculations via linear interpolation. Time invariant boundary conditions prescribed in the model are surface albedos in the visible and near infrared solar spectrum, surface roughness, vegetation type, surface geopotential height, and subgrid-scale standard deviation of terrain height (used in gravity-wave-drag-parameterization). The solar zenith angle dependence of surface albedo is taken into account depending on the surface type. Atmospheric CO₂ concentration is prescribed as 330 parts per million volume (ppm) for the present day (control) simulation.

CCM2 uses state of the art physical parameterizations for calculation of various energy and moisture exchange processes at the atmosphere-surface (land, ocean, sea ice), atmospheric boundary layer (ABL)-free atmosphere interfaces, convective processes, radiation transfer, diagnosis of clouds and their optical characteristics, gravity wave drag etc. Delta-Eddington approximation is used for calculation of solar radiation transfer through the atmosphere (Briegleb 1992). The solar spectrum is divided into 18 spectral intervals. Radiative heating rates are calculated at time steps of one hour. Longwave absorptivities and emissivities are updated every 12 hours. Cloud optical properties i.e., effective cloud droplet radius and liquid water depth are prescribed as a function of latitude, height and the surface beneath (i.e., marine and continental). For longwave radiation transfer, cloud emissivity is calculated as a function of cloud liquid water content. A simple mass flux scheme of Hack (1994) is used for parameterization of moist convection and convective precipitation. Cloud amount is diagnosed using a generalized scheme similar to that introduced by Slingo (1987), and depends on relative humidity, vertical velocity, atmospheric stability, and convective mass flux associated with parameterized moist convection. Three types of clouds viz., convective cloud, layered cloud, and low-level marine stratus are diagnosed by this scheme. A non-local diffusion scheme developed by Holtslag and Boville (1993) which depends on atmospheric stability is used for parameterizing ABL fluxes. The surface exchange of heat, moisture, and momentum at the atmosphere-surface (land,ocean,

and ice surface) interface are treated with a bulk-exchange formulation. Soil wetness and land snow cover are calculated interactively in the model using a bucket type soil hydrology with a bucket capacity of 15cm. Surface albedos are modified whenever snow cover is predicted by this scheme in the model grids.

Horizontal diffusion coefficient which governs the fine scale horizontal diffusion of dynamical variables, and threshold relative humidity used in prediction of stratiform cloud amount are different for the two resolutions and values arbitrarily tuned at different horizontal resolutions similar to those used by Bonan (1994) are used in this study.

Detailed description of CCM2 physics and numerical formulation are given in a technical note (Hack et al 1993).

2.2 The Present Indian monsoon

2.2.1 Summer mean precipitation and circulation

Indian climate is a typical example of monsoon climate. This region experiences seasonal reversal of wind (low level southwesterlies during summer and northeasterlies during winter) and distinct wet and dry seasons (wet summer and dry winter) primarily because of the seasonal changes in land-sea thermal contrast (e.g., Keshavamurthy and Sankar-Rao 1996; Pant and Kumar 1997; Webster et al 1998).

Fig. 2.1 shows the summer (June, July, August, September) mean climatological precipitation, 850 and 200 hPa wind from National Center for Environment Prediction (NCEP) reanalysis (Kalnay et al 1996). Major precipitation areas over India are along the west coast due to the orographic influence of western ghats, and north-east India coming under the influence of monsoon trough over Bay of Bengal. There is a secondary precipitation maximum over southern Indian ocean between $\sim 10^{\circ}\text{S}$ to equator. Precipitation over equatorial northern Africa exhibits

NCEP Reanalysis JJAS composites

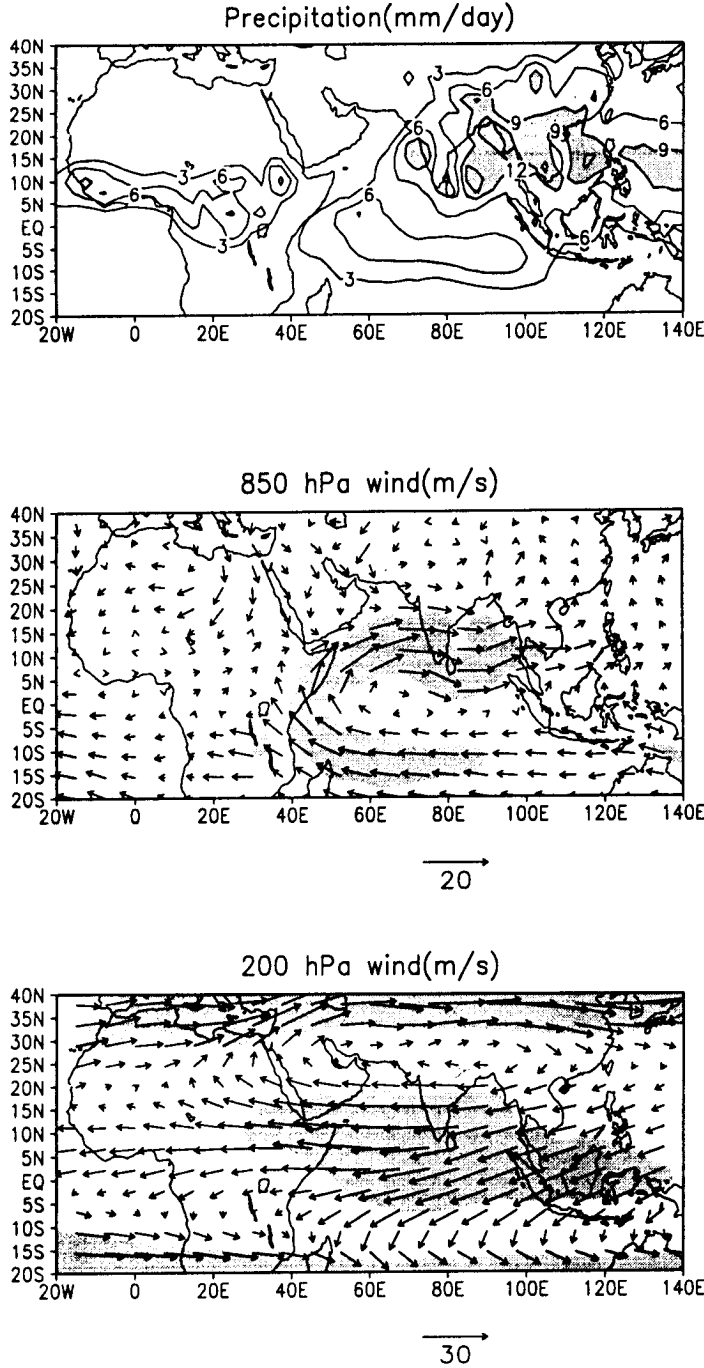


Fig. 2.1 Geographical pattern of the present day June, July, August, September (JJAS) mean climatologies of precipitation(P), 850 and 200 hPa wind from NCEP reanalysis. Contour interval for P is 3 mm/day and shaded areas represent $P \geq 9$ mm/day. Shaded areas for 850(200) hPa wind pattern represent wind speed $\geq 8(15)$ m/s.

a zonally uniform pattern compared to that over India and is confined to a narrow latitude band similar to intertropical convergence zone (ITCZ) over oceans. NCEP reanalysis data being model based is by and large consistent with the other climatologies based on observations. Xie and Arkin (1996) precipitation climatology which is mainly based on observational data and hence less contaminated with the model systematic errors is shown in Fig 2.2. Xie and Arkin data distinguishes between the precipitation associated with the monsoon trough and Pacific warm pool, compared to NCEP reanalysis. Also secondary precipitation maximum over the southern Indian ocean is more prominent in Xie-Arkin data and the precipitation belt is well off the east coast of equatorial Africa. However, NCEP reanalysis is the best source of other monsoon related variables such as evaporation, wind field, etc. and these fields are mutually consistent as they are derived from reanalysis using a common model. Hence we use NCEP reanalysis data for these climatologies as well as precipitation.

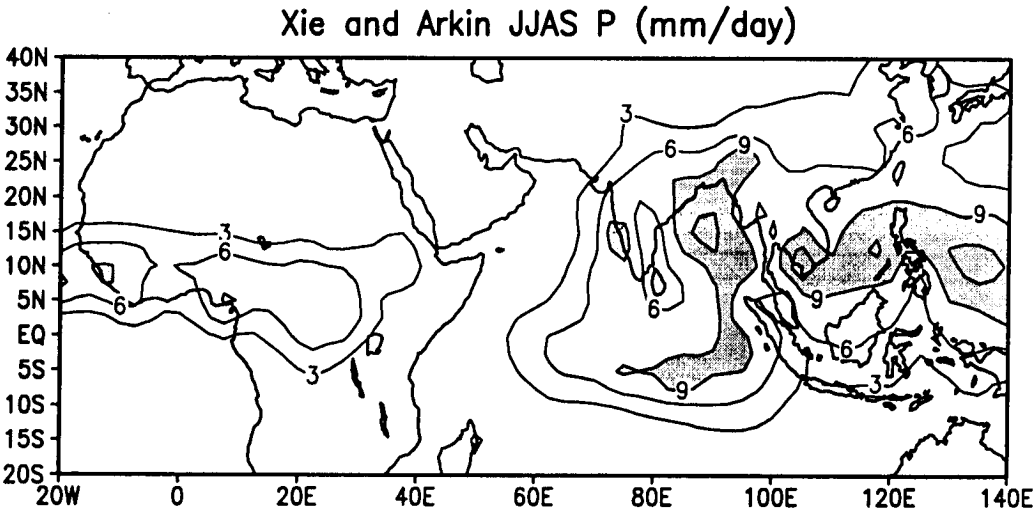


Fig. 2.2 JJAS precipitation climatology from Xie and Arkin (1996).

Within the annual cycle, monsoon onset is marked by abrupt increase of westerly wind speed, and precipitation around end of May or beginning of June, followed by a rainy season with gradual return to dry conditions around September-October. After the onset, the wet spell over India is never continuous. There are break (dry spell) and active (wet spell) phases. The intraseasonal variability is reflected in the wind speed also (Webster et al 1998). Once the monsoon sets on, convective processes play an important role in determining the further strength and evolution of the monsoon. Low level summer mean circulation over Indian monsoon domain (850 hPa wind field in Fig 2.1) consists of strong cross equatorial southerly winds off the east coast of equatorial Africa, followed by westerlies over Indian peninsula extending upto southeast Asia. Coriolis force is responsible for the cross equatorial winds to swirl into westerlies in the northward direction. At upper levels (200 hPa wind in Fig 2.1), flow consists of easterlies over a broad region from western Pacific to tropical northern Africa known as tropical easterly jet (TEJ) with a broad anticyclonic circulation over southern Tibet centered around 25°N. Modelling studies attribute many of these circulation features to land-sea distribution, elevation of the Tibetan plateau, and the presence of orographic features such as east African highlands (Webster et al 1998).

2.2.2 Monsoon Variability

Many features of mean monsoon circulation are explained fairly well. However, the variability of the monsoon on various time scales is not well understood and is an active area of research. Webster et al (1998) reviews the current status of monsoon variability research.

Indian monsoon variability on a large scale is studied by using all-India average rainfall index (AIRI) which is the seasonal (June to September) mean precipitation anomaly from the climatological (1871-1993) value (Parthasarathy et al 1994). The seasonal mean is calculated by averaging over all the meteorological subdivisions of India. If AIRI is more(less) than two standard deviations, then

that particular year is said to receive excess (deficient) rainfall. Analysis of time series AIRI shows variability predominantly on intraseasonal, biennial, ENSO, and decadal time scales (Torrence and Webster 1998) and is highly aperiodic and complex in nature.

Variations on the intraseasonal time scale comprises of a number of active and break phases within the season. Modelling studies suggest that the intraseasonal oscillations (ISO) being a manifestation of complex hydrodynamical processes taking place over the monsoon region are chaotic (unpredictable) in nature (e.g., Srinivasan et al 1993). However, it has been noticed that during many years of excess(deficient) monsoon the number and duration of active phases are respectively unusually higher (smaller) and longer (shorter) than other years (Gadgil and Asha 1992). Thus there is some codependence of variability at different time scales. These aspects are yet to be investigated in detail.

There is a predominant interannual variability on ENSO time scales which appears to be due to changes in Walker circulation during ENSO events. Walker circulation is an atmospheric circulation cell similar to Hadley circulation, but arising due to differential heating along the zonal (east-west) direction (mainly tropical Pacific). In the tropical Pacific ocean, there is an east-west SST gradient with higher SSTs in the western Pacific (also known as the Pacific warm pool) compared to eastern Pacific in the climatological sense. As a result, a thermally driven Walker circulation cell exists in this region with one of its rising branch over the Pacific warm pool and sinking branches over the eastern Pacific and the western Indian ocean. SSTs in the tropical eastern Pacific undergo fluctuations on interannual time scales (~ 3 -5 years) leading to the well known ENSO events. During warm ENSO events (when eastern Pacific SSTs are higher than the climatological average), the Walker circulation weakens and shifts eastward, thereby shifting the sinking branch from western Indian ocean to the Indian subcontinent, resulting in the suppression of convective activity and hence the monsoon strength. During cold ENSO events, there may be an westward movement of the major convection zone, leading to

a stronger monsoon. These explanations are robust, physically meaningful, and supported by observational and modelling studies (eg. Shukla 1987, Webster et al 1998). However, during the recent decades, the monsoon appears to be normal over India despite the occurrence of several warm ENSO episodes (Webster et al 1998). Krishna Kumar et al (1999) emphasize the warming trend over Eurasia during winter and southeastward shift of ENSO related circulation anomalies presumably due to the global warming trend (and the resulting expansion of Pacific the warm pool in the southeastward direction) in the recent decade as a possible explanation for the break down of the historical relationship between ENSO and monsoon.

Indian monsoon also exhibits variations on biennial time scales. Observational studies suggest that it may be intrinsic to the monsoon system independent of ENSO (eg., Meehl 1994). A hypothetical explanation given by Meehl (1994) suggests that a strong(weak) monsoon during a particular year alters the thermal state of the ocean (by means of wind speed-evaporation-SST feedback) and the land surface in such a way that the land surface conditions such as Eurasian snow cover, soil moisture, and SSTs during the subsequent year favour a weak(strong) monsoon. This hypothesis is yet to be investigated in more detail by means of modelling and observational studies.

Thus the monsoon varies on many time scales, processes behind which appear to be from within as well as outside the monsoon domain and there is some codependence of various time scales. Naturally, the observed variability of the monsoon is quite complex and each aspect requires careful investigation.

2.2.3 Monsoon Indices

In order to quantify the monsoon strength using a single quantity which may be a convenient tool to study the interannual variability of the monsoon, several indices are being used (eg., Webster and Yang 1992, Parthasarathy et al 1994, Goswami et

al 1999, Wang and Fan 1999). Many of these indices are defined with a view to study the present interannual variability of the monsoon. Our sensitivity simulations using orbital parameters of 6(115) ka favour strong(weak) summer monsoon circulation over India relative to present. Hence these indices serve to infer the relative changes in monsoon circulation during these periods. We have used the following indices of monsoon strength.

Pressure Index (PI) defined as a difference of seasonal mean sea level pressure (MSLP) averaged over land and ocean of a broad area covering the Indian sub-continent (45°E , 15°S - 45°N). This index is a good measure of land sea thermal contrast associated with the monsoon (Prell and Kutzbach 1987).

Precipitation (P) and Precipitation-Evaporation (P-E) averaged over India (10°N 70°E - 100°E).

Meridional Hadley Index (MHI) defined as meridional wind shear averaged over 10°N , 70°E - 110°E (Goswami et al 1999).

Wang and Fan (1999) discuss these indices and suggest the following other indices, which are found to correlate significantly with other monsoon indices barring a few instances, and are a good measure of the Indian monsoon strength. **Convection Index (CI)** which is the outgoing longwave radiation (OLR) over Bay of Bengal 10°N , 70°E - 100°E (Wang and Fan 1999).

Westerly wind shear index (WSI) which is the zonal wind shear (U_{850} - U_{200}) over 5°N , 40°E - 80°E (Wang and Fan 1999).

Southerly shear index (SSI) similar to MHI, but defined as the sum of southerly wind shear (V_{850} - V_{200}) over two regions where, the meridional wind shear is higher, namely over southern Indian ocean (0°S 40°E - 55°E) and eastern Tibet (15°N 85°E - 100°E) (Wang and Fan 1999).

JJAS mean climatological values of these indices from NCEP reanalysis are given in Table 2.1. Though precipitation is a good measure of monsoon strength, considering the complex processes associated with it, many attempts have been made to define monsoon indices using dynamical variables which are thought to be more reliable components simulated by AGCMs than precipitation. The domain over

which WS and SSI are calculated are such that the monsoon zonal and meridional wind shears in the vertical directions are quite strong.

Table 2.1 Climatological values of Monsoon Indices calculated from NCEP reanalysis.

Monsoon Index	NCEP reanalysis value
PI (hPa)	2.6
P (mm/day)	6.4
P-E (mm/day)	2.9
MHI (m/s)	2.5
CI (W/m ²)	285
WSI (m/s)	27.6
SSI (m/s)	14.8

2.3 Simulation of the present day monsoon using CCM2

This section gives a brief account of the simulation of the present day summer monsoon by CCM2 at the two horizontal resolutions. The results presented here are averages of last four years of 5 year and 30 days integrations at both the resolutions. The model integration starts from initial data for September 1, 1987, provided with the model and runs upto 5 years 30 days. Though there was considerable interannual variability in the model monsoon as well as observations, we believe the average of four years is adequate in our study of monsoon sensitivity to orbital parameters as our primary aim is to investigate the model sensitivity and its dependence on horizontal resolution than a rigorous simulation and comparison with palaeo-data. Fig 2.3 shows JJAS composites of precipitation simulated using CCM2 at T42 and T21 horizontal resolutions. The model captures broad scale features of summer monsoon over India and northern Africa at both the resolutions. When compared with NCEP reanalysis, T42 appears to be better than T21 in capturing certain features such as zonal pattern of precipitation over northern Africa. However, the spatial patterns of precipitation simulated by the model

at both the resolutions indicate that the model underestimate the precipitation associated with the Bay of Bengal trough. Both the resolutions fail to simulate the rainshadow effect of the western ghats and the secondary precipitation belt over the southern equatorial Indian ocean seen in observations.

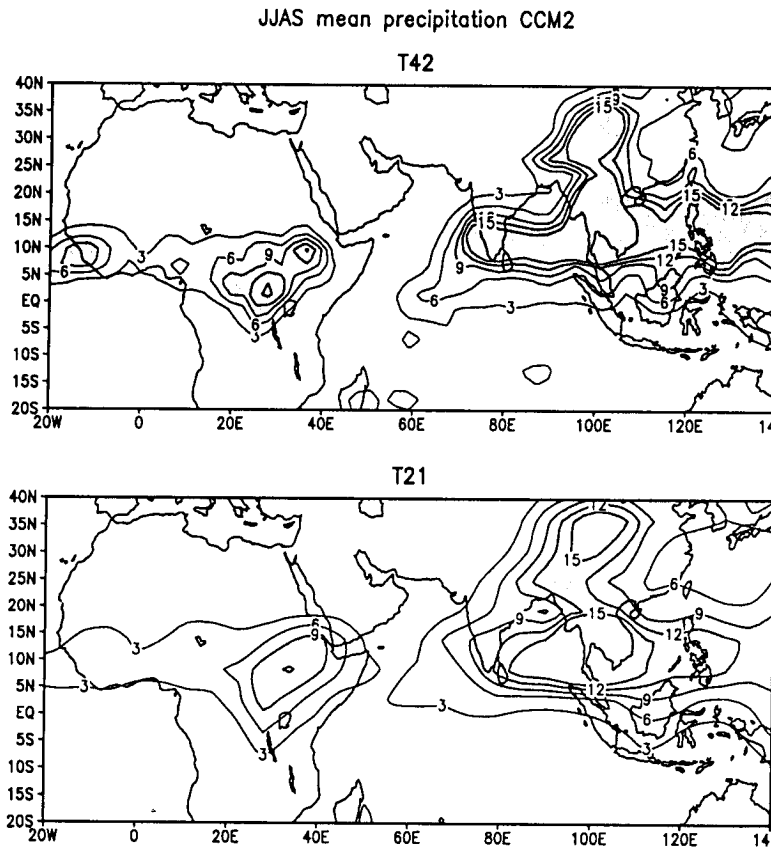


Fig. 2.3 JJAS composites of precipitation rate (mm/day) simulated by CCM2 at T42 and T21 horizontal resolutions.

On the other hand there is too much precipitation on the southern planks of the eastern Tibetan plateau and southern peninsula, Indonesian warm pool region, giving a typical horse-shoe like spatial pattern. Though the model underestimates precipitation over areas like north-east India, precipitation rates are unrealistically high on a broad scale compared to observations. This is diagnosed to be due to unrealistic non-linear interaction between ABL and convection parameterizations in the model (Hack 1994). These deficiencies are common to many of the existing

AGCMs (Gadgil and Sajani 1997) and the simulation of many aspects of seasonal mean monsoon is still an unresolved problem (Stephenson et al 1998). Figs 2.4 and 2.5 show JJAS composites of wind field at 850 and 200 hPa levels simulated by CCM2 at T42 and T21 resolutions. The model captures the major wind patterns at both the resolutions at upper as well as lower levels. Low level westerly winds

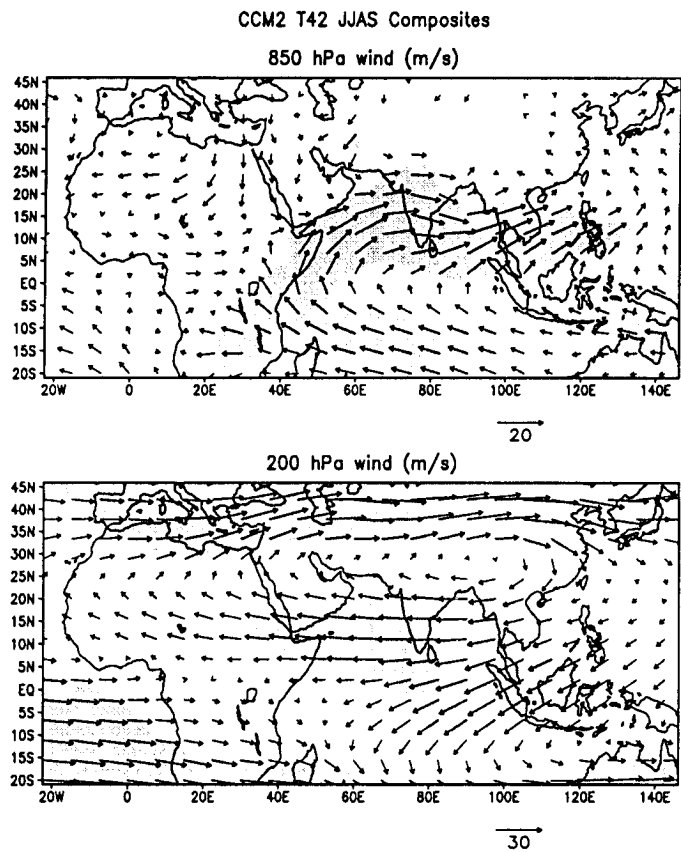


Fig. 2.4 JJAS composites of wind field (m/s) at 850 and 200 hPa simulated by CCM2 T42. Shaded areas denote the same features as in Fig 2.1.

extend too far east as well as north compared to observations at both the resolutions. T42 appears to compare better with the NCEP reanalysis (Fig 2.1) than T21. At upper levels, both T42 and T21 underestimate the longitudinal extent of the tropical easterly jet (shaded regions of 200 hPa wind in Figs 2.1, 2.4, and 2.5). T42 horizontal resolution better simulates the spatial pattern of wind field such as

the strength and the position of the Somali jet. This may be because, at this resolution the model resolves east African highlands and western ghats to a greater extent compared to T21 resolution.

Table 2.2 Monsoon indices simulated by CCM2 at T42 and T21 horizontal resolutions along with their standard deviation (sd).

Monsoon Index	T42	sd	T21	sd
PI (hPa)	3.2	0.26	5.4	0.5
P (mm/day)	7.4	0.6	8.2	0.9
P-E (mm/day)	4.3	0.4	3.8	0.4
CI (W/m ²)	248	6.2	241	5.8
MHI (m/s)	1.8	0.3	3.7	0.4
WSI (m/s)	30.0	1.8	32.1	1.7
SSI (m/s)	12.3	1.1	13.5	1.4

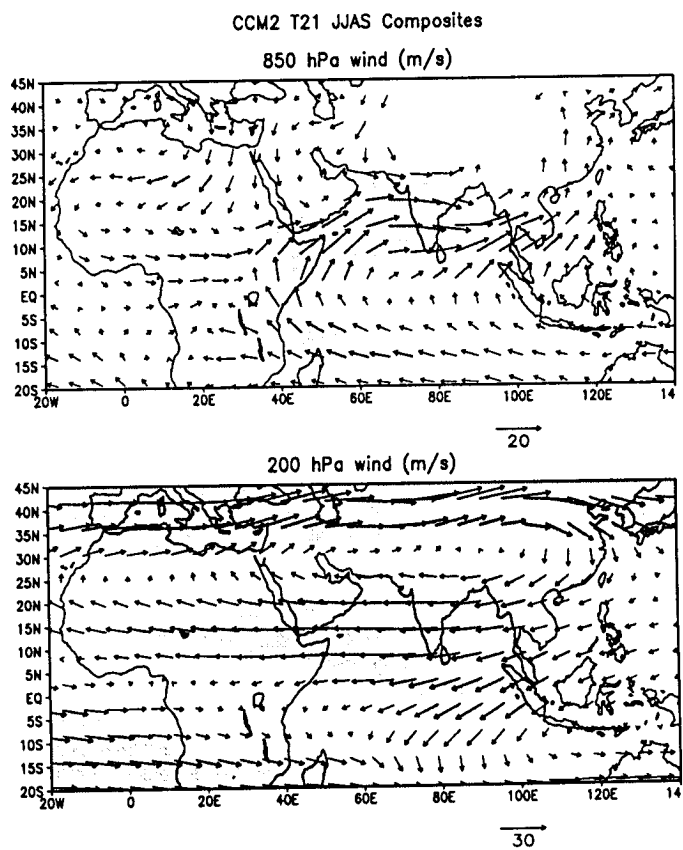


Fig. 2.5 JJAS composites of wind field (m/s) at 850 and 200 hPa simulated by CCM2 T21. Shaded areas denote the same features as in Fig 1.

On a broad scale the circulation pattern indicates that the monsoon circulation is stronger compared to observations. This is also evident when model monsoon indices are compared with those of observations (Table 2.2). These indices indicate that the low resolution model has quite stronger monsoonal circulation in many respects. However, both the resolutions, underestimate the SSI compared to NCEP reanalysis. This may be because of slight differences between the model and observations in the location of regions of strong southerly wind shears. Broadly speaking, many of the observed features of the monsoon are simulated by the model at both the resolutions. Though there are some systematic differences from the observations, the model can be used in palaeoclimate sensitivity studies.

Sensitivity Experiments I

3.1 Insolation changes during 6 and 115 ka

Variations in the seasonal cycle of insolation driven by changes in orbital parameters of the earth is primarily responsible for changes in monsoon strength on geological time scales. Orbital parameters of the earth vary in time primarily because of a slightly non-uniform distribution of mass in the earth from equator to poles and the resulting gravitational torque exerted by the sun (because of its mass), moon (because of its proximity to the earth) and other planets of the solar system (relatively less significant compared to the sun and moon). These orbital parameters can be calculated quite accurately up to a few million years backward (also forward) in time using the basic laws of celestial mechanics. Such calculations show that the three orbital parameters of the earth, namely eccentricity, axial tilt, and precession of longitude of perihelion undergo quasi-periodic oscillations with periodicities ~ 100 , 41, and 22 kilo years respectively (Berger and Loutre 1991). Records of past monsoon strength show predominant variability on time scales of 19 to 23 kilo years unlike that of high latitude climatic records where the influence of tilt and eccentricity cycles are dominant (e.g. Ruddiman and McIntyre 1984). This is so because the monsoon circulation is primarily driven by land-ocean thermal contrast and hence responds to significant seasonal changes in insolation brought about by the precession cycle. For instance, during 6 kilo years ago (ka) longitude of perihelion occurred near boreal summer in contrast to the present situation where it occurs during boreal winter which lead to increase in boreal

summer insolation relative to the present. During 115 ka the eccentricity(tilt) was higher(lower) compared to that of the present day resulting in significant reduction of boreal summer insolation. The orbital parameters of these time periods are ideally suited for model sensitivity studies of the monsoon circulation to insolation variations on orbital time scales. In this thesis we use the orbital parameters of these periods for examining the CCM2 AGCM monsoon circulation sensitivity to summer insolation changes.

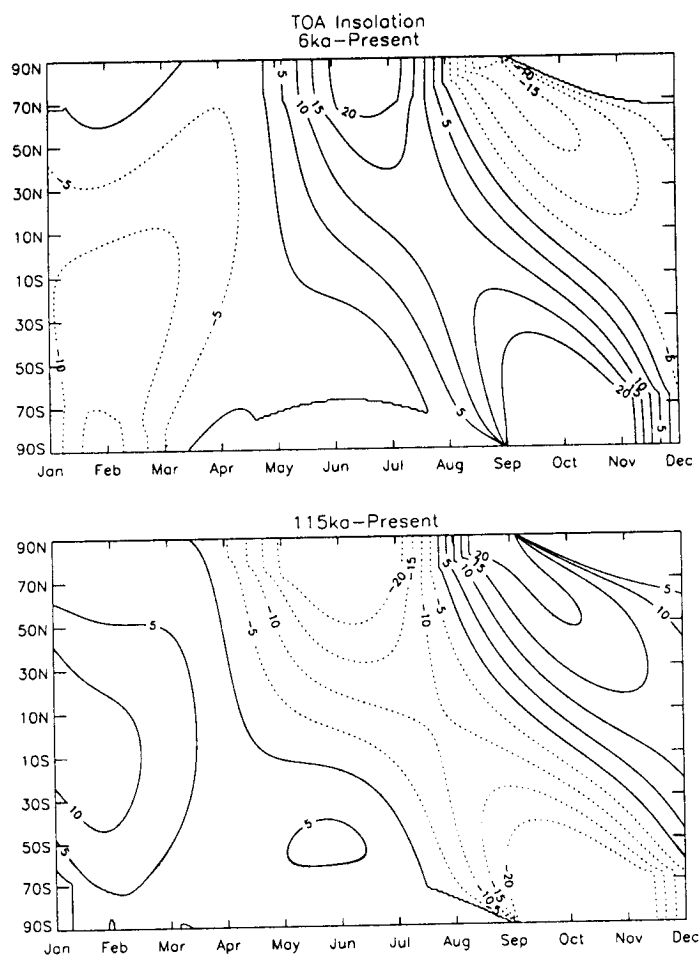


Fig. 3.1 Insolation anomalies (W/m^2) at TOA for 6 and 115 ka relative to present.

The orbital parameters of these time periods and the percentage deviation of northern hemisphere summer insolation at the top of the atmosphere (TOA) relative to the present day are given in Table 3.1. Latitude-time contours of insolation anomalies at TOA relative to the present are calculated using standard formulae (Berger

and Loutre 1994) are shown in Fig 3.1.

Table 3.1 Orbital parameters and mid July northern hemisphere averaged insolation anomaly (in percent) from the present.

Period	Eccentricity	Longitude of perihelion	Solar declination	Summer Insolation anomaly(%)
6 ka	0.019249	180.00	24.1 ⁰	≈ 5
115 ka	0.043983	289.54	22.44 ⁰	≈ -8

It is clear from Fig. 3.1 that the northern hemisphere summer insolation at TOA increased (decreased) during 6 (115) ka relative to the present. Similar changes in insolation are likely to occur at the surface which will result in changes in land-ocean thermal contrast relative to the present day leading to changes in the monsoon circulation. The AGCM sensitivity studies for the orbital parameters of these two periods will help in understanding the major changes in monsoon circulation to both increase and decrease of seasonal summer insolation relative to the present and provide a basis for interpreting the palaeo-data in terms of atmospheric circulation changes.

3.2 Inferences from palaeoclimate reconstructions

In this section we give a brief overview of monsoon variations as inferred from palaeoclimate reconstructions. Over continents, a majority of palaeomonsoon records is from geochemical and fossil pollen studies of lake sediments (eg., Singh et al 1974, Bryson and Swain 1981, Wasson et al 1984, Street-Perrott et al 1989). The lake level records are broadly categorized in qualitative terms as high, intermediate, and low throughout the past several thousand years relative to their present levels. Street-Perrott et al (1989) give details of factors such as dating uncertainties, quality of data etc., taken into account in this categorization. A majority of these records

over northern Africa and southern Asia is from the areas where the present monsoon rainfall is weak or completely absent (Sahara, Arabia, north-western India and the Chinese monsoon region) and are mostly regions of transition from monsoonal to desert/extratropical climate. These records clearly indicate that there is a wide spread increase in lake levels during early and middle Holocene (~ 9 to 6 ka) relative to the present. Changes in lake level during 6 ka in qualitative terms is shown in Fig 3.2. Over marine regions, upwelling indices such as foraminiferal species abundances, geochemical indicators of wind strength such as dust, pollen, etc are the major proxies (eg. Van Campo et al 1982, Pokras and Mix 1985, Prell 1984, Sarkar et al 1990, Sirocko 1996b). Van Campo et al (1992) and Pokras and Mix (1985), using the wind blown fresh water diatom record extending up to 150 ka showed that equatorial north African lakes were drier at the time of glacial inception (115 ka). Prell (1984) reconstructed the monsoon upwelling intensity for several thousand years by measuring the abundance of *G. bulloides*, a species of foraminifera more abundant in cooler sea surface conditions. Such cooler surface conditions over this region are induced mainly by the southerly summer monsoon winds (Findlater jet) and hence the abundance of *G. bulloides* in the oceanic sediment cores is an indicator of the strength of Findlater jet. This index showed variations similar to that of northern hemisphere summer insolation, thereby indicating that the strength of the Findlater jet is mainly influenced by summer insolation. The extent of monsoon winds over the Arabian sea inferred from the geochemistry of dust grains deposited in the oceanic sediments reveal that the summer monsoon weakened during the LGM (~ 21 ka), increased during early and middle Holocene (~ 10 to 6 ka), and decreased to present extent in tandem with seasonal summer insolation and glacial surface conditions (Sirocko 1996b). Sirocko (1996b) also showed that glacial events over high latitude regions such as Younger Dryas(YD) around 10.5 ka do not seem to influence the summer monsoon winds over Arabian sea, as summer insolation was higher during this period while the signature of such events are strong in the winter monsoon proxies. However, during the LGM, when insolation pattern was almost the same as that of

the present day, glacial conditions affected both the summer and winter monsoon winds to a great extent (e.g., Sirocko 1996b, Sarkar et al 1990). Thus it is likely that the competing influence of glacial conditions and summer insolation, that determine the strength of the Indian monsoon on millennial time scales. Clemens et al (1991), based on geochemical study of southern Indian ocean cores, concluded that apart from direct insolation forcing, internal forcing associated with the latent heat transport from southern Indian ocean is also important. Glacial events such as YD are found to affect the north African summer monsoon even though the summer insolation was higher relative to present. This is due to the proximity of northern Africa to north Atlantic ocean which is the main source of moisture influx for this monsoon. A few records of the monsoon strength such as vegetation proxies from peat bogs from southern India have also been unearthed (Sukumar et al 1993). But given the large spatial variability associated with the present day Indian monsoon, it is difficult to infer from these studies whether they are representative of large scale changes in monsoon strength over the surrounding areas. Overall, there is a definite indication that the monsoon strength changes with changes in seasonal cycle of insolation on orbital time scales, though there is a considerable gap in the regional coverage of palaeomonsoon reconstructions over the Indian subcontinent.

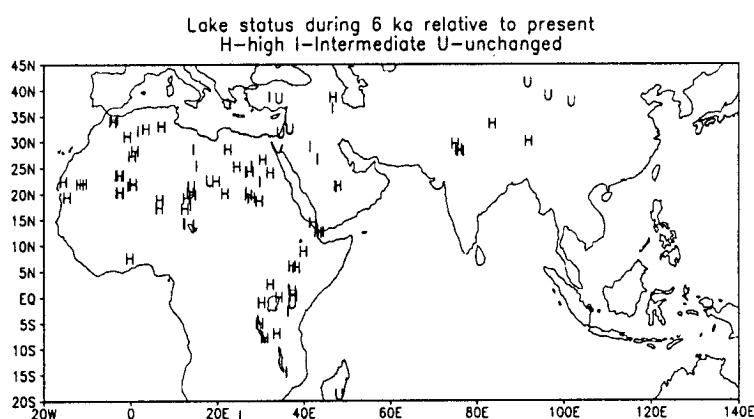


Fig. 3.2 Qualitative indices of lake status during 6 ka relative to the present (Street-Perrott et al 1989).

3.3 Modelling studies of the past monsoons

Here we give a brief overview of modelling studies related to past summer monsoon over southern Asia and northern Africa. The range of models used for study varies from AGCMs to coupled atmosphere-ocean-biosphere models. Many early modelling studies used relatively low resolution AGCMs in perpetual mode to simulate characteristic features of extreme summer(July) or winter(January) months to changes in insolation and glacial boundary forcings (e.g., Prell and Kutzbach 1992). Some studies used very low resolution AGCMs in annual cycle mode or to simulate seasons (Gates 1976; Kutzbach and Otto-Bleisner 1982). These studies were in qualitative agreement with the palaeo indicators of monsoon strength such as Arabian sea upwelling index (Prell 1984) and supported the inference from proxy records that the summer monsoon intensity is primarily controlled by insolation changes at the precessional frequency of the earth's orbit (~ 19 to 23 kilo years). They illustrated the changes in monsoon strength due to summer insolation changes by means of model derived large scale monsoonal indices such as averages of precipitation over Indian and north African monsoon regions, pressure index, southerly wind speed averaged over western Arabian sea, land surface temperatures, etc. The quantification of monsoon strength in these studies was thus on a large spatial scale and reasonably explained the monsoon evolution on long time scales as due to a combined effect of tectonism, insolation, glacial conditions, and atmospheric CO_2 concentration (Prell and Kutzbach 1992). Many of these studies did not take into account the internal feedback processes associated with soil moisture, precipitation, and snow cover. Some of the recent models used in palaeoclimate modelling studies which treat many of the processes such as surface hydrology, and impact of vegetation more interactively are listed in Table 3.2. A relatively high resolution AGCM which incorporated interactive soil hydrology was used by Dong et al (1996) to investigate the sensitivity of the atmospheric circulation to changes in insolation and glacial boundary conditions (CLIMAP 1981). The results of this study indicate that the monsoon strengthened(weakened) due

to changes in insolation during 6(115) ka and weakened substantially during the Last Glacial Maximum(~21,000 years ago).

Table 3.2 Some of the models used in recent palaeomonsoon studies. Except CLIMBER2, all other models are AGCMs. Some AGCMs incorporate land surface model and some are also coupled to an ocean general circulation models (OGCM).

Model	Resolution	Features	Reference
UGAMP	T42, L19	Interactive surface hydrology	Dong et al 1996
LMD4	48*36, L11	Bucket type soil hydrology	deNoblet et al 1996
CCM2	T42, L18	coupled to a land surface model	Kutzbach et al 1996
GEN2	T31, L18	coupled to land surface and ocean circulation model	Kutzbach and Liu 1999
CCM3	T42, L18	coupled to a land surface model	Broström et al 1998
NCAR CSM	T31, L18	CCM3 synchronously coupled to an ocean GCM	Otto-Bliesner, 1999
GFDL	R30, L14	coupled to GFDL global ocean model	Bush, 1999
CLIMBER2	51°X10°	Climate-Biosphere model of intermediate complexity	Claussen et al 1999

These results are in qualitative agreement with the previous studies. This study shows that the incorporation of interactive soil hydrology has significantly increased the monsoon sensitivity compared to fixed hydrology, thereby emphasizing the importance of interactive soil moisture in palaeoclimate simulations. This study also supports the view of Clemens et al (1991) who based on the geochemical evidence from the southern Indian ocean sediment cores suggested that a large part of the Indian summer monsoon variability is not only due to direct insolation changes, but also due to the internal forcing associated with the latent heat transport from the southern Indian ocean. The monsoon significantly decreased during LGM in this simulation while some previous studies (e.g., Prell and Kutzbach 1992) reported only a modest decrease.

In another study, deNoblet et al (1996), using a relatively lower resolution AGCM for the insolations of present day, 6, 115, and 126 ka, focussed on sensitivity to insolation changes of 6, 115, and 126 ka alone keeping all other boundary

conditions the same as that of the present day. This study shows that the insolation induced increase(decrease) of the land-sea thermal contrast during 6 and 126 ka (115 ka) induces a major shift of convergence zone associated with the monsoon towards northwest(southeast), resulting in increase(decrease) of precipitation over land of the monsoon regions at the expense of decrease(increase) of precipitation over the ocean. They point out that such shifts in convergence zone are observed during weak/strong monsoon events of the present day monsoon due to El Niño/La Niña. They infer that the model monsoon increase(decrease) due to insolation increase(decrease) is brought about by increase(decrease) in the frequency of high precipitation events.

Model intercomparisons under common forcings and boundary conditions relevant to 6 and 21 ka began with the inception of Palaeoclimate Modelling Intercomparison Project (PMIP) (Joussaume and Taylor 1995). In PMIP, models of diverse formulations under common boundary forcings were examined. Inter-model comparison studies are very useful as they have the potential to indicate whether, any characteristic feature of the simulation is specific to the model or is likely to be a robust response of the climate system. These studies reveal the role of model formulations such as horizontal resolution, differences in the simulation of present day climate, and physical parameterizations on the model sensitivity and come up with the most probable candidate mechanisms behind climatic changes. In one such study Joussaume et al (1999) compare sensitivities of monsoonal climates over northern Africa and southern Asia to 6 ka insolation in 18 participating models of PMIP. This comparison shows that all the models show a northward expansion of rainbelts over south Asian and north African regions and underestimate the northward extent of rainfall over northern Africa. Kutzbach et al (1996) using CCM2 AGCM coupled to a land surface model found that the inclusion of orbital parameters alone does not explain the extent of hydrological and vegetation changes over northern Africa, and the sensitivity increases with the inclusion reconstructed vegetation of 6 ka, but still inadequate to explain the observed northward extent of vegetation and precipitation. Kutzbach and Liu

(1997) find that the inclusion of oceanic feedbacks using a coupled ocean atmosphere GCM gives higher rainfall over northern Africa during 6 ka as inferred from palaeo records, but still not adequate to explain the reconstructed hydrological changes. A detailed study of land surface feedbacks associated with palaeo vegetation, and lakes and wetlands, during 6 ka using CCM3 AGCM which incorporates a land surface model also shows that none of these factors simulate the observed northward extent of vegetation and expansion of lakes (Broström et al 1998). Thus additional feedback processes may be necessary to explain the extent of rainfall over northern Africa as seen in palaeoclimate reconstructions. Joussaume et al(1999) point out that the data-model discrepancies over northern Africa may be due to the omission of synergistic interaction between ocean, vegetation and surface-water storage. The recent work of Ganopolski et al (1998) using a climate biosphere model of intermediate complexity wherein synchronous coupling between vegetation and atmosphere-ocean circulation is incorporated, indicates that the explanation of the observed extent of hydrological and vegetation changes over northern Africa during middle Holocene requires dynamic atmosphere-ocean-land-vegetation feedbacks. Using the same model Claussen et al (1999) arrived at an interesting explanation for the abrupt desertification of northern Africa around 5 ka. They performed transient simulations from 9 ka to present starting from the surface and oceanic boundary conditions of 9 ka obtained from an equilibrium simulation of 9 ka. The only input forcings for their model were insolation and CO_2 and the rest of the parameters such as vegetation etc., are interactively calculated in the model. More importantly vegetation interacts synchronously with the atmosphere-ocean system and vice versa in their model. The transient simulations from this model showed that the rapid desertification occurred around 5 ka within a few hundred years. They argued that the Saharan and Arabian desertification were triggered by subtle decreases in insolation which were strongly amplified by vegetation-atmosphere feedbacks. This study also implies that the vegetation-atmosphere interaction is more important than oceanic changes in causing desertification, thereby supports and extends the Charney's

(1975) pioneering work on desertification. However, due to the coarse resolution ($51^{\circ}\times 10^{\circ}$) this model does not adequately distinguish changes over western and eastern Africa. Hence additional studies are required with comprehensive AGCMs which include this feedback so as to assess this result and its geographical significance.

While vegetation-atmosphere feedbacks are important for explaining past north African monsoon, sensitivity of the Indian monsoon to insolation changes is related to ENSO(El Niño-Southern Oscillation) events. Some researchers based on geoarchaeological evidence and faunal indicators of warm conditions suggest the existence of semi-permanent warm conditions typical of present day El Niño events in the equatorial eastern Pacific along with an absence of interannual variability from ~ 11 to 5 ka (Rollins et al 1986, Sandweiss et al 1996, DeVries et al 1997). Bush(1999) uses an AGCM forced by fixed SSTs and also couples it to an ocean general circulation model to test the possibility of existence of such semi-permanent warm conditions over the eastern equatorial Pacific during mid-Holocene (6 ka). He finds that when the model is forced with SST distribution typical of warm ENSO events with 6 ka orbital parameters, there is a drastic reduction in Indian monsoon rainfall contrary to observations inferred from proxies. When AGCM is coupled with OGCM and run with 6 ka orbital parameters, Indian monsoon intensifies and the Walker circulation strengthens which in turn interacts dynamically with the equatorial eastern Pacific resulting in enhanced upwelling and more La Niña-like situations. Another similar study by Otto-Bliesner (1999) using NCAR Climate System Model (CSM) which is a synchronously coupled atmosphere-land-ocean-sea ice model suggests that the frequency and strength of El Niño events during 6 ka remained similar to that of present day. She suggests that faunal indicators of warmer conditions developed in narrow embayments and are not representative of large scale sea surface conditions like ENSO.

Thus the modelling studies continue to offer insights into mechanisms of monsoon variability. It is also important to analyze and understand any major

uncertainties within a model due to various factors like horizontal resolution, convection parameterization etc. In this thesis we focus on this aspect and study the impact of horizontal resolution and two different convection parameterizations on CCM2 AGCM monsoon sensitivities to 6 and 115 ka orbital parameters. In this chapter we describe the sensitivities of the standard version of CCM2 which uses a simple mass flux scheme for convection parameterization (Hack 1994) at two (T42 and T21) horizontal resolutions.

3.4 Sensitivity experiments

The orbital parameters of 6 and 115 ka are used as forcing factors to CCM2. A total of four simulations each of 1125 days duration are carried out at the two horizontal resolutions by prescribing these orbital parameters as forcings to CCM2. Sun-earth distance factor (inverse of the square of the sun-earth distance, also known as eccentricity factor) and solar declination which are functions of the orbital parameters of the earth are prescribed in the model as Fourier series functions of the time of the year. We have calculated these quantities for an annual cycle using the orbital parameters at sufficiently high temporal resolution and fitted them to Fourier series functions of time with the same number of terms as used in the standard version of the code. Pre-industrial CO₂ concentration of 267 ppm is used for both 6 and 115 ka experiments. SST and other boundary conditions are prescribed same as that of the present day. Thus our studies are not strict simulation studies where all the boundary conditions have to be specified or calculated by the model. Our aim is to study the impact of horizontal resolution and convection parameterization on model monsoon sensitivities when the forcing is significantly different from that of the present, and thereby infer any major uncertainties in the model sensitivities due to these factors. As AGCMs form a major component of the climate system models, an understanding of the impact of these factors may be useful in inter-model comparisons (Gates 1992).

3.5 6 ka results

As shown in Fig 3.1, boreal summer TOA insolation increases during 6 ka relative to the present. This insolation anomaly increases the land surface temperatures relative to the present day resulting in increase of land ocean thermal contrast and strengthening of the monsoon circulation. In the following subsections we describe the model monsoon circulation of 6 ka in detail.

3.5.1 Summer mean precipitation and circulation

Increase in monsoon strength can be examined by examining several parameters simulated by the model. Fig 3.3 and 3.4 show the precipitation(P) and precipitation minus evaporation(P-E) anomalies(6 ka-control) simulated by the model at T42 and T21 resolutions respectively. As the spatial distribution of precipitation simulated by the model for the present day is not very good (Fig 2.3) and precipitation rates are overestimated in regions of warm pool and southern planks of Tibet, the anomalies over these regions are higher compared to elsewhere. Nevertheless, the model simulates coherent changes in P and P-E over a broad region with increase over northern India and Africa, north-eastern China, and decrease over southern India, parts of warm pool region and oceanic regions at both the resolutions. T21 anomalies appear to be less compared to T42. Thus there appears to be increase of P over certain regions at the expense of decrease elsewhere at both the resolutions. Interestingly, the range of summer mean daily precipitation rates decreases for 6 ka especially due to decrease of precipitation rates over Pacific warm pool at both the resolutions. This is also indicative of major changes in precipitation pattern due to changes in land surface and atmospheric heating induced by insolation anomalies. In particular, there is a major change in the large scale convection pattern.

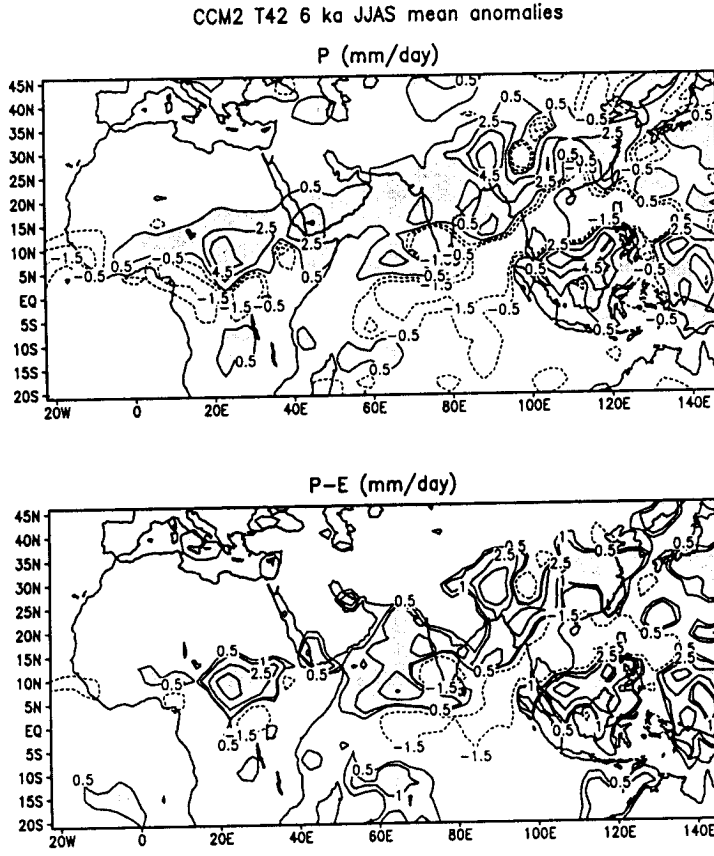


Fig. 3.3 6 ka P and P-E anomalies simulated by CCM2 T42. Shaded areas denote anomalies ≥ 0.5 mm/day.

The 850 hPa wind anomalies at the two resolutions are shown in Fig 3.5. The increase of westerlies is of the order of 2-4 m/s. Both the resolutions show increase in the strength of the westerlies over northern Africa and India, whereas T42 shows smaller increase in the low level wind speed over the Indian subcontinent compared to T21. At upper levels (200 hPa), both the resolutions show increase in TEJ strength (not shown), north of $\sim 15^\circ\text{N}$. Thus precipitation, upper and lower level wind anomalies simulated by the model at both the resolutions indicate that there is a strengthening of the monsoon circulation especially over northern latitudes, and there is a corresponding decrease over southern tip of India, Indo-Pacific warm pool, and equatorial northern Africa. Thus the model simulation at both the resolutions qualitatively indicates that there is an extension of rainbelts towards north of Africa, north-west India and east Asia.

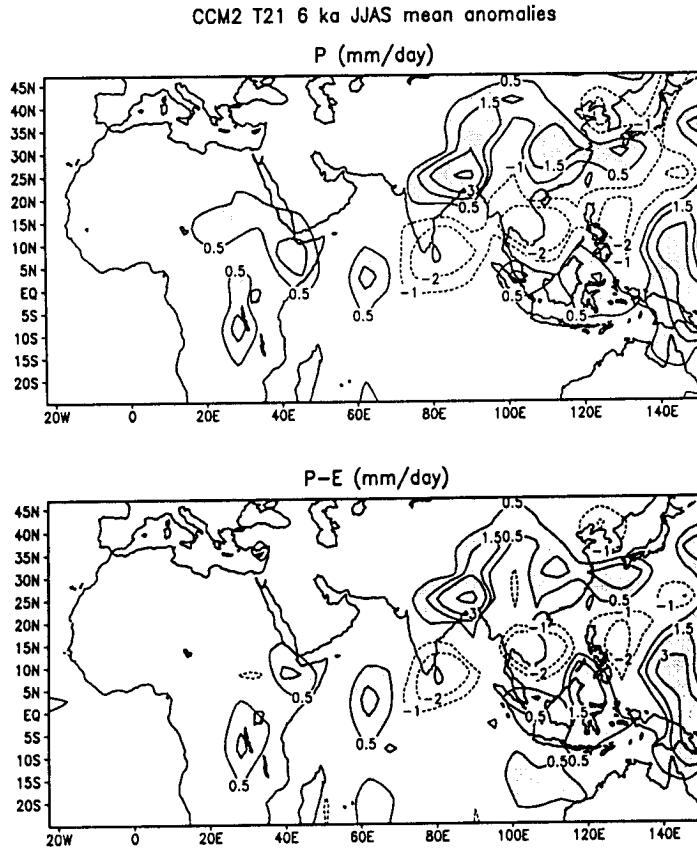


Fig.3.4 Same as Fig 3.3 but for CCM2 T21.

This extension of rainbelts appears to be due to major changes in the location of convergence zones for 6 ka relative to the present. Fig 3.6 shows meridional wind speed at 850 hPa (V850) averaged over the Arabian sea sector (45-65°E) for the present and 6 ka simulation of the model at the two resolutions. Between equator and 30°N, V850 reverses in sign and the latitude where it goes to zero, indicates a confluence zone or tropical convergence zone (TCZ). TCZ over the Indian region is a very complicated structure unlike the ITCZ over oceans, wherein rainbelt is confined to a narrow latitude band. Nevertheless, such a quantity may provide an elegant explanation for model simulated P and P-E anomalies.

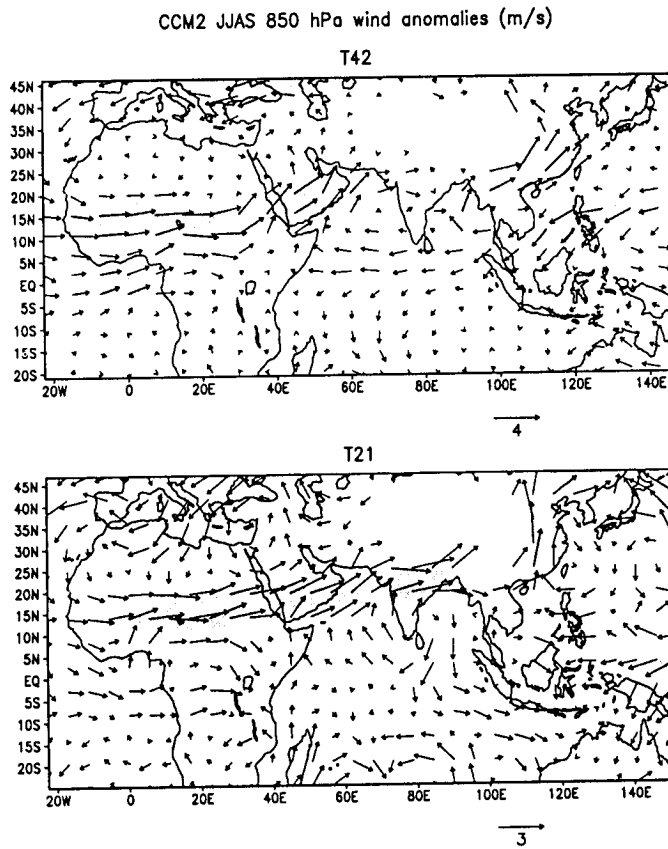


Fig.3.5 CCM2 6 ka 850 hPa wind anomalies. Shaded areas represent wind speed anomalies $>2\text{m/s}$.

It is evident from the figure, that the value of V_{850} increases, which is a clear indication of increase in monsoon strength. Also the latitude of TCZ is further north relative to the control. Thus the increase in land surface thermal contrast appears to favour the movement of monsoon trough slightly more north compared to the control. This is one of the reasons for decrease in P and P-E over southern tip of Indian at both the resolutions. A similar mechanism also seems to be there over northern Africa also as evident from P and P-E changes. Thus the geographical features of the seasonal mean anomalies of P, P-E, and wind field indicate that there are features common to both the resolutions mainly northward shift of rainbelts and a corresponding decrease over oceanic regions.

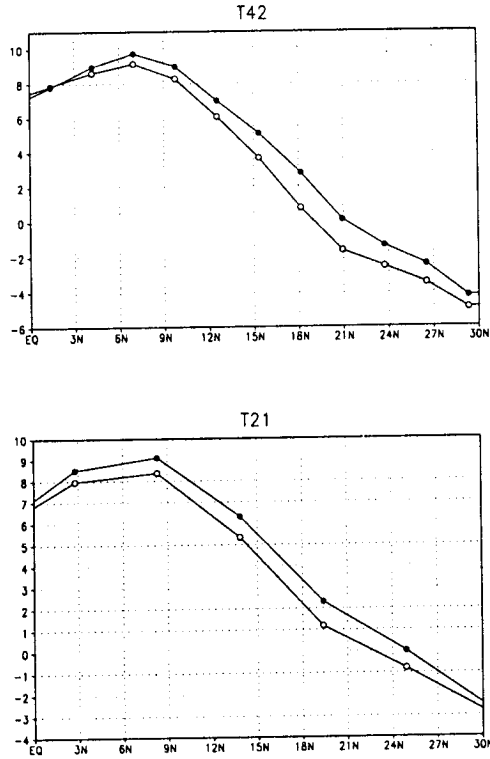


Fig.3.6 V850 (m/s) averaged over Arabian sea sector (45-65°E). Legends: open circle for 0 ka, and filled circle for 6 ka.

3.5.2 Anomalies in monsoon indices

The anomalies in monsoon indices simulated by the model at both the resolutions are given in Table 3.3. The anomalies at T42 resolution are higher compared to T21. However, one can notice a common feature of these anomalies at both the resolutions. The monsoon indices follow a similar pattern of changes both in sign and order of magnitude indicative of a robust mechanism behind the changes represented at both the resolutions. At both the resolutions most sensitive parameter is MHI. As MHI is a broad scale index of Hadley circulation associated with the monsoon, it implies that both the resolutions show an increase in Hadley circulation strength, which is mainly driven by land-ocean thermal contrast. Thus MHI increase at both the resolutions for 6 ka orbital parameters is consistent with increase in PI which is a measure of land-ocean thermal contrast.

Table 3.3 Anomalies (6 ka-Present) in monsoon indices. Values in parentheses indicate percentage deviations from the control run. These anomalies are statistically significant to a confidence level > 99%.

Monsoon Index	T42	T21
PI (hPa)	1.4 (43.75)	1.5 (27.7)
P (mm/day)	1.47 (19)	0.95 (11.6)
P-E (mm/day)	0.94 (21.8)	0.85 (22.4)
CI (W/m^2)	-19.3 (-7.8)	-11.5 (-4.8)
MHI (m/s)	1.4(77.7)	1.6(43.2)
WSI (m/s)	1.6(5.3)	0.6(1.8)
SSI (m/s)	0.9(7.3)	1.0(7.4)

Hence a major change in the monsoon circulation at both the resolutions is because of the strengthening of Hadley circulation. Thus the model simulations at both the resolutions indicate that much of the changes in P and P-E pattern may be related to changes in Hadley circulation over this region. However, other monsoon indices like SSI, WSI, and CI show much smaller increase compared to MHI. Thus, the monsoon index anomalies at both the resolutions indicate that a major mechanism behind monsoon rainfall changes due to 6 ka orbital parameters is the strengthening of the Hadley circulation cell.

3.5.3 Seasonal transitions

Observational analysis of intraseasonal variation of TCZ over the Indian monsoon region reveal a number of active and break phases with repeated northward propagation of TCZ playing a major role in revival from break phases (Sikka and Gadgil 1980). It has been recognized that subseasonal variations in monsoon rainfall, particularly the transition period between the active and break phases can affect the seasonal mean precipitation to a certain extent (Gadgil and Asha 1992). The recovery from break phase can take from a few days to weeks depending on the time at which the break occurs and surface conditions such as soil moisture, evaporation,

and runoff (e.g., Webster et al 1998). The mechanism and the transition time associated with the northward propagation of TCZ is explained to be due to interactive surface hydrology (Webster and Chou 1980, Nanjundiah et al 1992, Srinivasan et al 1993) and are inherently unpredictable due to the highly non-linear interactions involved. Figs 3.7 and 3.8 show P and P-E (averaged over the Indian region) average seasonal transition for the present day, 6 and 115 ka at T42 and T21 resolutions. It can be noticed that the seasonal transition consists of increasing trend in P and P-E during onset (June) reaching maximum during the established phase (July-August), and decreasing trend during withdrawal phase for all the cases. Both the resolutions show increase in P and P-E for 6 ka especially during onset and established phases. This is more noticeable at T21 than T42 resolution. Though large scale increase in monsoon strength is more at T42 as inferred from some monsoon indices (e.g. change in PI and MHI), due to the regional differences between the two resolutions in precipitation pattern, T21 appears to show more increase in P and P-E than T42. Figs 3.9 and 3.10 show seasonal transition of latent and sensible heat flux (LHFLX and SHFLX) averaged over the Indian region at both the resolutions. Both T42 and T21 show that as the season progresses LHFLX increases and SHFLX decreases due to increase in P for 6 ka indicative of increase in surface soil moisture. This is consistent with increase in P and P-E throughout most of the 6 ka summer and clearly indicate strengthening of the monsoon circulation. Also, P and P-E variations are almost similar indicating that increase in P-E is due to increase in P over this region.

Another quantity to study the seasonal transition of the monsoon is atmospheric kinetic energy averaged over the region 40-90°E, 5-20°N at 850 and 200 hPa. During the monsoon onset, westerly(easterly) winds dominate this region

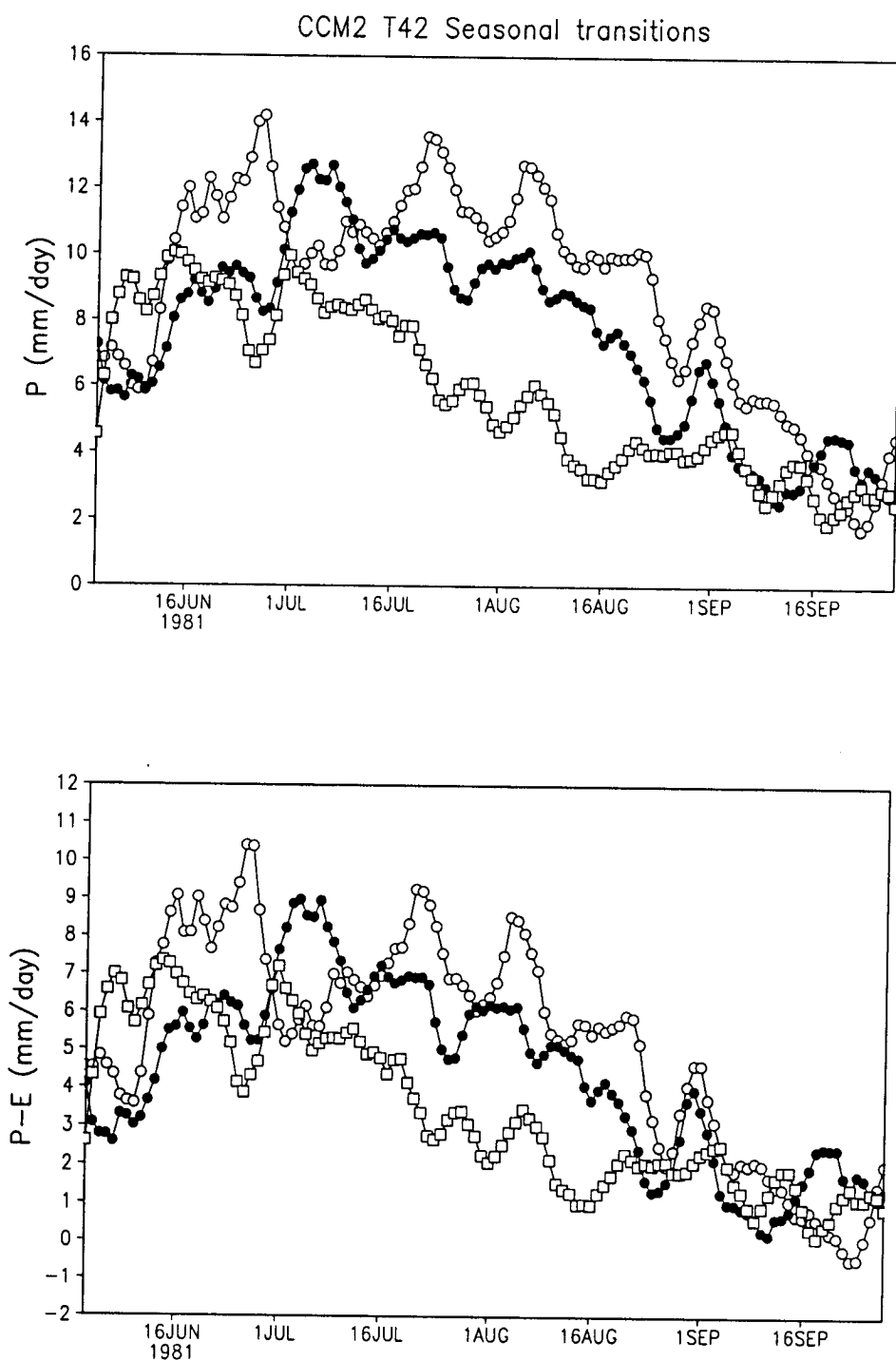


Fig.3.7 Seasonal transition (from June to September) of P and P-E averaged over India simulated by CCM2 T42. Legends: filled circle - 0 ka, open circle - 6 ka, open square - 115 ka.

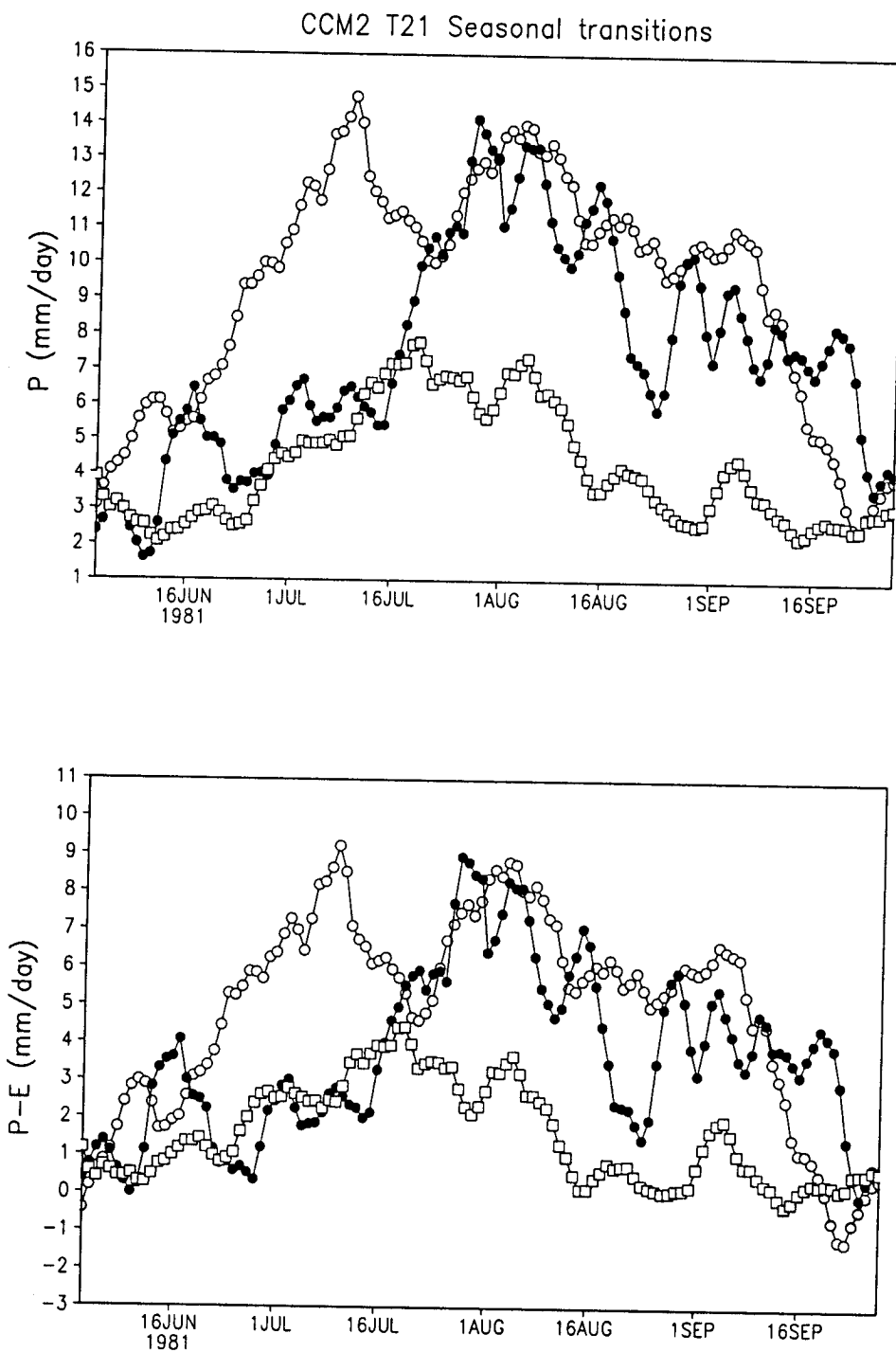


Fig.3.8 Same as Fig3.7 but for CCM2 T21.

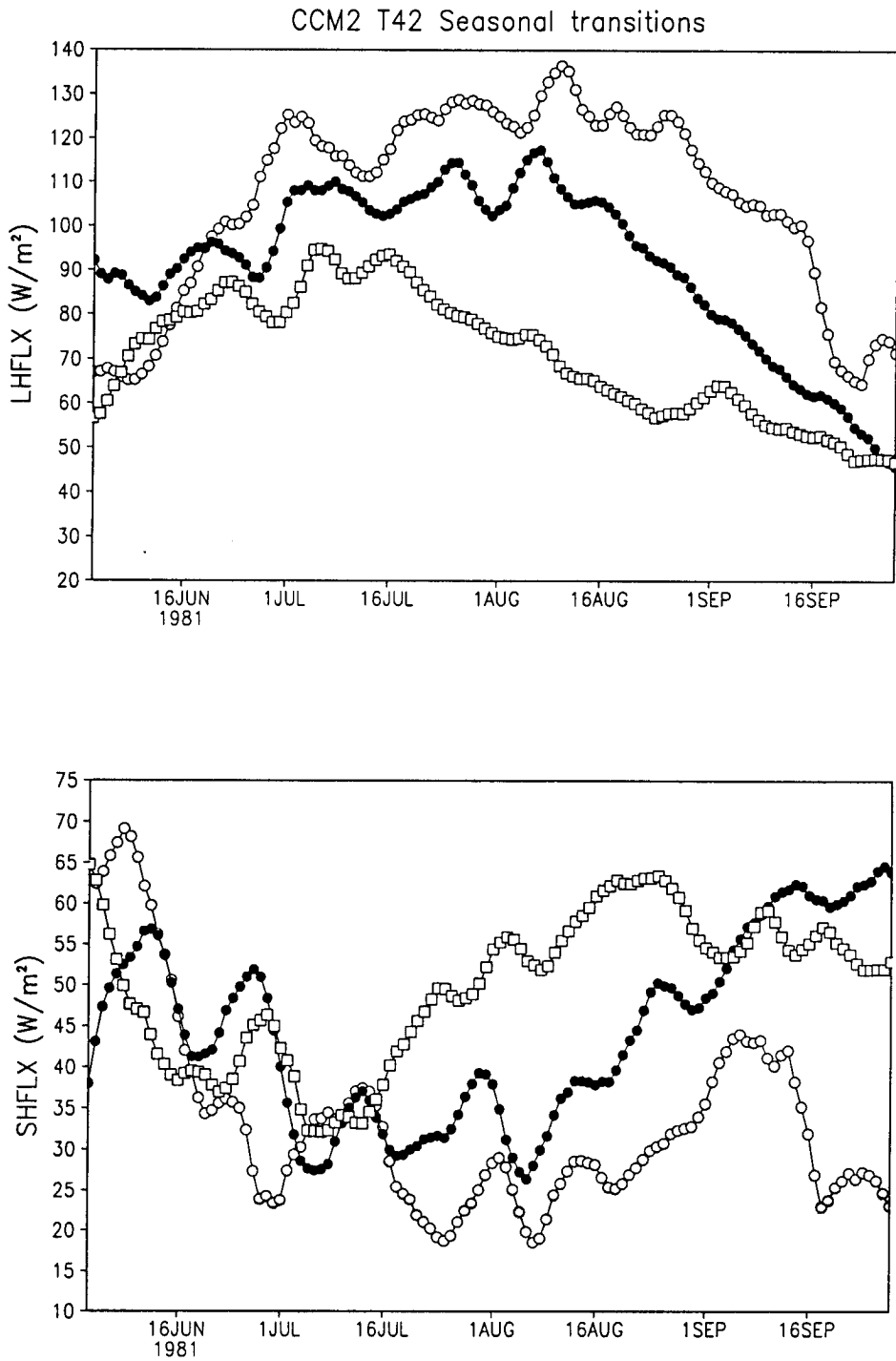


Fig.3.9 Seasonal transition of latent and sensible heat fluxes averaged over the Indian region simulated by CCM2 T42. Legends: filled circle - 0 ka, open circle - 6 ka, open square - 115 ka.

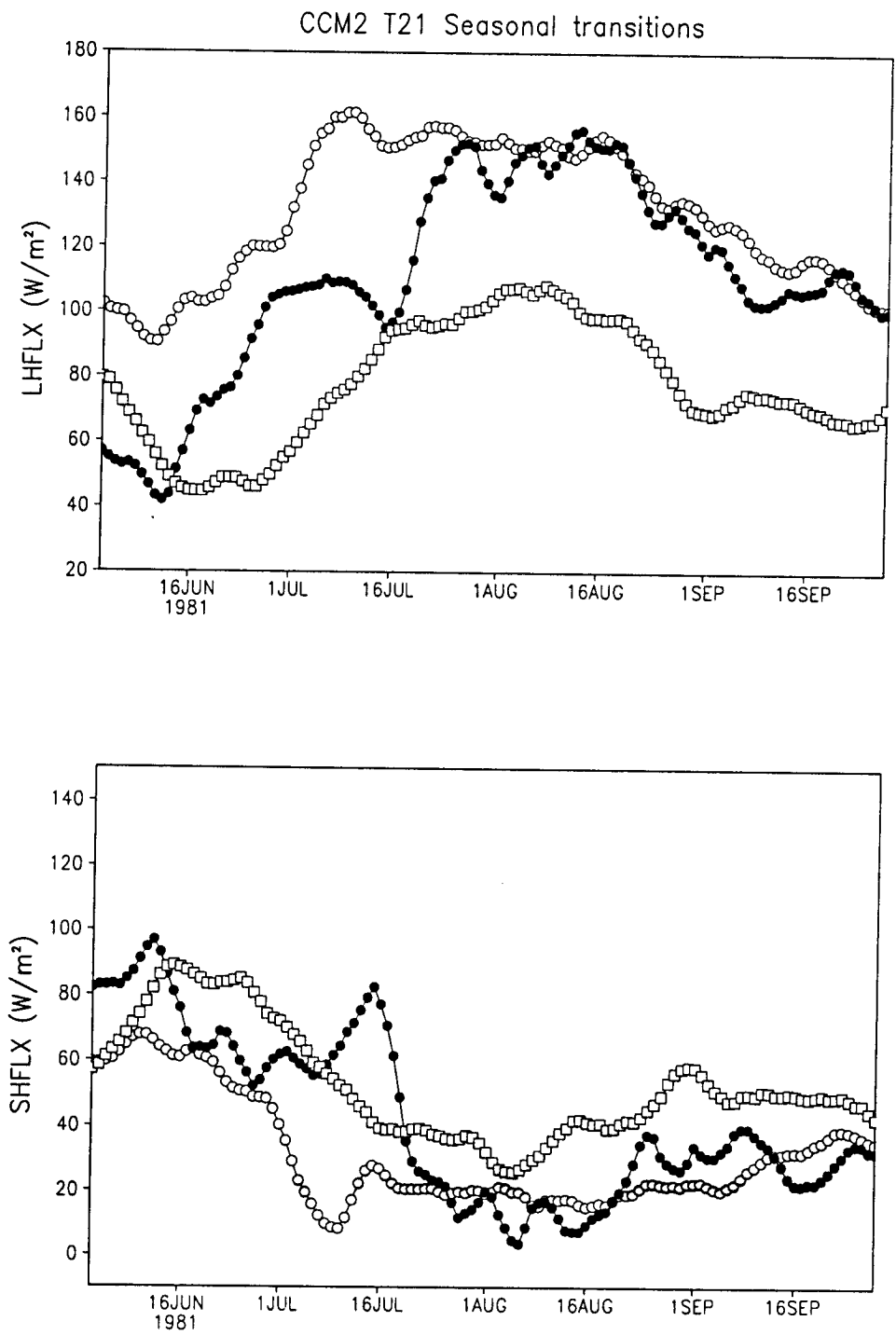


Fig.3.10 Same as Fig3.9 but for CCM2 T21.

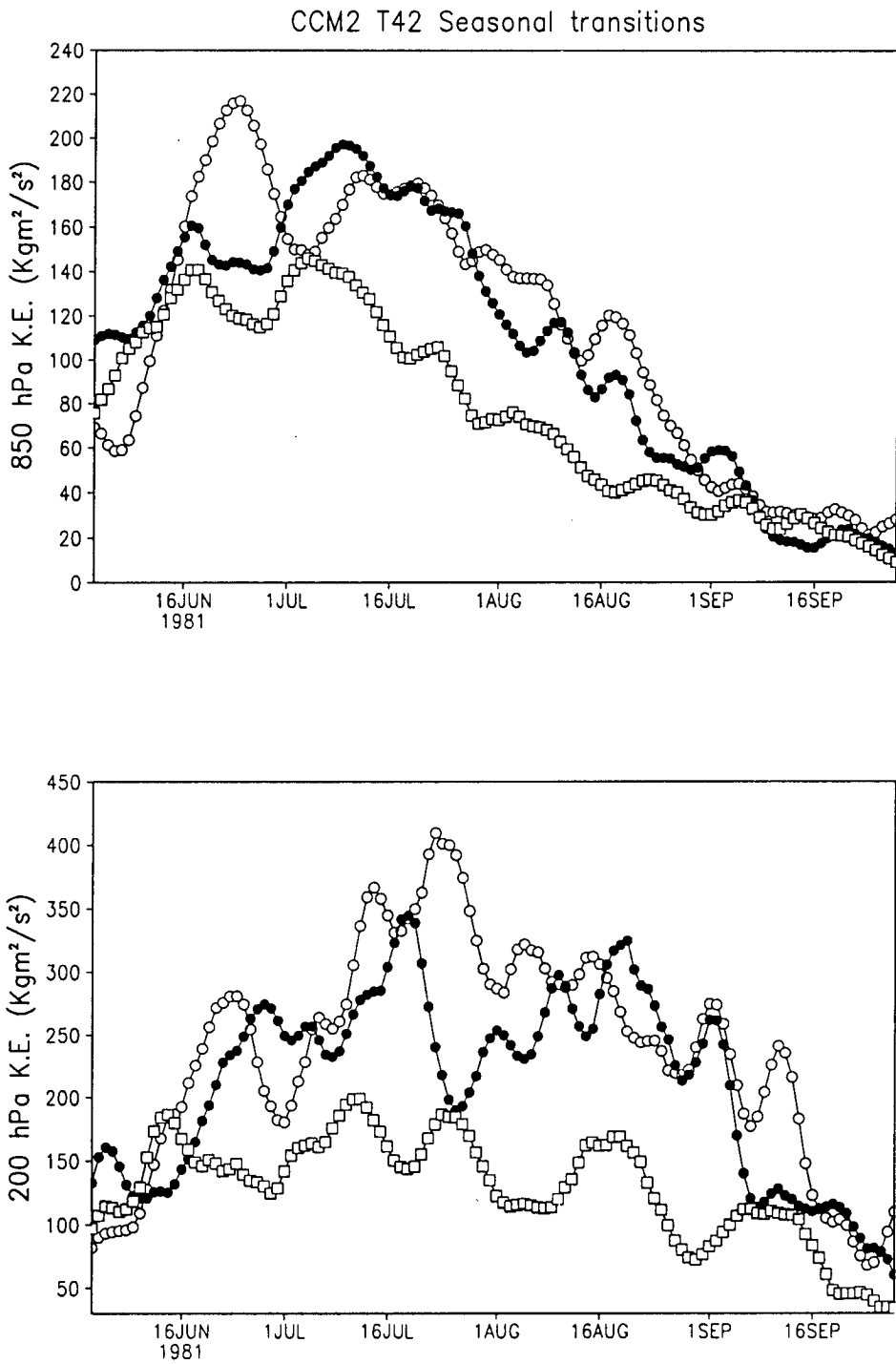


Fig.3.11 Seasonal transition of atmospheric kinetic energy averaged over the Indian monsoon region at 850 and 200 hPa simulated by CCM2 T42. Legends: filled circle - 0 ka, open circle - 6 ka, open square - 115 ka

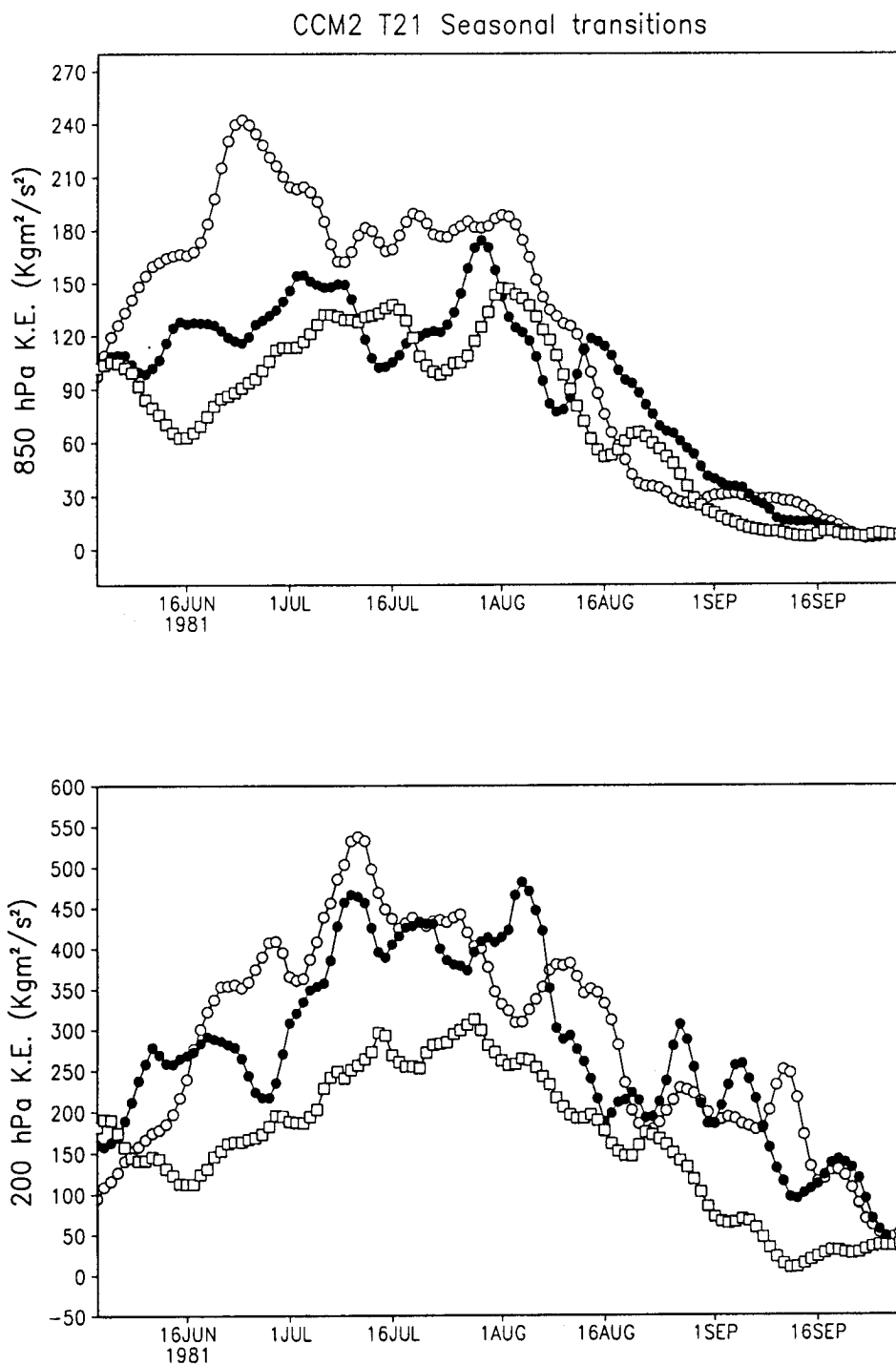


Fig.3.12 Same as Fig3.11 but for CCM2 T21.

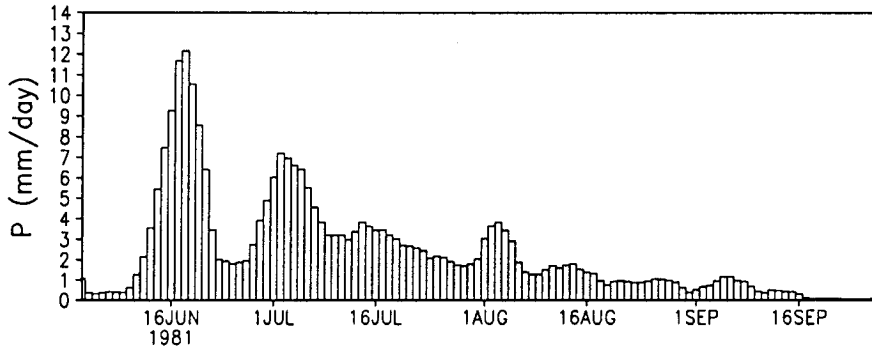
at lower(upper) tropospheric levels. Consequently one can see increase in atmospheric kinetic energy at both the levels during onset, which reaches maximum during the established phase and decreases during withdrawal phase. Figs. 3.11

and 3.12 show the seasonal transition of this quantity at T42 and T21 resolutions. It can be noticed that there is a slight increase in this quantity at 850 and 200 hPa levels at T42 levels for 6 ka, while at T21 the increase is much more pronounced at 850 hPa. This is consistent with the differences in P and P-E seasonal transition between the two resolutions.

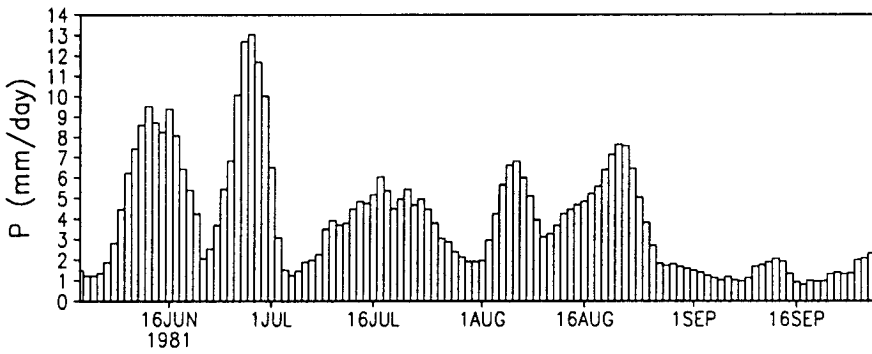
Increase in monsoon strength during 6 ka as illustrated by various quantities in the above discussion do not reveal much about the active-break phases of the monsoon. Precipitation averaged over central India ($70-85^{\circ}\text{E}$, $15-30^{\circ}\text{N}$) clearly shows active and break phases of the Indian monsoon for the present day at both the resolutions, though may not be in good agreement with the observed climatology. For 6 ka, the daily precipitation rates clearly show increase in the duration of active phase relative to the present day at both the resolutions (Figs 3.13 and 3.14). The range of daily precipitation rates however remain similar to that of the present day. Thus seasonal transition of monsoon precipitation over India simulated by CCM2 at both the resolutions indicate increase in the duration of active spell. These precipitation events may be classified into low, medium and high precipitation rates. While frequency of high precipitation events ($\sim 10-12$ mm/day) is small, middle range (~ 5 mm/day) dominate the active phase of the monsoon. It is seen that these middle range precipitation events increase for T42 6 ka and result in a prolonged active phase compared to the present. However, in T21 there is considerably more increase in high precipitation events than T42. These features may be related to the model control precipitation pattern at both the resolutions. T21 simulates considerably high precipitation over central India than T42. Overall, both the resolutions show increase in the duration of active spell during 6 ka relative to the present. Similar results are noted by deNoblet et al (1996) in their AGCM sensitivity study. However, they use the model at low resolution and with same CO_2 concentration as the present day and notices increase in frequency of heavy precipitation events similar to T21 results presented here.

CCM2 T42

Present



6 ka



115 ka

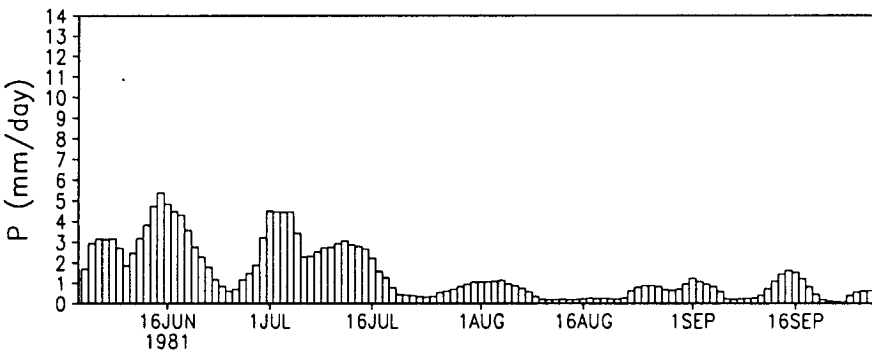


Fig.3.13 Bar chart of daily precipitation rates averaged over central India simulated by CCM2 T42.

CCM2 T21

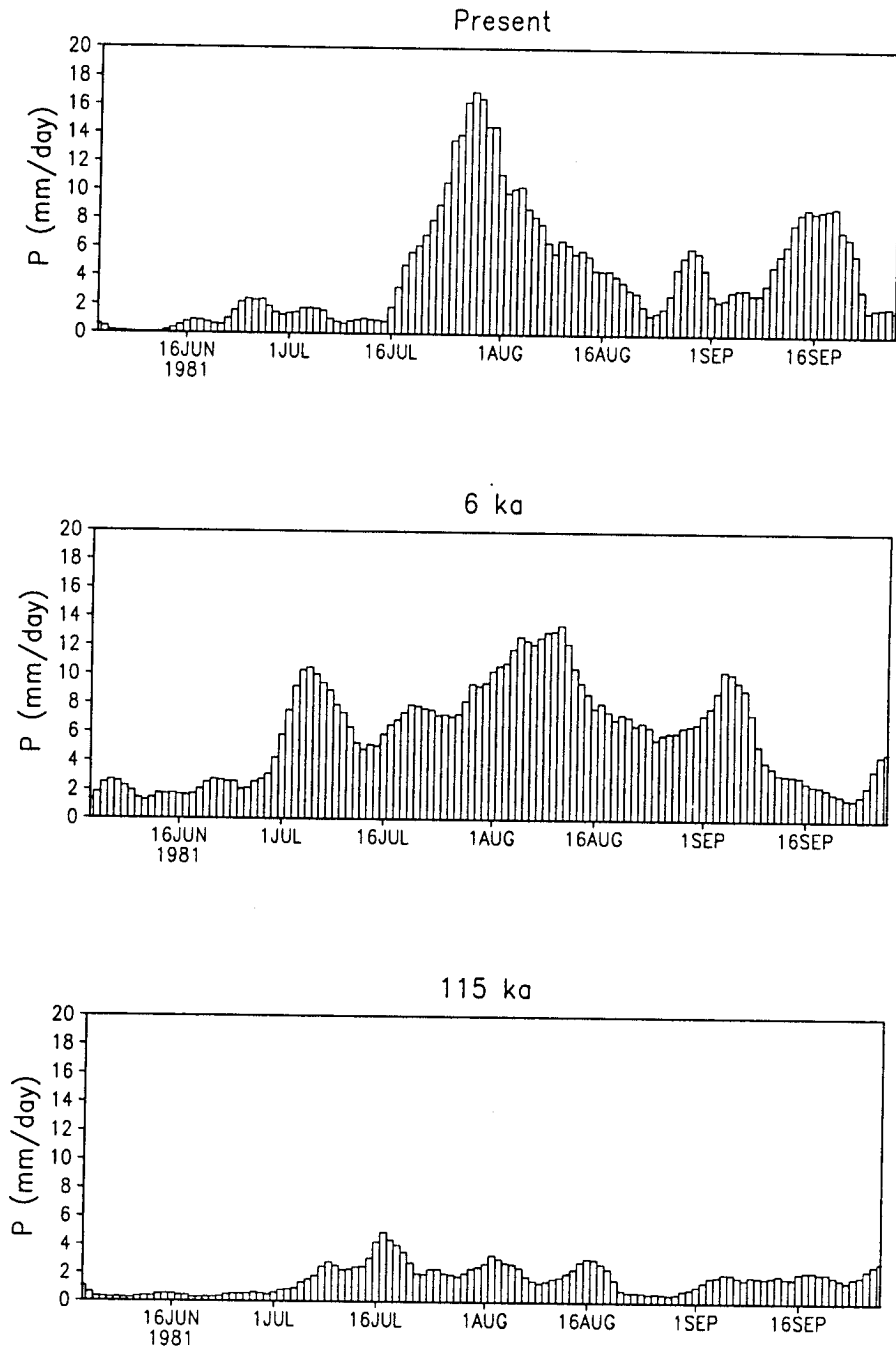


Fig.3.14 Bar chart of daily precipitation rates averaged over central India simulated by CCM2 T21.

3.6 115 ka results

As insolation anomalies are negative during 115 ka, the land surface will be relatively cooler than the present. This leads to weakening of the monsoon circulation relative to the present.

3.6.1 Seasonal mean precipitation and circulation

Figures 3.15 to 3.16 show JJAS mean P, P-E, and 850 hPa wind anomalies. The geographical pattern of P anomalies are nearly opposite to that of 6 ka on a broad scale with decrease of precipitation over a broad area comprising of northern Africa, India, north-east China and increase over southern tip of India, Pacific warm pool, equatorial western Africa at both the resolutions. P and P-E anomalies are also similar. The model precipitation rates range from ~ 0 -35 mm/day in the case of the present day over the monsoon region and the Pacific warm pool. This range further increases for 115 ka with highest values around 45 mm/day. This is due to increase of precipitation over Pacific warm pool relative to the present. Over the continents the precipitation decreases considerably. Noting that, the model precipitation rates are unrealistically high in the control run, due to unrealistic non-linear interaction between ABL and convection scheme, it is likely that the model monsoon sensitivity to 115 ka may be underestimated. The inference that the rainbelt shrinks towards equator relative to the control is also consistent with the circulation features. The 850 hPa wind decreases over the Indian monsoon region and northern Africa (Fig 3.17). The upper level circulation shows that the center of the Tibetan anticyclone shifts $\sim 5^\circ$ equatorward relative to the control at both the resolutions. Thus the seasonal mean TCZ is equatorward compared to the present. This is evident from the latitudinal variation of 850 hPa wind averaged over the Arabian sea sector (45 - 65°E) (Fig 3.18). It is evident from the figure that the TCZ position shifts by $\sim 5^\circ$ towards the equator relative to the present at both the resolutions.

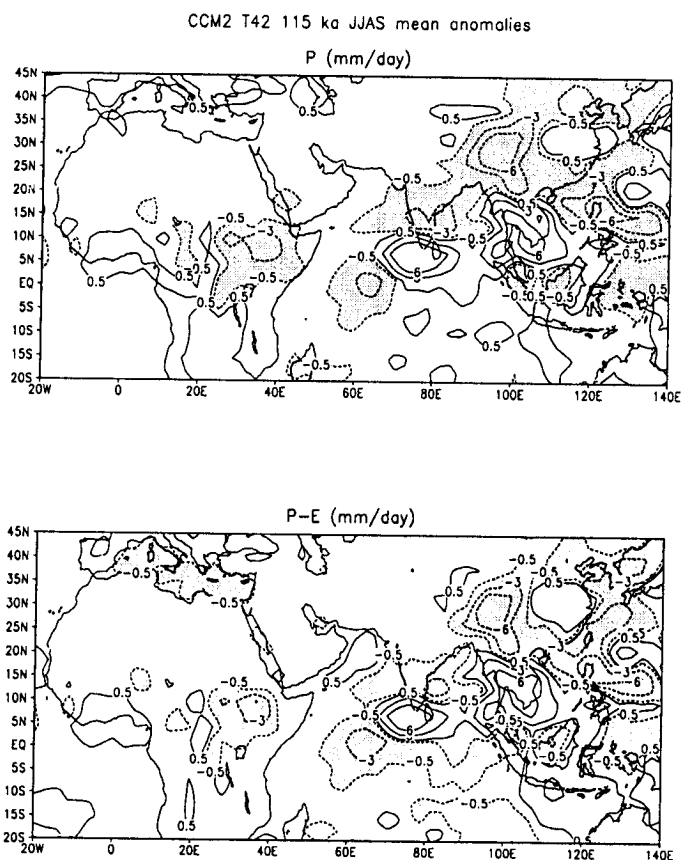


Fig.3.15 CCM2 T42 115 ka P and P-E anomalies. Shaded areas denote anomalies < -0.5 mm/day.

On a broad scale the geographical pattern of these anomalies appear to be similar at both the resolutions. Overall, the model geographical pattern of anomalies at both the resolutions indicate weakening of the monsoon over northern India, northern Africa, and strengthening over southern tip of India, southward of equatorial Africa, Indian ocean, and southeast China. These changes in geographical pattern are brought about by southward displacement of summer mean TCZ over India. Thus 115 ka anomalies of monsoon variables are broadly opposite of 6 ka anomalies suggesting that some changes in monsoon strength are brought about by relative latitudinal displacement of mean TCZ in response to insolation anomalies. These aspects are yet to be inferred in detail from palaeo-data over this region.

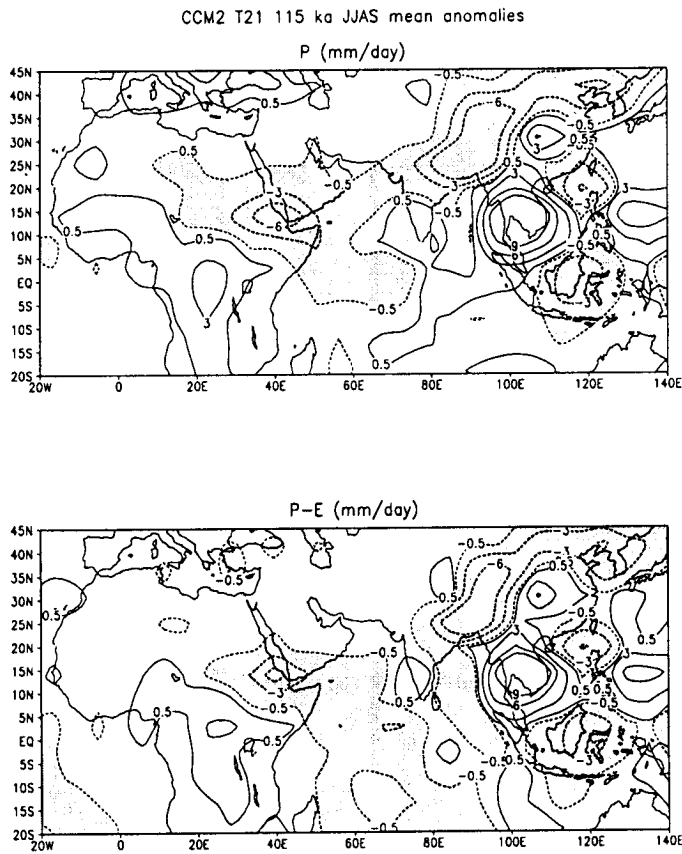


Fig.3.16 CCM2 T21 115 ka P and P-E anomalies. Shaded areas denote anomalies less than -0.5 mm/day.

Noting that the SSTs are prescribed same as that of the present day, in all the experiments, it is quite possible that the model response may be sensitive to prescribed SSTs to a large extent. Thus it is also necessary to infer palaeo-SSTs over these regions so as to study their possible role in determining the model sensitivity. For instance Texier et al (2000) decreases SSTs over the upwelling regions of the Arabian sea and increases it over Bay of Bengal and do sensitivity experiments using an AGCM with 6 ka orbital parameters. They find that the reduction in SSTs over Arabian sea (off east African coasts) enhances the monsoon circulation over Arabia, eastern Africa and India, and increasing SST over Bay of Bengal reduces land-sea thermal contrast and decreases monsoon strength over north India, and China.

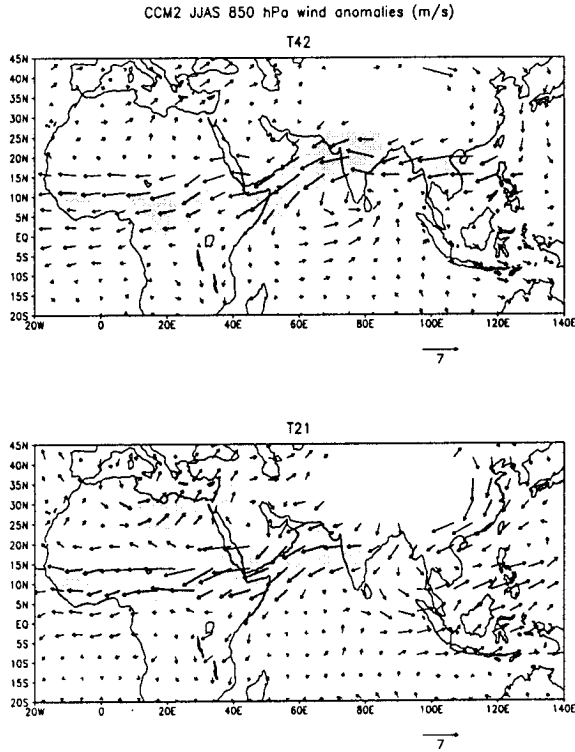


Fig.3.17 CCM2 115 ka 850 hPa wind anomalies. Shaded areas denote anomalies < -2 m/s.

Thus seasonal variations in palaeo-SSTs could be an important factor in knowing the model response such as northward displacement of mean TCZ to 6 ka orbital parameters etc. More modelling studies are required to with the help of inferred palaeo-SST, vegetation boundary conditions along with the palaeomonsoon indicators such as P-E, wind strength etc. As many of the monsoon circulation features like Findlater jet, extent of northwesterlies over Arabian sea, are fairly well characterized and long time series of the indices of these features are now available (e.g., Prell 1984; Sirocko, 1996b), a more direct comparison with AGCM sensitivities would be helpful both in evaluating the models as well as inferring the causes of variations in these features. In particular it would be interesting to infer the spacial extent of influence of remote boundary conditions like north-Atlantic SSTs, over the Indian region. Such remote changes in boundary conditions are often thought to affect the monsoon through teleconnections such as Eurasian snow cover and modelling studies support this view to a certain extent (e.g. Overpeck

et al 1997).

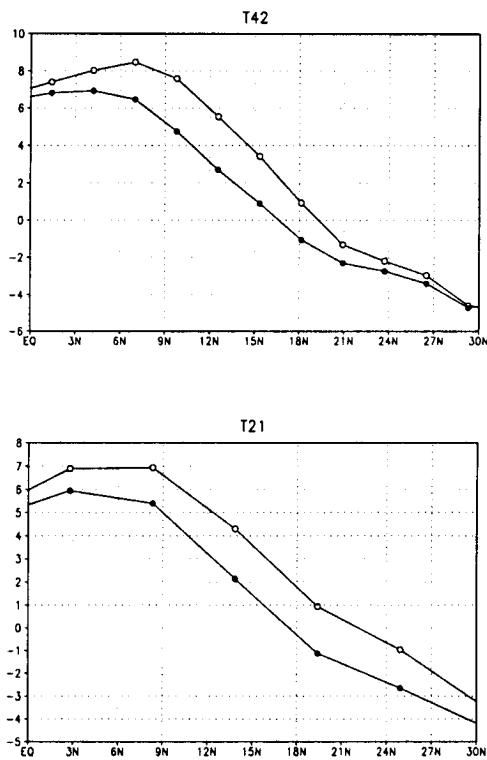


Fig.3.18 V850 (m/s) averaged over Arabian sea sector (45-65°E). Legends are open circle for 0 ka, and filled circle for 115 ka.

3.6.2 Anomalies in monsoon indices

Anomalies in monsoon indices for 115 ka are given in Table 3.4. All the indices show a decrease in monsoon circulation over India. PI and MHI anomalies at T42 horizontal resolution are higher than those of T21. All other indices are higher at T21 than T42. It may be noted that apart from PI and MHI, the other indices are recommended for use as indices of Indian monsoon strength (Wang and Fan 1999). These differences are thus likely to be due to differences between the two resolutions in capturing the regional details of the present Indian monsoon. However, the nature of the anomalies are similar at both the resolutions. Most sensitive index at both the resolutions is MHI and the least sensitive is CI.

Table 3.4 Anomalies (115 ka-Present) in monsoon indices. Values in parentheses indicate percentage deviations from the control run.

Monsoon Index	T42	T21
PI (hPa)	-3.5(-109)	-3.8(-70)
P (mm/day)	-1.7(-22.9)	-4(-48.8)
P-E (mm/day)	-1.0(-23.2)	-2.3(-60.5)
CI (W/m ²)	1(0.4)	4.6(2)
MHI (m/s)	-2.3(-128)	-3.5(-95)
WSI (m/s)	-7.8(-26.0)	-9.9(-30.8)
SSI (m/s)	-4.6(-37)	-7.3(-54)

3.6.3 Seasonal transitions

On an average seasonal transition of 115 ka model monsoon variables showed variations similar to that of the present day i.e., the monsoon during 115 ka is also characterized by onset, established and withdrawal phases. Due to decrease in summer insolation during 115 ka, monsoon strength also decreased. This is reflected in the average seasonal transitions of P, P-E, LHFLX, SHFLX, and atmospheric kinetic energy at 850 and 200 hPa levels over Indian monsoon region (Figs 3.7 to 3.12) at both T42 and T21 resolutions. Both the resolutions show decrease in P and P-E during established phase of the monsoon consistent with the decrease in latent heat flux, and increase in sensible heat flux. While there is an increase in KE during the monsoon season during 115 ka, this is smaller than the increase during 6 ka, clearly indicating a weakened monsoon circulation consequent to a reduced land-sea thermal contrast. T42 shows a more clear decrease in atmospheric kinetic energy at 850 and 200 hPa while T21 the seasonal transition is relatively closer to that of the present day. These differences between the two resolutions are also seen in P, and P-E thereby indicating that the differences are due to regional discrepancies between the two resolutions in the monsoon simulation. Nevertheless, there is a clear decrease in atmospheric kinetic energy at both the resolutions. Dong et al (1996) note that the maximum atmospheric kinetic energy is simulated for 115 ka

orbital parameters during the monsoon season in their AGCM sensitivity study. Our simulations indicate a rather direct response of atmospheric kinetic energy to changes in summer insolation. These differences may be due to the relatively long simulations used by Dong et al (1996) also as compared to our simulations. Such an increase in atmospheric kinetic energy as noted by their study is due to increase in monsoon winds over equatorial Indian ocean for 115 ka. Our simulations also simulated increase in precipitation and wind over the equatorial Indian ocean in addition to decrease of precipitation and winds over northern India. Thus it is likely that the length of the model simulations have some stabilizing effect on this quantity. However, no extensive data on P and P-E changes are available to verify the model simulated changes over the equatorial Indian ocean. Such changes are seen in palaeoclimate reconstructions over equatorial Africa (e.g., Pokras and Mix 1985).

Bar chart of daily precipitation rates averaged over central India shown in Figs 3.13 and 3.14 show that the precipitation rates are in the lower end ($\sim 0\text{-}5$ mm/day) at both the resolutions for 115 ka and hence appears similar to a prolonged break.

3.7 Comparison with palaeo-data

Increase in precipitation, over northwest India, region of China influenced by the Indian monsoon, Arabia and eastern Africa are in qualitative agreement with the palaeo-data of lake levels, geochemical indicators of wind strength etc. for 6 ka (Singh et al 1974, Bryson and Swain 1981, Wasson et al 1984, Prell 1984, Street-Perrott et al 1989, Sirocko 1996a). Decrease of monsoon strength simulated at both the resolutions for 115 ka is also in agreement with the wind blown fresh water diatom record extending up to 150 ka (e.g., Van Campo et al 1982, Pokras and Mix 1985).

Both the resolutions are similar in their spatial details of P-E changes of 6 ka

except over the central Indian region due to the model control simulation. Both the resolutions show spatially coherent increase in P-E over northern Africa, northern India, Chinese monsoon region, and decrease over eastern China, southern India, parts of the Indian ocean and Pacific warm pool, and equatorial Africa. There is a strong east-west gradient in the P-E pattern over eastern China and lake level indices also support such a feature. There are regional discrepancies between the two resolutions notable among them are, spatially extensive increase in P-E over north India(northern Africa) at T21(T42) than T42(T21). These features are related to differences between the two resolutions in their simulation of the present day climate. As T21, simulates more P-E in the control, than T42 over India, and so are the anomalies for 6 ka. However as noted in the monsoon indices, overall, the sensitivity hydrological changes at T42 is higher compared to that of T21.

However there are many aspects of the model simulations verification of which needs more spatial coverage of palaeo-data within and close to the Indian regions over both the ocean and the land. Both the resolutions shows a decrease in P-E over southern India, and Indian ocean. There also appears to to be an northeast-southwest gradient in P-E pattern over the Indian region, with increase in P-E over northern India, southwest Tibetan plateau, and decrease over southern peninsular India and equatorial Indian ocean for 6 ka. According to the model, the mechanism which gives rise to these changes in P-E within the domain of the Indian monsoon is major shift of convergence zone towards the land in response to insolation induced land-surface heating anomalies strengthened by soil moisture feedbacks. Thus over a span of a few thousand years, wherein there is significant change in summer insolation, one can expect differences in the sign and phase of evolution of the monsoon strength over different regions, which need to be analyzed. Such an analysis could serve as a crucial test for a set of model experiments conducted at different time slices which can help in understanding the palaeo-monsoon dynamics to a great extent.

3.8 Concluding remarks

The aim of the sensitivity experiments presented in this chapter was to infer any major differences in the model Indian monsoon sensitivity due to horizontal resolution. We find that there is a remarkable amount of similarity in the monsoon sensitivities as inferred from the analysis of geographical patterns of precipitation and circulation anomalies, and monsoon indices. Both the resolutions show that to a first approximation, model monsoon sensitivity to insolation changes are due to changes in the meridional Hadley circulation. The similarity of anomalies in monsoon indices of both the resolutions for 6 and 115 ka indicates that the processes associated with the changes are similar at both the resolutions on a broad scale. There are certain differences between the two resolutions in both the geographical pattern of the anomalies as well as monsoon indices. Notable of them are (i) Relatively large sensitivity in PI and MHI at T42 than T21.

(ii) Other indices also show larger sensitivity for 6 ka at T42.

However, T21 is more sensitive than T42 for 115 ka in these indices. These differences indicate that on a broad scale hydrological changes simulated by the model are more intense in the case of high resolution, relative to low resolution. Rind (1988) studied the impact of resolution on warm (double CO₂) and cold (ice age) climates by an AGCM and found that finer resolution is generally warmer (colder) relative to coarse resolution in double CO₂(ice age) experiments. Thus our results also give similar dependency on horizontal resolution, though for insolation changes. Thus it appears that the model hydrological cycle and associated feedbacks are more intense in high resolution to changes in forcing factor that affects the hydrological cycle. The results of this study also indicate the importance of interactive hydrology on the model sensitivities. In the absence of interactive hydrology sensitivities would be grossly different. In a similar study, Jagadheesha et al (1999) noticed that high(low) horizontal resolution is more(less) sensitive to

decrease(increase) in summer insolation relative to the present day due to the differences in the net surface solar radiation and latent heat fluxes at both the resolutions. But the model simulations in that study are for perpetual July with fixed hydrology. Hence the small differences in the model present day at both the resolutions amplified giving rise to different sensitivities. In this study such differences appear to reduce and the nature of sensitivities and processes associated with them are similar at both the resolutions. Thus the broad scale nature of monsoon sensitivities and the processes appear to be similar at both the resolutions when the forcing is strong from that of the present day.

The poor simulation of the present day P and P-E by the model at both the resolutions, limits the comparison with the palaeo-data. Also the palaeo-data is very sparse over the Indian region. Nevertheless, the model shows an increase in P and P-E for 6 ka over northwest India, northeast China which are periphery regions influenced by the Indian monsoon in qualitative agreement with the palaeo-data.

Sensitivity Experiments II

4.1 Introduction

There are many physical parameterizations in CCM2 AGCM which lead to improvements in the simulation of the present day climate when compared to previous versions of NCAR AGCMs CCM0 and CCM1 (Hurrell et al 1993). One of them is the parameterization of moist convection and the associated precipitation. As a major component of the forcing that drives the monsoon circulation is the convective latent heat release in the atmosphere (e.g. Webster et al 1998), it is important to understand the role of various convection parameterizations in modifying the model monsoon sensitivity. Zhang (1994) investigates the present day monsoon simulation in an AGCM with and without moist convection parameterization and notices significant improvements in the simulation of the monsoon circulation and precipitation pattern when a penetrative convective parameterization namely mass flux scheme is used as compared to no convection parameterization and moist convective adjustment (MCA) parameterization of Manabe (1969). In the model without moist convection parameterization, in order to prevent the atmosphere from being statically unstable, the adjacent vertical layers are successively checked for dry static stability starting from the lowest model level and if found unstable, the heat and moisture are mixed in the two layers until the dry adiabatic lapse rate is reached. Any moisture in excess of saturation amount is removed as large scale condensation after this mixing. In MCA parameterization, similar mixing procedure is followed except that (i) the layers are checked for moist

static stability, and (ii) condensation is allowed during mixing (convective precipitation). Any moisture left after mixing in excess of saturation is then removed as large scale condensation. Thus both dry and moist convective adjustments are local in nature and inefficient in terms of transferring heat and moisture to upper troposphere over the tropics. As a result, the model vertical humidity profiles are biased to give excess(deficient) moisture at lower(upper) troposphere compared to observations when MCA scheme is used to parameterize moist convection. In the tropical atmosphere, humidity is quite high and hence both dry adiabatic adjustment plus large scale condensation and MCA plus large scale condensation tend toward moist adiabat. Hence the model without and with MCA scheme gives almost similar circulation and precipitation pattern over the tropics (Zhang 1994). On the other hand when a penetrative convection parameterization such as a mass flux scheme is used, the entire vertical column of the atmosphere is checked for moist static stability and the heat and moisture are directly transported to the upper troposphere from the lower troposphere resulting in the drying of the lower troposphere, moistening of the upper troposphere, and more realistic distribution of humidity and precipitation than in the case of MCA scheme. The resulting circulation and precipitation pattern over the Indian monsoon and western Pacific region also become more realistic than that of MCA scheme.

Hack (1994) reports the changes in the present day climate simulation of CCM2 when the convection parameterization is changed from MCA to a simple mass flux scheme. The major improvements attained by using the mass flux scheme are, more realistic vertical distribution of moisture, and geographical pattern of monsoon precipitation. There are some discrepancies also, such as unrealistic non-linear interaction between ABL and convection schemes resulting in higher precipitation rates than observed. In spite of this drawback the improvements in the simulation of the present day monsoon from MCA scheme to mass flux scheme are noticeable in many respects.

It is interesting to know the effect of changing convection parameterization

on the model monsoon sensitivity to changes in orbital parameters and infer any major changes in sensitivity. However, in intermodel comparisons it is difficult to distinguish the effects of convection parameterizations alone. Hence intramodel sensitivity studies such as the one presented in this chapter may provide useful information and hints for explaining differences in intermodel sensitivities. From this point of view, using moist convective adjustment scheme (Manabe 1969) for convection parameterization we simulated the CCM2 response to the present day, 6 ka, and 115 ka orbital parameters at T21 horizontal resolution. All the experiments were run for 3.5 years starting from September 1 initial data provided with the standard version of CCM2. Model sensitivities are then inferred from the average of the three summer seasons (JJAS composites) simulated by the model for each case. Except for change in the convection parameterization, other details of the model runs are same as those explained in chapters 2 and 3.

4.2 Simulation of the present day monsoon

In this section we describe the present day monsoon simulation using CCM2 T21 with MCA scheme (T21MCA hereafter).

4.2.1 Geographical pattern

Fig 4.1 shows JJAS composites of precipitation(P), 850 and 200 hPa wind simulated by T21MCA for the present day. Spatial distribution of the precipitation is significantly different from that of the observations (Figs 2.1 and 2.2). Precipitation associated with the monsoon is confined mainly to the Indo-Pacific warm pool. The precipitation over India and northern Africa is weaker compared to observations with almost no precipitation over northern India. The precipitation over western Pacific is confined to near equatorial latitudes in the observations, whereas

CCM2 T21MCA 0 ka JJAS composites

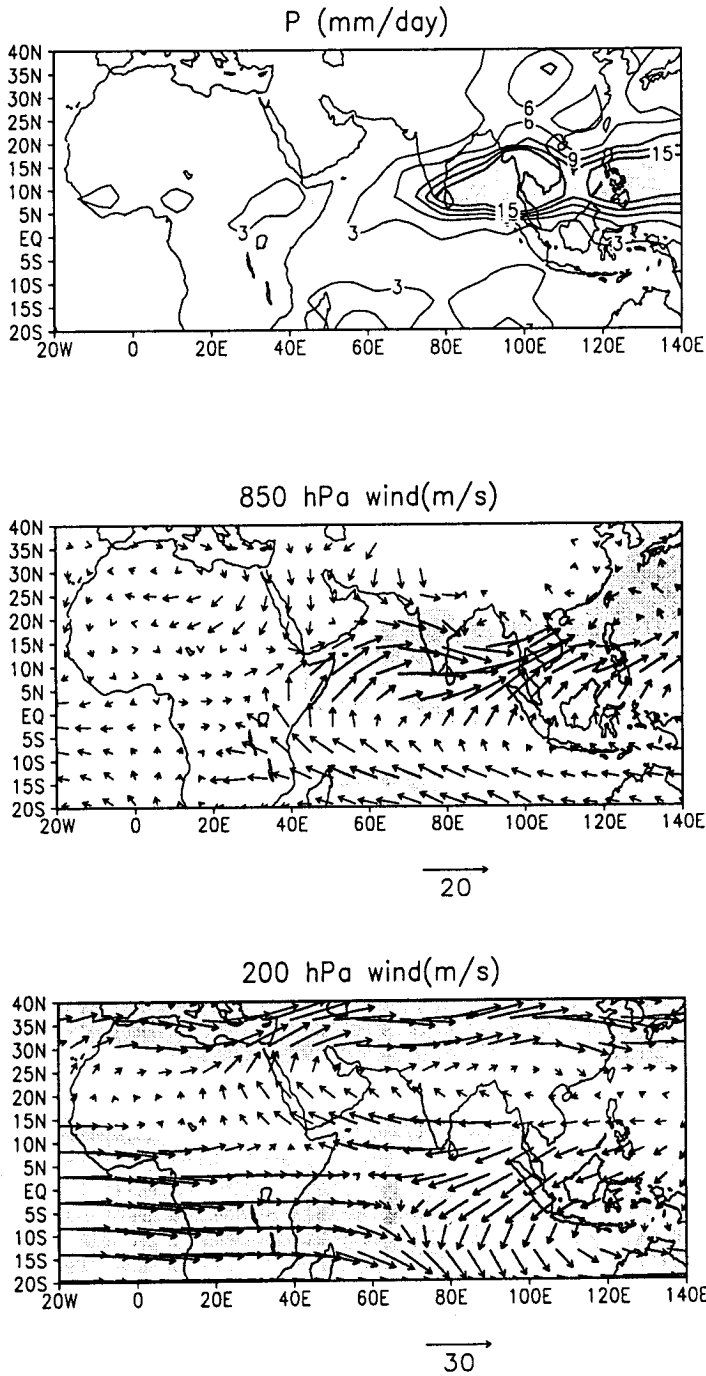


Fig. 4.1 The present day JJAS composites of precipitation rate (mm/day), 850 and 200 hPa wind (m/s) simulated by T21MCA.

it extends more northward in T21MCA. In comparison with the CCM2 simulations with a simple mass flux scheme for convection parameterization (T21MFX

hereafter) described in chapter 2, T21MCA gives less precipitation over India and northern Africa. Orographic precipitation over the Himalaya/Tibetan plateau region is higher in T21MFX than in T21MCA. The geographical pattern of difference of precipitation rates between T21MFX and T21MCA clearly shows relatively less rain over land regions in T21MCA (Fig. 4.2).

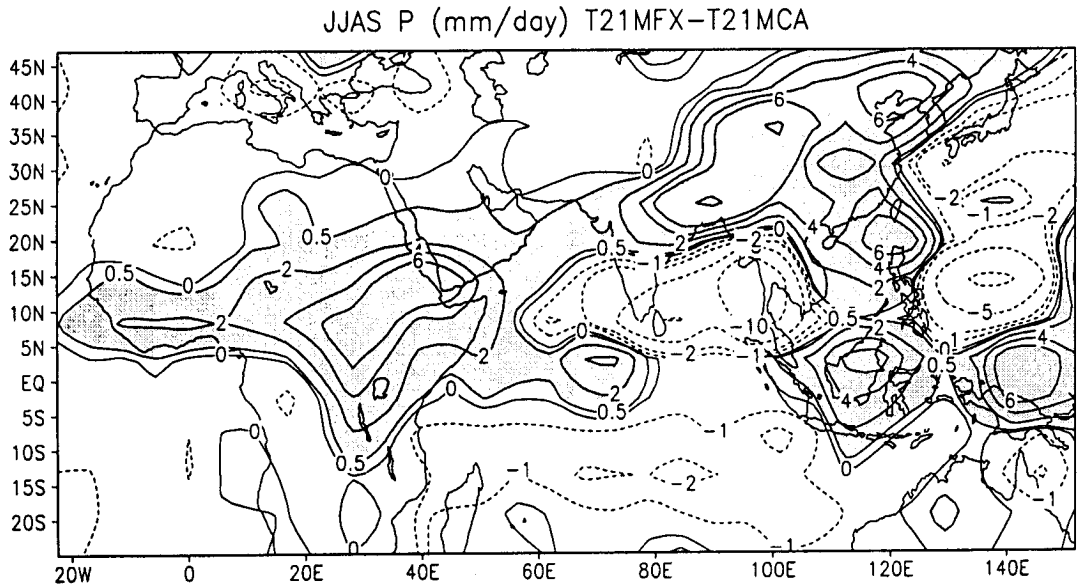


Fig. 4.2 The present day JJAS composites of precipitation rate (mm/day), T21MFX-T21MCA.

The broad scale pattern of 850 hPa wind is closer to the observations except that the monsoon westerlies extend too far east compared to the observations. The 200 hPa anticyclonic circulation centered over India is also simulated. However, the 200 hPa southern hemisphere subtropical westerly jet extends more equatorward compared to the observations. Tropical easterly jet (TEJ) is mainly confined to the Indian ocean region in the model, whereas it extends to as far as 10°S and covers equatorial Africa in the observations. These features of T21MCA are consistent with the far eastward extent of 850 hPa wind and weak precipitation over

India and northern Africa. It can be noticed that the 200 hPa winds are more north-easterly in T21MCA whereas they are easterly in the observations over the Indian ocean region. This is due to the fact that the major convective heat source lies over south-east China and equatorial Indian ocean in T21MCA. Thus the weak Indian monsoon in T21MCA gives rise to significant differences in TEJ compared to the observations. As we have described in chapter 2, TEJ features are captured quite well by the model with the mass flux scheme for convection.

Thus many of the features of T21MCA such as far eastward extent of monsoon westerlies, weak TEJ and precipitation over India, etc are similar to those noted by Zhang (1994) in an AGCM sensitivity study. However, in CCM0 and CCM1 (Hurrell et al 1993) which use MCA scheme for convection parameterization, near surface westerlies are quite strong and there is considerable precipitation over northern Africa. Consequently, 200 hPa TEJ, though weak compared to observations, is stronger than in T21MCA. It is possible that these aspects are not seen in T21MCA due to improvements in other parameterizations such as cloud radiative effects and consequent reduction in warm bias in the surface temperatures over northern hemisphere as compared to CCM0 and CCM1. Hence precipitation zone in T21MCA is confined mainly over warm oceanic regions where local moist static instability is high with weak precipitation over the continents, relative to CCM0 and CCM1. Thus it is important to note that the CCM0 and CCM1 TEJ are closer to observations than T21MCA in this study due to changes in other physical parameterizations.

4.2.2 Monsoonal indices

Monsoonal indices simulated by T21MCA give some insight into the nature of processes behind the model simulated monsoon (see chapter 2 for definition of monsoon indices and related references). As noted from the geographical pattern of changes, the monsoon circulation is weak compared to the observations is also evident from the monsoonal indices simulated by T21MCA (Table 4.1).

Table 4.1 The present day Monsoon Indices.

Monsoon Index	T21MCA	T21MFX	NCEP
PI (hPa)	1.03	5.4	2.6
P (mm/day)	3.9	8.2	6.4
P-E (mm/day)	1.5	3.8	2.9
MHI (m/s)	-0.57	3.7	2.5
CI (W/m^2)	237.7	241	285
WSI (m/s)	15.4	32.1	27.6
SSI (m/s)	7.5	13.5	14.8

It can be noted that all the monsoonal indices except convection index are indicative of the weaker Indian monsoon in the model. The lower value of convection index compared to observations mainly comes from a different area where oceanic precipitation is high in the model and hence may not be comparable with the observed OLR in order to infer the Indian monsoon strength. The smaller values of PI, MHI, WSI, and SSI compared to the observations indicate that the overturning of the airmass associated with the monsoon circulation is of lesser vertical extent than the observation. Geographical pattern of 500 hPa JJAS composite vertical velocity pattern for T21MCA and T21MFX also indicate this inference (Fig 4.3). It can be clearly noticed that the region of ascent (indicated by negative values of vertical pressure velocity) is concentrated over warm oceanic region centered around south east China in T21MCA and is of limited spatial extent compared to T21MFX. The only similarity of T21MCA monsoonal indices with the observations is that the vertical wind shears are higher for the zonal wind than for the meridional component. Thus T21MCA is less realistic than T21MFX in the particular context of the present day simulation of the Indian monsoon. The monsoonal indices such as WSI, MHI, and SSI which are a measure of baroclinicity of the monsoon circulation are closer to NCEP reanalysis in T21MFX whereas they are grossly underestimated in T21MCA. Thus from the circulation perspective, T21MFX may be regarded as a significant improvement as far as the simulation of the large scale aspects of the present day Indian monsoon is concerned.

JJAS Composite 500 hPa Vertical Velocity (hPa/s)

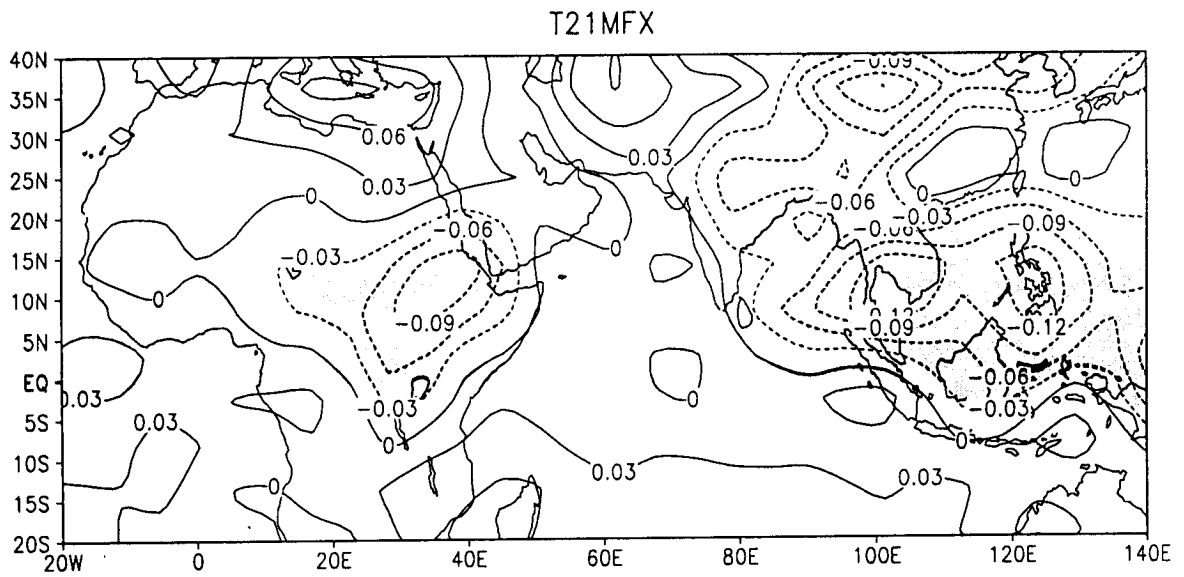
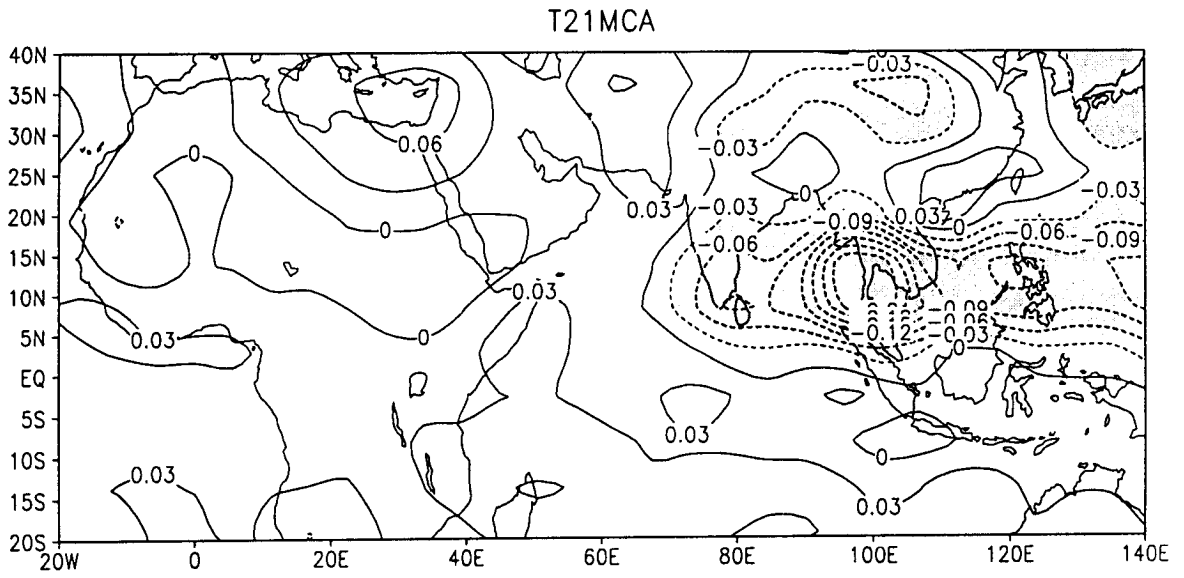


Fig. 4.3 JJAS composites of vertical pressure velocity pattern simulated by T21MCA and T21MFX.

4.3 6 ka results

In this section we describe the T21MCA monsoon sensitivity to 6 ka orbital parameters.

4.3.1 Geographical features

Fig 4.4 shows geographical pattern of P, P-E, and 850 hPa wind anomalies simulated by T21MCA for 6 ka orbital parameters. T21MCA does simulate increase in P and P-E over the Indian subcontinent and southeast China. Increase in P and P-E mainly takes place over the Indian subcontinent and eastern China south of $\sim 25^\circ\text{N}$. There is a corresponding decrease in P and P-E also over the equatorial Indian ocean and southeast China. There is not much change in P and P-E pattern over northern Africa except a slight change over eastern Africa and equatorial northern Africa. Thus unlike CCM0 and CCM1 sensitivity studies (Qin et al 1998) which use MCA scheme for moist convection parameterization, T21MCA does not indicate any northward penetration of P and P-E over northern Africa. As we have already noted, apart from convection parameterization, there are other changes in CCM2, important one being the reduction in warm bias of surface temperatures over northern hemisphere in CCM2 relative to CCM0 and CCM1. Also, while CCM0 experiments were done using fixed soil moisture in perpetual July mode, CCM1 experiments were done with mixed layer slab ocean model and hence may have shown different sensitivities than T21MCA presented here. Both T21MCA and T21MFX show a northward precipitation of the monsoon rain-belt vis-a-vis the control simulation. As the spatial pattern of precipitation differs between T21MCA and T21MFX, so are the regions which experience increase in precipitation. Thus in the case of T21MCA, as most of the precipitation is over southeast China, northward penetration into the Indian subcontinent and southwest China is relatively weak, whereas it is relatively high over northeast China compared to T21MFX.

CCM2 T21MCA 6 ka anomalies JJAS composites

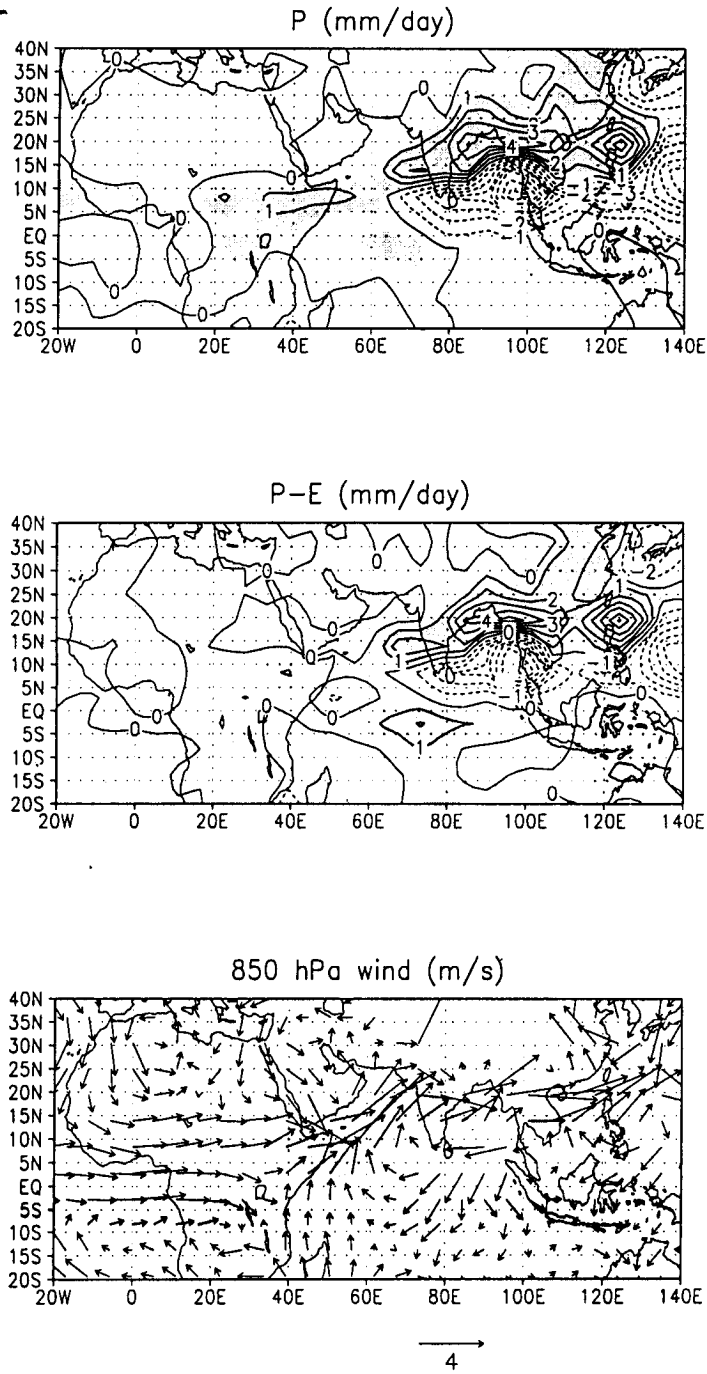


Fig. 4.4 JJAS composites of 6 ka P, P-E, and 850 hPa wind anomalies simulated by T21MCA.

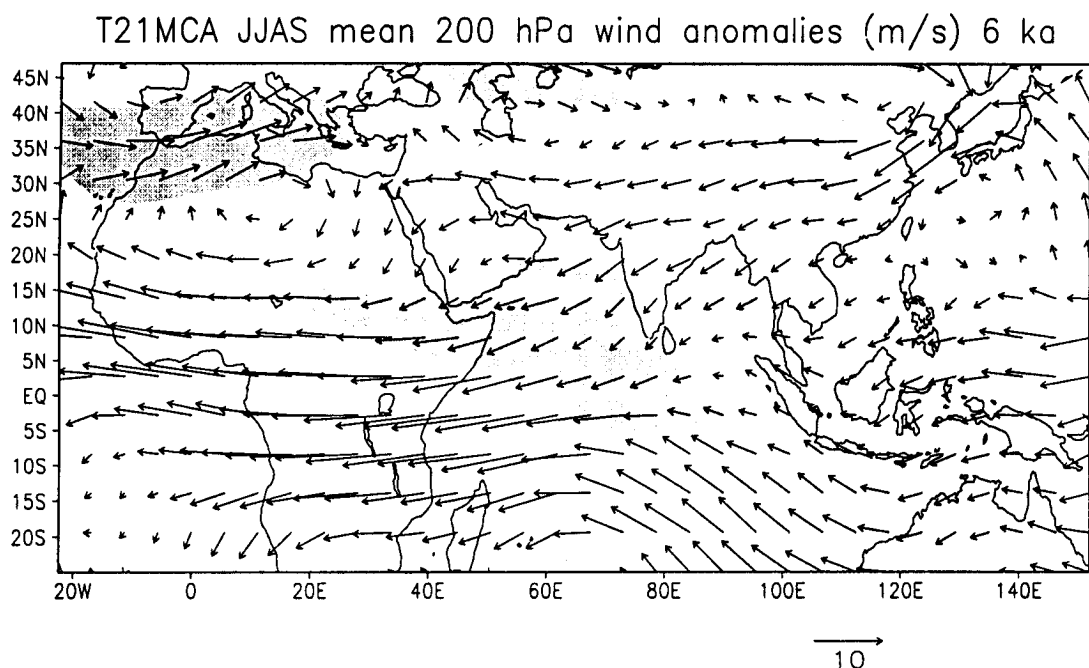


Fig. 4.5 JJAS composites of 6 ka 200 hPa wind anomalies simulated by T21MCA.

However, the lake data indicate changes of intermediate(high) level over north-west India (southwest Tibet and China) indicating that the expansion of the monsoon rainbelt is mainly in the northeastward direction. The lake level data also appears to indicate east-west gradient in moisture balance over China, with evidence of some lake levels being dry or no change (wet or high) from their present level in eastern (Southwestern) China during 6 ka (Qin and Yu 1998 and references listed there). T21MCA does not capture these features of P-E changes. However, T21MFX appear to capture the direction of changes fairly well (Fig 3.4). Thus geographic pattern of seasonal mean P and P-E anomalies is influenced by the model present day pattern of these quantities. It also indicates that the Indian and north African summer monsoons show different sensitivities to orbital forcing. Monsoon being stronger over India due to the typical shape of the subcontinent bringing it into proximity to ocean, and presence of high elevation Tibetan orography to the north (Webster et al 1998). Thus once the monsoon onset takes place over India, moisture feedbacks together with enhanced land sea thermal contrast gives rise to

stronger monsoon circulation and precipitation zone extends to as north as 30°N. Over northern Africa, the precipitation zone is close to ITCZ over the oceans and confined to equatorial northern Africa for the present day. Many AGCM sensitivity studies show that northward penetration of rainbelt takes place over northern Africa when realistic vegetation of 6 ka is prescribed in the model (e.g., Texier et al 2000). Thus the sensitivity of the north African monsoon is generally weak compared to the Indian monsoon for 6 ka summer insolation changes.

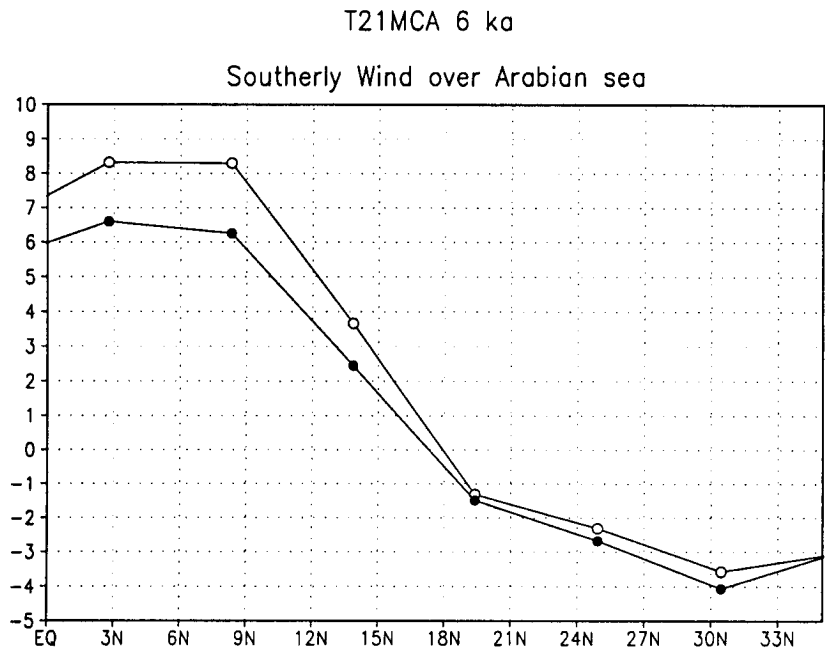


Fig. 4.6 T21MCA 850 hPa meridional wind averaged over Arabian sea sector (45-65°E). Legends: filled circle for 0 ka, and open circle for 6 ka.

850 hPa wind also shows increase over the Indian monsoon region, equatorial northern Africa, and China consistent with increase in P and P-E over these regions except over northern Africa where there is a small increase in P and P-E. 200 hPa wind also shows increase in anticyclonic circulation (Fig 4.5), and a slight southward displacement of the southern hemisphere subtropical westerlies over Africa. Otherwise there is not much change in the overall pattern from the present

day. Noting that the present day simulation of the TEJ and the precipitation pattern is poor in T21MCA, the actual extent and influence of the monsoon simulated for 6 ka by the T21MCA also appears to be underestimated consistent with the spatial pattern of P-E anomalies.

As the monsoon trough itself appears to be over the oceanic region the northward displacement of mean TCZ as inferred from the latitude of confluence of meridional wind over the Arabian sea is also smaller compared to that of T21MFX (Figs 3.6 and 4.6). Thus unlike CCM0 and CCM1 simulations (Qin et al 1998), which show some northward displacement of the mean TCZ in the Indian region relative to the present, T21MCA does not show any significant displacement. Rather, the precipitation increase appears to be there over the entire Indian subcontinent including southern tip of Indian peninsula. However, such a northward displacement is there and quite strong compared to T21MFX over the southeast China due to the fact that the control precipitation zone is centered around this region. Thus T21MCA and T21MFX differ quite significantly in the geographical features of the anomalies.

4.3.2 Anomalies in monsoonal indices

The anomalies in monsoon indices simulated by T21MCA are given in Table 4.2. Note that the anomalies are quite high compared to those of T21MFX in terms of percentage change. However, qualitatively the nature of response is the same for T21MCA and T21MFX. As in T21MFX, the most sensitive index is MHI. Thus the mechanism behind the increase in monsoon strength is the same for both T21MCA and T21MFX i.e., increase in meridional Hadley circulation driven by changes in land sea thermal contrast. It is to be noted that the overall circulation of the monsoon is weaker in T21MCA than T21MFX in the control run. However, the sensitivities are higher for T21MCA than for T21MFX. Thus differences in convection parameterizations can partly explain the discrepancies in the model sensitivities in

intermodel comparisons. The monsoon is a highly non-linear system with a number of feedback processes modulating it and the interaction between sub-models such as the interaction between cumulus convection, cloud determination and radiation could be very different when one of the sub-models is changed, leading to differing simulations.

Table 4.2 Anomalies (6 ka-Present) in monsoon indices. Values in parenthesis indicate percentage deviations from the control run. These anomalies are statistically significant to a confidence level of > 99%.

Monsoon Index	T21MCA	T21MFX
PI (hPa)	1.37(133)	1.5(27.7)
P (mm/day)	1.5(27.7)	0.95(11.6)
P-E (mm/day)	1.0(66.6)	0.85(22.4)
CI (W/m^2)	-10(-4.2)	-11.5(-4.8)
MHI (m/s)	2.02(354)	1.6(43.2)
WSI (m/s)	10.4(67.5)	0.6(1.8)
SSI (m/s)	5.3(72.6)	1.0(7.4)

Another feature to notice is that increase in PI and MHI are an order of magnitude higher (in terms of percentage changes) in T21MCA than T21MFX. Thus the sensitivities of these quantities are more subtle in T21MFX than in T21MCA. Noting that the meridional Hadley circulation associated with the monsoon can be affected by various factors such as Eurasian snow cover, it is important to examine this aspect in detail in intermodel comparisons of 6 ka simulations. It is quite possible that as there is significant precipitation over the land regions of southern Asia in T21MFX as compared to T21MCA, cloud radiative feedbacks may reduce the 6 ka heating anomalies and hence land sea thermal contrast to a certain extent. In T21MCA, due to lack of precipitation over land, the radiative heating of the land surface and hence the increase in land sea thermal contrast relative to the present day is higher compared to T21MFX, even though the spatial extent of P and P-E increase is actually less compared to T21MFX.

4.3.3 Seasonal transitions

There are considerable fluctuations in the onset, number of active and break phases, and withdrawal from year to year in the three year simulations, making the seasonal transition of the monsoon also to vary from year to year for both the present day and 6 ka simulations of T21MCA. However, seasonal transition of P and P-E clearly show increase during the established phase of the monsoon (mainly during July and August). Fig 4.7 shows average time series (from June beginning to end of September) of P and P-E averaged over the Indian region from the three summers simulated by the model for the present day (0 ka), and 6 ka. The figure clearly shows that the monsoon onset phase (June) is marked by increase of P, followed by established phase where P reaches maximum (July and August), and withdrawal phase (September) where P decreases. The same pattern is simulated for 6 ka also, with notable increase during established phase. Both P and P-E seasonal transitions are similar indicating that the changes in P-E are mainly brought about by changes in P in this region.

Seasonal transition of the monsoon is also illustrated by using atmospheric kinetic energy at 850 and 200 hPa averaged over the region 40-90°E, 5-20°N where the lower and upper level winds which are characteristic features of the Indian monsoon circulation exhibit distinct seasonal transitions as seen in observations (Ju and Slingo 1995, Soman et al 1994, Dong et al 1996). The onset of the monsoon is marked by transition of low level easterly winds to westerly and upper level westerly winds to easterly in this region. The withdrawal is characterized by features opposite of the onset. As the monsoon circulation intensifies during the onset the 850 and 200 hPa kinetic energy shows increasing trend, reaches maximum during established phase, and begins to decrease during withdrawal phase (September). The time series of atmospheric kinetic energy at 850 and 200 hPa averaged over this region constructed from the averages of three model simulated time series of the summer season of T21MCA 0 and 6 ka simulations are shown in Fig 4.9. The increase of this quantity is seen mainly during the established phase

of the monsoon and the basic evolution characteristics remain similar for both the present day and 6 ka and exhibit similar characteristics of P and P-E. However, compared to T21MFX, the time evolution of atmospheric kinetic energy is quite smooth for 6 ka. In T21MFX, there is a rapid decrease from the beginning of August for 6 ka (Fig 3.11). However, both T21MFX and T21MCA, show a distinct change in atmospheric kinetic energy for 6 and 115 ka relative to the present while the changes are relatively small in CCM2 T42. Thus over the Indian region, both T21MFX and T21MCA show more increase in monsoon strength than T42MFX as also seen from P and P-E indices.

Surface latent heat flux which depends on the surface air temperature and soil moisture also shows similar seasonal transition as that of P and P-E (Fig 4.8). As the season progresses, this quantity increases, indicating that as the monsoon strengthens, surface moisture increases, which in turn lead to increase in surface evaporation and hence latent heat flux. This contributes to the moist static energy of the atmosphere resulting in increased convective activity and intensifies the monsoon circulation (e.g. Webster et al 1998). Hence a major factor responsible for the strengthening of the Indian monsoon of 6 ka relative to the present is intensification of soil moisture feedbacks. Due to relatively more surface moisture during 6 ka, the surface sensible heat flux shows a seasonal transition opposite of the surface latent heat flux (Fig 4.8). As the seasonal transition of latent heat flux is similar to that of P and P-E, soil moisture changes during 6 ka increases mainly due to increase in P over this region.

It is important to note that, in the absence of interactive surface hydrology, the evolution of P, P-E, surface latent and sensible heat flux would have been different and the present day prescribed soil moisture would hold a greater influence on the model sensitivity. For instance Jagadheesha et al (1999) show that when CCM2 AGCM is run in perpetual July mode, the model sensitivities to orbital parameter changes are constrained by the model present day surface reaching solar radiation and latent heat flux. Thus in the absence of interactive hydrology,

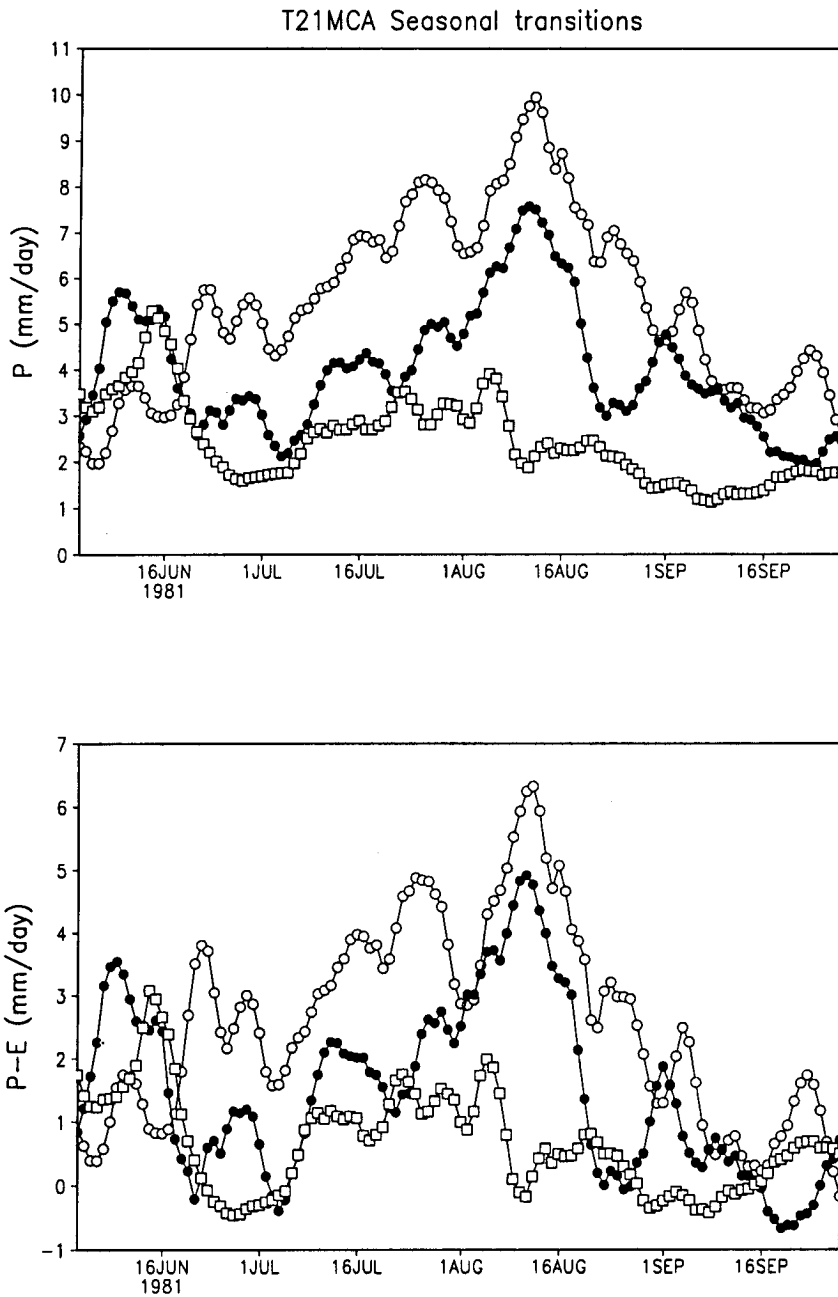


Fig. 4.7 Seasonal transition of P and $P-E$ averaged over India (5 day running mean is plotted so as to smooth the data). Legends: Filled circle - Present, Open circle - 6 ka, open square - 115 ka. Ignore the year tag on time axis.

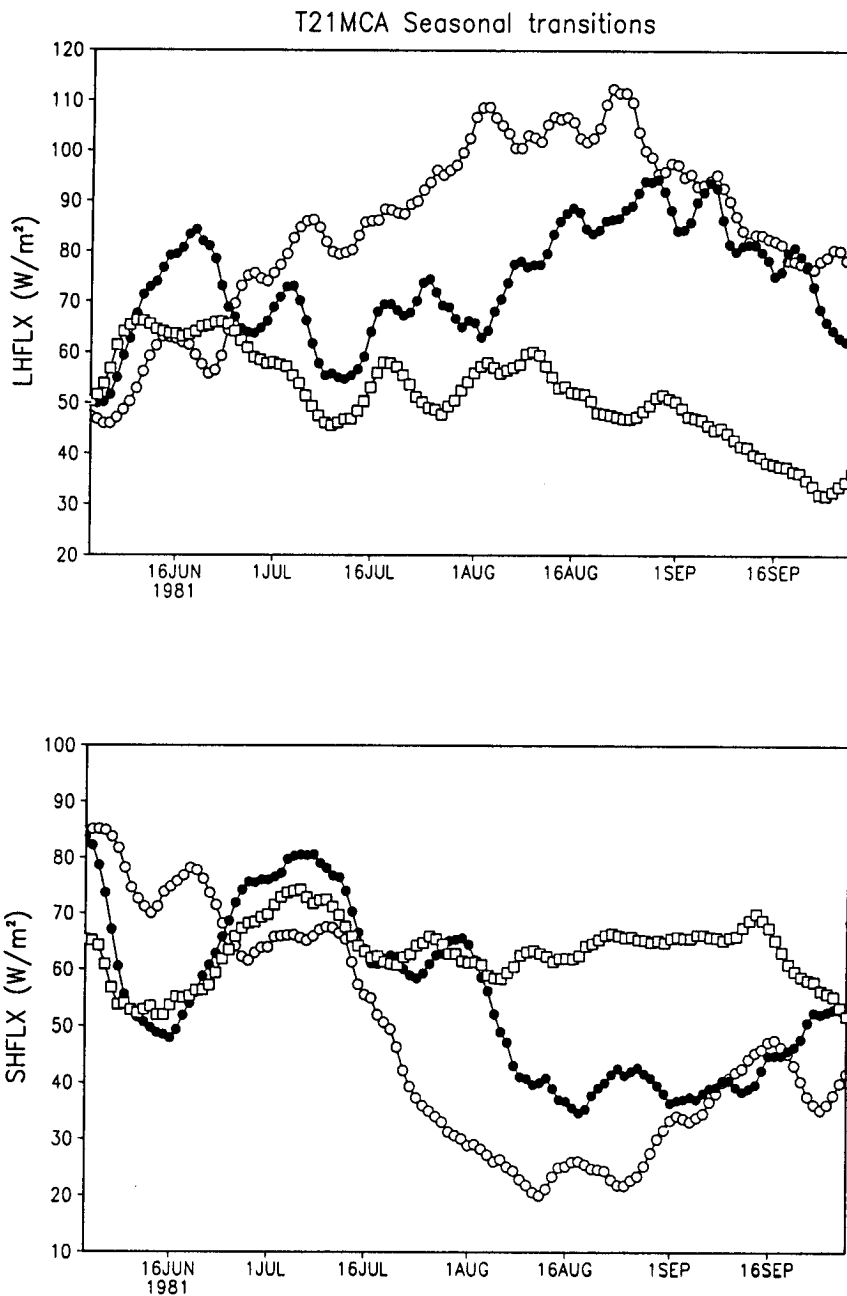


Fig. 4.8 Same as Fig 4.7 except for surface latent and sensible heat fluxes (LHFLX and SHFLX).

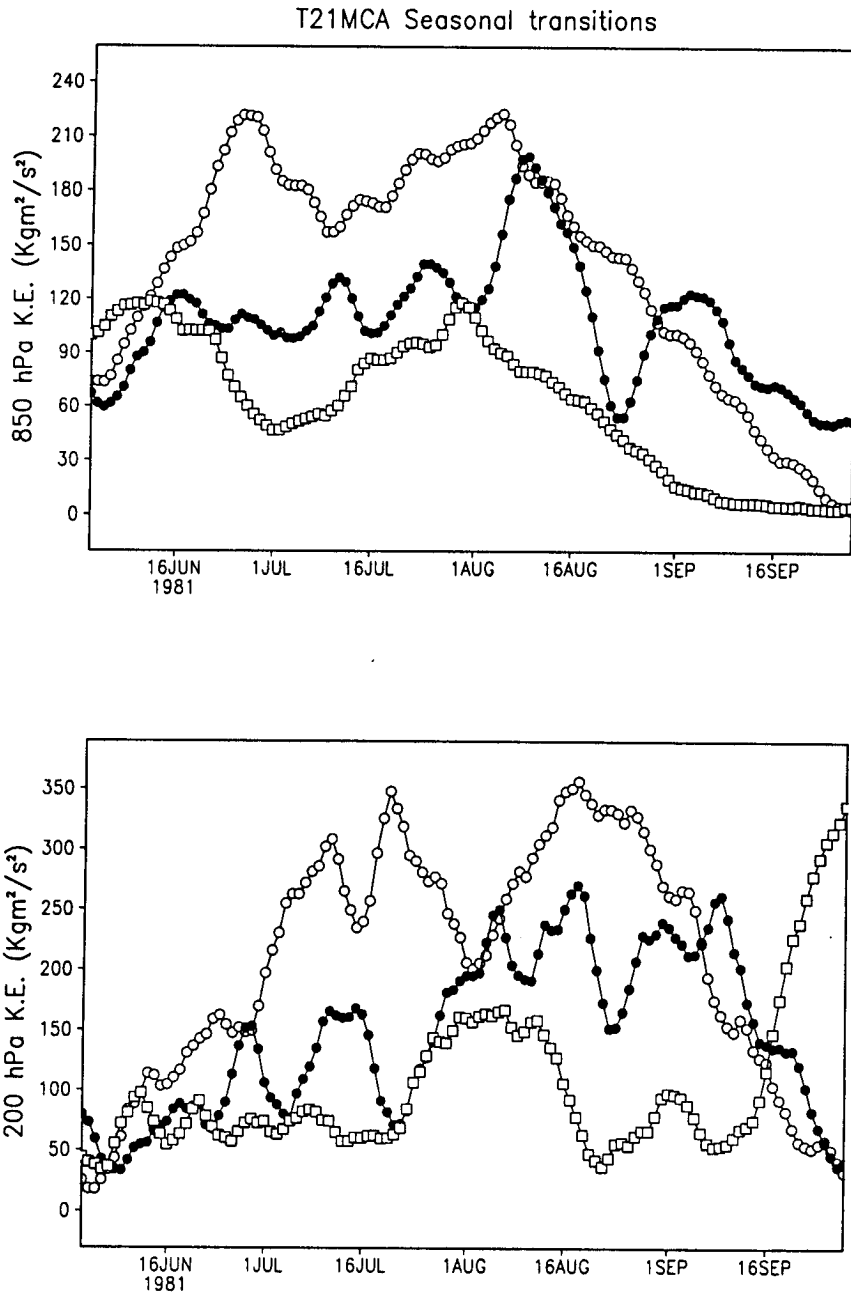


Fig. 4.9 Same as Fig 4.8 except for 850 and 200 hPa atmospheric kinetic energy averaged over 45-90°E 5-15°N.

it appears that the sensitivities are mainly influenced by the control surface absorbed solar radiation and latent heat flux resulting in asymmetry (i.e., the model which more(less) sensitive to increase(decrease) in summer insolation relative to another model which is less(more) sensitive to increase(decrease) in insolation) in

the model sensitivities. However, when interactive hydrology is incorporated, this asymmetry tends to reduce on a large scale as we have seen in chapter 3.

Fig 4.10 shows a bar chart of daily precipitation rates averaged over central India (15-30°N, 70-85°E). Active-break phases of the monsoon can be clearly noticed in this figure. Relative to the present day, the duration of the active phase increases for 6 ka similar to T21MCA results described in chapter 3 (Fig 3.14). The range of precipitation rates does not change, but the frequency of medium to high precipitation rates increases resulting in enhancement of the duration of active phase during 6 ka. These results are similar to the one of T21MCA and other studies (e.g. deNoblet et al 1996).

In summary, qualitatively the seasonal transition of the monsoon related parameters such as P, P-E, etc., show a similar evolution in T21MCA as in T21MFX, except for the fact that, the withdrawal of monsoon during 6 ka is more abrupt in T21MFX than T21MCA. This may be one of the reasons for increased sensitivity of monsoonal indices in T21MCA, than T21MFX (Table 4.2). As the season progresses, the soil moisture increases resulting in increased surface latent heat flux, monsoon circulation, P, P-E, and reduced sensible heat over the Indian region. Thus soil moisture feedbacks contribute to increase in monsoon strength during the established phase of the monsoon. The duration of the active phase of the monsoon also increases as compared to the present day.

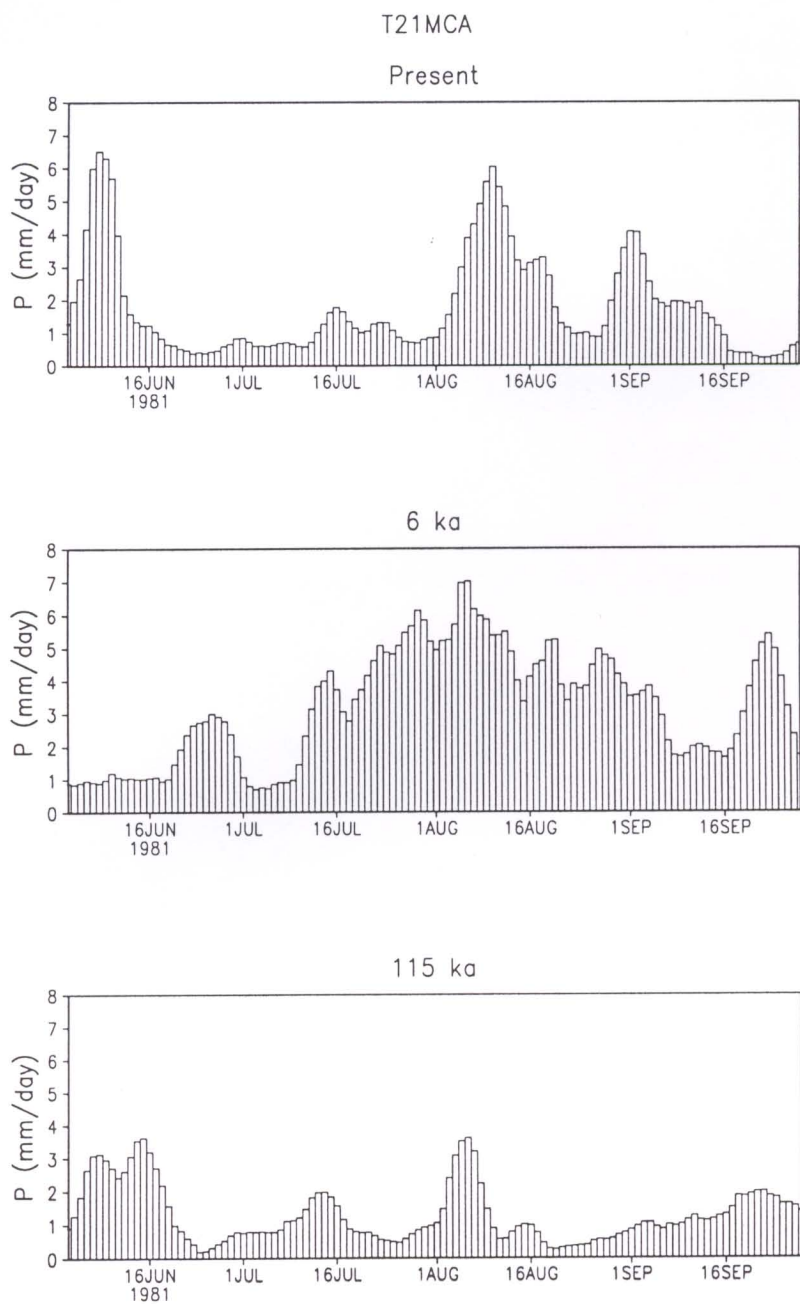


Fig. 4.10 Bar chart of daily precipitation averaged over central India simulated by T21MCA.

4.4 115 ka results

In this section we describe 115 ka anomalies simulated by T21MCA.

4.4.1 Geographical features

The precipitation anomalies for 115 ka are centered around the control rainbelt. Even though there are significant differences in the spatial pattern between T21MFX and T21MCA, the direction of changes are largely similar over the Indian ocean region, indicative of similar mechanism behind the changes (Fig 4.11). In both T21MFX and T21MCA, there is increase of precipitation in the southeastward direction over China, and southwestward increase over India. However, there is an increase in maximum precipitation rate for 115 ka in T21MFX, over the Indo-Pacific warm pool, whereas there is a decrease for T21MCA as most of the precipitation appears to be over Indo-Pacific warm pool in the control. Strength of the low level circulation over the Indian monsoon region also decreases consistent with decrease in precipitation. The decrease in the wind speed is simulated over entire Indian peninsula covering a broad region of Indian ocean (Fig 4.11). However, decrease in wind speed is mainly confined to the Indian region in T21MCA, whereas it covers region of equatorial northern Africa in T21MFX. It is expected as the influence of monsoon circulation is confined to Indian ocean region in T21MCA. The TEJ strength almost diminishes and subtropical westerlies dominate as far as $\sim 15^{\circ}\text{N}$ over northern Africa whereas in T21MFX, the decrease is not as prominent as that of T21MCA (Fig 4.13). This is due to the weak 200 hPa TEJ of T21MCA in the control relative to the present. The 850 hPa meridional wind averaged over Arabian sea which is used to infer the latitude of mean TCZ shows that it does not change for 115 ka in T21MCA, whereas there is some $\sim 5^{\circ}$ southward displacement in latitude is simulated by T21MFX (Figs 3.18 and 4.12).

Eolian evidence for the tropical Africa indicates that monsoon decreased over north of the equator while south of the equator the conditions were moist

during 115 ka (Pokras and Mix 1985) consistent with the geographic pattern of P and P-E changes simulated by T21MCA.

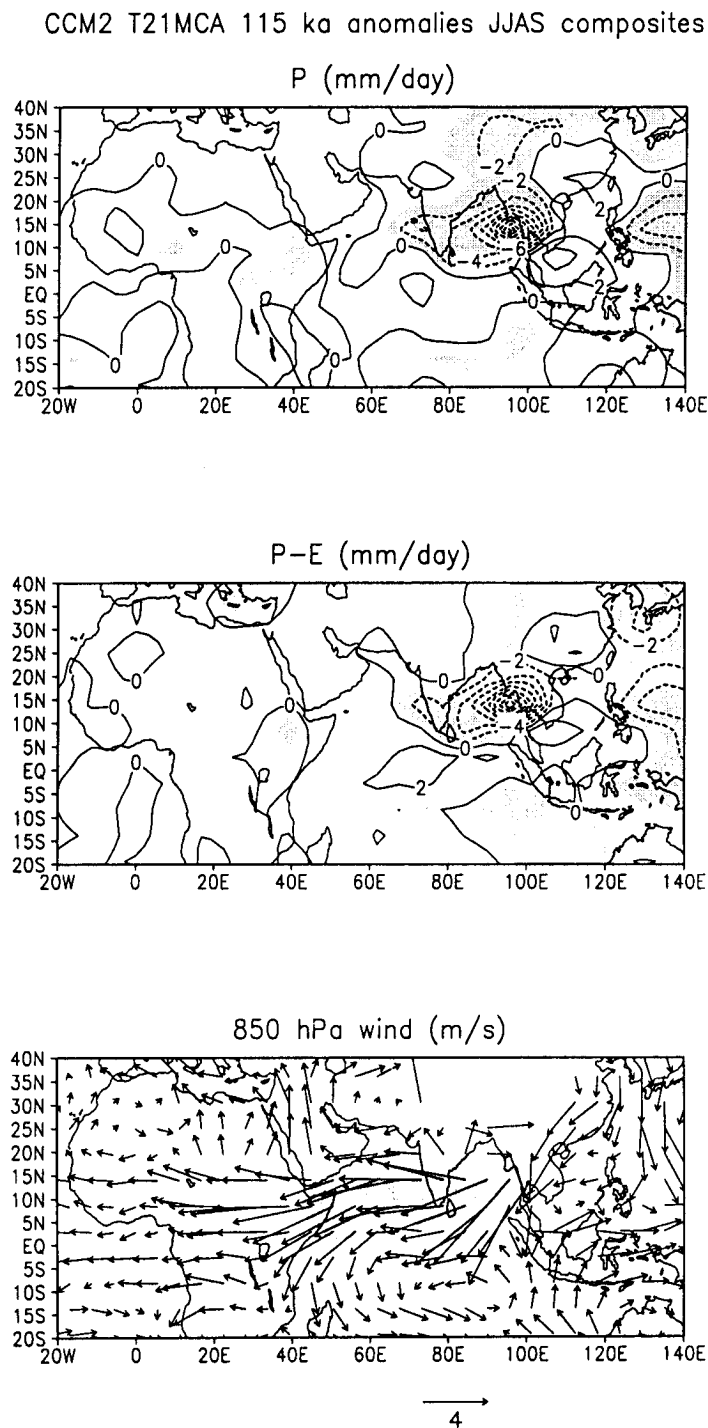


Fig. 4.11 JJAS composites of 115 ka P, P-E, and 850 hPa wind anomalies simulated by T21MCA.

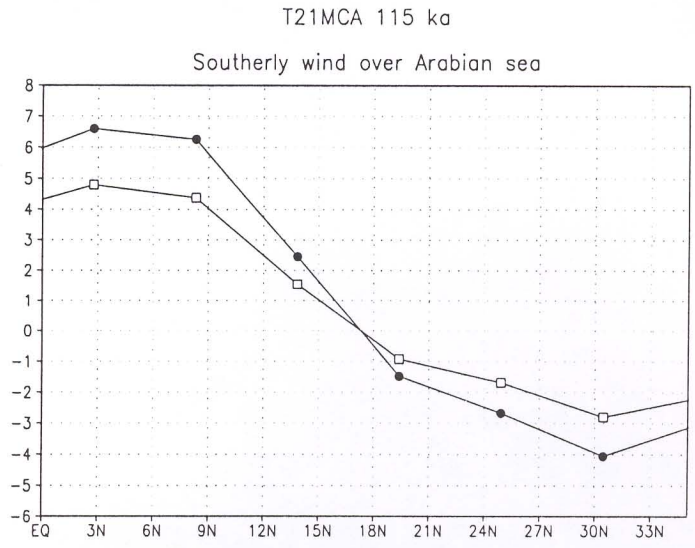


Fig. 4.12 T21MCA 850 hPa meridional wind averaged over Arabian sea sector (45-65°E). Legends: filled circle for 0 ka, and open square for 115 ka.

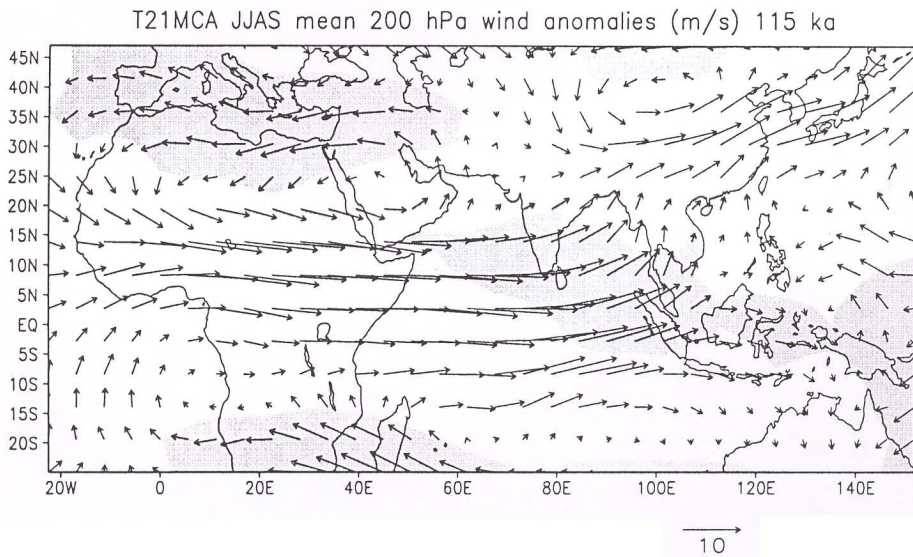


Fig. 4.13 T21MCA 200 hPa wind anomalies (m/s). Shaded areas denote anomalies < 2 m/s.

4.4.2 Anomalies in monsoonal indices

Anomalies in monsoonal indices for T21MCA 115 ka simulations are given in Table 4.3. All the monsoonal indices indicate decrease of monsoon strength. There are many similarities in qualitative sense with T21MFX sensitivities. Most sensitive index in both T21MCA and T21MFX is MHI. In terms of percentage change, the sensitivities of PI, MHI, WSI, and SSI are quite high in T21MCA compared to T21MFX. However, P and P-E changes are slightly less in T21MCA compared to T21MFX. This is due to the fact that these quantities are averaged over land areas only and as the P and P-E are less over land in the T21MCA control relative to observations and T21MFX. Thus, even though there appears to be a drastic reduction in monsoon circulation in T21MCA relative to T21MFX, simulated changes in P and P-E are broadly similar.

Table 4.3 Anomalies (115 ka-Present) in monsoon indices. Values in parenthesis indicate percentage deviations from the control run. These anomalies are statistically significant to a confidence level of $> 99\%$.

Monsoon Index	T21MCA	T21MFX
PI (hPa)	-2.68(-260)	-3.8(-70)
P (mm/day)	-1.4(-36)	-4(-48.8)
P-E (mm/day)	-0.8(-53)	-2.3(-60.5)
CI (W/m^2)	22(9.2)	4.6(2)
MHI (m/s)	-3.28(-575)	-3.5(-95)
WSI (m/s)	-8.1(-52.6)	-9.9(-30.8)
SSI (m/s)	-5.53(-73.7)	-7.3(-54)

As MHI and PI are the indices that are most sensitive in T21MCA, the mechanism behind the changes are associated with the reduction in meridional Hadley circulation and change in land-sea thermal contrast. Hence although MHI, and PI changes are more in T21MCA than T21MFX, these indices have a small influence

on P and P-E changes in T21MCA than in T21MFX.

4.4.3 Seasonal transitions

The seasonal transition of P, P-E, 850 and 200 hPa atmospheric energy, surface latent, and sensible heat fluxes show the features that are broadly opposite of 6 ka. The average summer time series (1 June to 30 September) of these quantities for 115 ka are shown in Figs 4.7 to 4.9 together with those of 0 and 6 ka simulations of T21MCA. P and P-E show a large decrease during the established phase of the monsoon relative to the present. As the monsoon progresses, there is a reduction in the intensity of the monsoon circulation brought about by reduction in the land-sea thermal contrast, modulated by soil moisture feedbacks.

Atmospheric kinetic energy also decreases during the established and withdrawal phases of the monsoon. Compared to T21MFX, the decrease of this quantity is more noticeable at 850 hPa. However, there is a gradual decrease of this quantity during withdrawal, a feature observed in T21MFX simulations also. Thus the change in this quantity is more subtle in T21MFX and T42 simulations described in chapter 3.

Latent heating decreases relative to the present mainly during July and August, and is of comparable magnitude during onset and withdrawal. Sensible heating shows evolution features opposite of that of the latent heat flux. Thus soil moisture feedbacks also contribute to decrease in the monsoon circulation. Time evolution of these quantities are broadly same as that of T21MFX.

While these features are qualitatively similar with other AGCMs (e.g. Dong et al 1996), there are notable differences. For instance, Dong et al reports that the highest kinetic energy during the established phase is simulated for 115 ka orbital parameters and the changes are relatively less compared to T21MCA. In chapter 3, we noticed that T42 also simulates a more subtle change in this quantity though

highest kinetic energy is simulated for 6 ka. Thus it is likely that the seasonal evolution of these quantities are horizontal resolution dependent. These differences between the AGCMs may also be related to differences in the precipitation anomalies in this region. However, no spatially coherent palaeoclimatic evidences exists in order to verify model simulated changes over this region. Geographical pattern of changes indicate that P, and P-E anomalies are of opposite sign over this region compared to northern boundary of the monsoon for 6 and 115 ka. The resulting heating anomalies can offset the increase or decrease in 850 hPa atmospheric kinetic energy brought about by increase or decrease of land-sea thermal contrast to a certain extent in this region. Also the length of the model durations reported in Dong et al (1996) is higher than our study and may be one of the reasons for these discrepancies.

Daily precipitation rates averaged over central India (Fig 4.10) show that the precipitation rates are reduced relative to the present day. However, active-break phases are still noticeable. Thus the reduction in seasonal mean precipitation is mainly due to the decrease in daily precipitation rates and the duration of the active-break phases appears to be comparable to that of the present day.

4.5 Concluding Remarks

The sensitivity of T21MCA to changes in orbital parameters are broadly similar to that of T21MFX in some respects. Qualitatively the nature of changes are similar at both T21MCA and T21MFX. The spatial pattern of changes are strongly influenced by the control climate. Both T21MFX and T21MCA show that the role of soil moisture feedbacks in determining the Indian monsoon strength to changes in summer insolation is stronger than that of the north African monsoon. Over northern Africa, this feedback is weak and hence the P and P-E sensitivity to insolation changes are quite dependent on the control precipitation.

However, there are notable differences between T21MFX and T21MCA sensitivities especially from the circulation perspective. Major differences are

- (1) The overall sensitivity of T21MFX is smaller than T21MCA in many respects. For instance change in PI and MHI are an order of magnitude higher (in terms of percentage change) than other monsoon indices in T21MCA. T21MFX simulates relatively small changes in these quantities compared to T21MCA.
- (2) The spatial pattern of P and P-E anomalies better compare with the spatial pattern of lake level changes for 6 ka in T21MFX than T21MCA over regions influenced by the Indian monsoon. T21MFX simulates relatively drier conditions over northeastern China, and wetter conditions over southwest China, northwest India, and northern and eastern Africa, and Arabia broadly in agreement with the lake status data over these regions. T21MCA fails to simulate increase in P-E over northern Africa, and decrease over northeast China. While T21MFX simulates some decrease in P-E over southern tip of Indian peninsula, T21MCA simulates decrease in P and P-E over a broad area from southeast China to southern tip of India.
- (3) Unlike CCM0 and CCM1 sensitivities (Qin et al 1998), T21MCA sensitivities are quite small over northern Africa as well as the northern boundary of the Asian monsoon. Thus the sensitivity due to MCA scheme reduces in terms of simulating P and P-E changes while it increases in terms of circulation changes. Thus the spatial pattern of P and P-E, in the control simulation plays an important role in determining the large scale model sensitivity.

Thus CCM0 and CCM1 sensitivities are higher than T21MFX sensitivities for 6 ka partly because of the use of different convection parameterizations and partly due to other parameterizations (e.g. cloud radiative effects) also. Though spatially coherent palaeo-indicators over the northern boundary of the Indian monsoon in qualitative terms are available, they are by no means comparable to model sensitivities in quantitative terms as yet. However, noting that the T21MFX better simulates the monsoon circulation features than T21MCA and gives somewhat

better geographical pattern of P-E changes as inferred from lake level changes, T21MFX may be regarded as better in simulating Indian monsoon changes compared to T21MCA. It is also to be noted that the model sensitivities are dependent on the simulation of the present day monsoon and hence a critical analysis of the model's ability to simulate the present day monsoon will also be helpful in ascertaining the role of other factors such as vegetation, SSTs, etc. on the monsoon sensitivity at various geographical changes. Within the Indian monsoon region, the monsoon changes are quite strong as inferred from model simulations. Over the north African region, AGCM sensitivities could be unreliable, in certain cases, where the model overestimates the control precipitation and its northward extent. Nevertheless, it has been shown that majority of existing AGCMs fail to simulate the northward extent of the north African water balance changes as inferred from palaeo-lake level changes (Joussaume et al 1999). Further analysis of the model sensitivities taking into account the model's ability to simulate the present day monsoon from circulation as well as hydrological perspective will be required to evaluate the model performances as well as palaeo-monsoon changes of the recent past. In particular it will be interesting to know whether the AGCMs which simulate the present day Indian monsoon better, perform better for palaeoclimate cases. What is the impact of biases in the model present day simulation with respect to observations on the model palaeomonsoon sensitivities? Examination of these aspects may be helpful in knowing the possible role of additional boundary forcings of vegetation, SSTs etc.

Summary, conclusions and future directions

5.1 Summary and conclusions

The monsoon over India is primarily driven by land-ocean temperature contrast and hence is expected to be influenced by changes in seasonal insolation, as shown by previous modelling studies. However, there is quite a number of changes in AGCM formulation and many of the current AGCMs show sensitivities that are quite small on a large scale when compared to previous versions. Are the changes in model sensitivities due to changes in physical parameterizations, or horizontal resolution or both? In order to obtain some inference on these model dependent factors and their role in determining the model monsoon sensitivity, we did some sensitivity experiments using CCM2 AGCM described in previous chapters.

We used CCM2 AGCM with T42(high) and T21(low) horizontal resolutions. The standard version of CCM2 described chapter 2 simulates many aspects of the present day monsoon at both the resolutions. There are some systematic differences between the two resolutions. On a large scale both the resolutions overestimate the monsoon strength as inferred from pressure index. T42 is closer to observations in pressure index. Both the resolutions indicate that the model underestimates the precipitation associated with the Bay of Bengal trough. Both the resolutions fail to simulate the rainshadow effect of the western ghats, the secondary precipitation belt over the southern equatorial Indian ocean, and distinction between

the Pacific warm pool precipitation and monsoon precipitation seen in observations. Also, there is too much precipitation on the southern planks of the eastern Tibetan plateau and southern peninsula, Indonesian warm pool region, giving a typical horse-shoe like spatial pattern at both the resolutions. 850 hPa southwestlies extend too far eastward compared to observations at both the resolutions. Zonal extent of 200 hPa winds are underestimated at both the resolutions relative to the NCEP reanalysis. Thus there are significant differences in between the observations and the model, in geographical pattern of monsoon circulation and precipitation. However monsoon indices which are used to quantify the model monsoon, show many features similar to observations. For instance, the order of magnitude of the model simulated and NCEP reanalysis monsoon indices are close to each other. Zonal wind shears are higher than the meridional wind shears in both the observations as well as the model. Hence eventhough the model geographical pattern of precipitation is significantly different from the NCEP reanalysis, the quantification using monsoonal indices indicate that the model monsoon is representative of the observed monsoon atleast from circulation perspective and can be used in palaeoclimate modelling studies.

In a previous study we found that the low resolution (R15) is more (less) sensitive to increase (decrease) in insolation relative to high resolution (T42). However, there are certain limitations in this study such as the model was integrated in perpetual July mode with fixed surface hydrology. Noting these limitations, the differences in the sensitivities between the two resolutions was traced to be due to the differences in the present day latent heat flux and net surface reaching solar radiation between the two horizontal resolutions. In order to verify whether such a difference in the sensitivities between the two resolutions exists when the model used with interactive hydrology and in annual cycle mode, we performed annual cycle integrations incorporating interactive surface hydrology with CCM2 at T42 and T21 horizontal resolutions, for 6 and 115 ka orbital parameters and examined the sensitivities relative to the model control (the present day) simulations

at the two resolutions. It was found that T21 simulated monsoon indices are relatively higher compared to T42 for the present day. However, the geographical pattern of P, P-E, and 850 hPa wind showed higher sensitivity at T42 than T21 for both increase and decrease of summer insolation relative to the present day. Over northern Africa, both the resolutions fail to simulate the northward penetration of rainbelt for 6 ka. However, both the resolutions show increase (decrease) in precipitation southward (northward) of the control precipitation zone. On a large scale, monsoon circulation is more sensitive to 6 and 115 ka summer insolation anomalies relative to present at T42 than T21. Over Indian region, T21 is relatively more sensitive in terms of changes in P, P-E, and SSI than T42 indicative of the fact that the regional pattern of P and P-E in the control simulation can still play an important role in determining the model monsoon sensitivity. When compared to qualitative indices of lake level change over the regions influenced by the Indian monsoon region, both the resolutions simulated the direction of the changes fairly well. The lake level data indicate east-west moisture gradients over northern China, with western part being under the influence of Indian monsoon experiencing wetter conditions and eastern part being relatively dry. These features as inferred from lake level changes are captured relatively well at T42 than T21. Examination of subseasonal evolution of P, P-E, latent and sensible heat fluxes revealed that both the resolutions show increased sensitivity during the established phase of the monsoon and the soil moisture feedbacks modulate the changes in monsoon strength brought about by insolation changes. It was found that as the season progresses the soil moisture and hence surface latent heat flux increases while sensible heat flux decreases for 6 ka summer and the opposite takes place for 115 ka summer as compared to the present day. Thus insolation induced changes in land-ocean thermal contrast change the monsoon strength which affect soil moisture which in turn feedback on the monsoon. Both the resolutions show enhanced soil moisture over the Indian region and there was a clear indication of increase of P and P-E for 6 ka summer insolation changes. However, over northern Africa, both the resolutions fail to simulate the increase of P-E north of 10°N as inferred from palaeo-lake level

data. The reason for the different sensitivities of the Indian and north African monsoon lies in the factors that determine their strength. The Indian monsoon extends as north as 35°N and is quite strong in terms of circulation as well as precipitation when compared to any other region experiencing the monsoon type climate due to the role of Tibetan plateau as an elevated source of heat during summer, and typical peninsular shape of the continent surrounded by ocean (e.g., Webster et al 1998, deNoblet et al 1996). However, the north African monsoon resembles more like the ITCZ over the ocean and is of limited latitudinal extent. Many recent AGCM studies have shown that the north African monsoon simulation requires a vegetation component which interacts with the atmosphere (e.g. Texier et al 2000). Thus our study shows that the horizontal resolution while has certain impact on the simulated spatial features and large scale monsoon indices, there is no major discrepancy in terms of mechanism of changes in monsoon circulation. The systematic differences between the two resolutions seem to be similar to that of earlier studies of resolution dependence of climate sensitivity (Rind 1988). Thus our results on the horizontal resolution dependence of sensitivity may be summarized as

- The high resolution is relatively more sensitive to insolation changes than the low resolution on a large scale. However, there are regional discrepancies over the Indian region, where the control precipitation pattern can play an important role in determining the model monsoon sensitivity. Over north African monsoon region, despite the low resolution control P, and P-E being higher, the sensitivities are lower compared to high resolution to summer insolation increase. Thus interactive surface hydrology significantly alters the model sensitivity over the north African region.
- The sensitivity over north African region at both the resolutions is lower compared to previous modelling results which use AGCMs in perpetual July mode with fixed hydrology as well as AGCMs with a slab mixed layer ocean model. In the case when the model is used with perpetual July mode, the

sensitivities are highly dependent on the model control simulation of P and P-E.

- Our results suggest that the intermodel differences in the sensitivities are more likely to be due to differences in physical parameterizations than on the horizontal resolution. Provided a model with almost similar physical parameterizations, then the results may show a dependence on horizontal resolution as inferred from this study.
- We have also found that the model control precipitation pattern can affect the regional scale sensitivity such as the Indian monsoon region. Hence model intercomparison projects and comparison with palaeo-data should in some way be constrained by the model's ability to simulate the present day climate over these regions where intermodel sensitivities show a strong dependence on the control climate. This could lead to better data-model comparison schemes.
- On a large scale the mechanism of monsoon changes are similar at both the resolutions, i.e., both the resolutions show a strengthening or weakening of meridional Hadley circulation associated with the monsoon circulation to changes in summer insolation.
- Over the Indian monsoon region there are features such as latitudinal displacement of mean TCZ as inferred from the latitude of confluence of meridional wind over the Arabian sea. This appears to lead to a decrease(increase) of P and P-E over southern tip of India during 6(115) ka summer. These features are yet to be verified from palaeo-data. This suggests a possibility that palaeo-monsoon indicators over different regions influenced by the Indian monsoon may not show a coherent change in monsoon strength and there will be a certain phase difference in the monsoon evolution over these regions. Palaeo-data are yet to provide constraints on these aspects of model sensitivities.

- Subseasonal variation of atmospheric kinetic energy averaged over the region where monsoon westerlies are strong at lower and upper levels indicated increase during the established phase of the monsoon for 6 ka and decrease for 115 ka. T42 showed smaller differences between this quantity among the present, 6 and 115 ka simulations. A recent study by Dong et al (1996) showed that this quantity reaches its maximum the monsoon season for 115 ka and the for the glacial boundary conditions of LGM this quantity was very small. However, our results indicate that there is a clear decrease in this quantity for 115 ka. These results may be dependent on the length of the model integrations also.

In order to infer the impact of moist convective adjustment (MCA) convection parameterization of Manabe(1969) previously used in many AGCM sensitivity studies we did simulations for the present day, 6 and 115 ka orbital parameters using MCA scheme. As convective latent heat release in the atmosphere plays an important role in driving the monsoon circulation, the convection parameterization can alter the monsoon sensitivity to a significant extent. The present day monsoon simulation using MCA scheme is weaker compared to the observations in many respects over India as well as northern Africa. Most of the precipitation is concentrated over the warm oceanic regions and there is not enough precipitation over the continental region. The low level monsoon westerlies extend too far eastward than the observations. Zonal extent of 200 hPa tropical easterly jet (TEJ) is also smaller compared to observations and there is not TEJ over equatorial northern Africa as inferred from observations and southern hemisphere subtropical westerlies extend too north compared to observations. Monsoon indices also suggest a weaker monsoon circulation. Thus the present day monsoon simulation with MCA scheme showed a weak, shallow, and localized monsoon circulation compared to observations similar to the one described in a sensitivity study by Zhang (1994). However, CCM0 and CCM1 simulations of the present day climate described in Hurrell et al (1993) show a significant precipitation and surface

westerlies are strong over northern Africa despite the fact that MCA scheme is used. Thus other parameterizations such as cloud radiative effects also play an important role in determining the overall strength of the monsoon. Nevertheless many characteristics such as far eastward extent of monsoon westerlies etc. are seen in those simulations also. For 6 ka orbital parameters, the sensitivity of the monsoon strength as inferred from the monsoon indices are more compared to the sensitivities of CCM2 T21 with a simple mass flux scheme (T21MFX) for moist convection parameterization. However, the geographical extent is very small compared to T21MFX. Over northern Africa, the sensitivities reduce further compared to T21MFX. Thus the previous sensitivity studies using CCM0 and CCM1 show increased monsoon strength over northern Africa due to the use of the model with the fixed soil hydrology in perpetual July mode and incorporation of slab mixed layer ocean model respectively. Also many features of the P-E changes such as east-west moisture gradient over northern China, are not captured. Thus even though the sensitivities seem to be higher in terms of circulation, the geographic extent of P and P-E still remain closer to the present day and as the present day simulation of the monsoon is poor, many palaeo-data inferred P-E changes are not captured. While T21MFX showed north-south displacement of mean TCZ, it is not evident with MCA scheme as the monsoon precipitation zone itself is centered around equatorial Indian ocean and southeast China. In summary

- With MCA scheme the model present day monsoon over India and northern Africa are weaker, shallow and localized over warm oceanic regions compared to observations. The sensitivities to 6 and 115 ka orbital parameters are higher than that of T21MFX in terms of monsoon indices. However, the geographical pattern of changes in P and P-E suggest that an underestimation as inferred from palaeo-data and there are significant discrepancies in spatial pattern too.

- Sensitivity over northern Africa is reduced compared to previous model sensitivity studies. This is due to the use of model in perpetual July mode with fixed hydrology and incorporation of mixed layer ocean model. Other parameterizations like cloud radiation parameterizations may also play an important role.
- Thus combination of MCA scheme together with the control precipitation pattern (which depends on other factors apart from convection parameterization) can lead to higher as well as lower sensitivities depending on the region.
- Unlike T21MFX, the atmospheric kinetic energy at lower and upper levels averaged over the Indian monsoon region where monsoon westerlies are quite strong, this simulation show a large differences among the control, 6 and 115 ka simulations indicating a more direct response to insolation changes. However, it is not clear if use of MCA scheme would have reduced the monsoon strength for LGM also to a great extent compared to T21MFX.

5.2 Future directions

With increasingly realistic simulation of the present day climate by AGCMs and also the grater spatial and temporal availability of the palaeo-monsoon data, a large number of sensitivity as well as simulation studies using AGCMs and more complete climate system models are required to model the mechanisms responsible for palaeomonsoon changes.

From the point of view of simulating of a particular time slice such as mid-Holocene and LGM, a large number of AGCM results are already done (e.g., Jousaume et al 1999). Our study shows a certain dependence of model sensitivities on the control simulation and physical parameterizations such as convection parameterizations. It would be useful to critically examine the model sensitivities from the intermodel comparisons in light of the model's ability to simulate all the aspects

of the present day monsoon apart from water balance change alone. For instance a model may simulate a fairly good precipitation pattern but poor in other aspects such as circulation features at upper level, the baroclinicity as inferred from observational reanalysis, etc. What is the impact on the model sensitivity? Also the model simulation of the present day monsoon is continually improving. A particular aspect is the intensity of hydrological cycle. There will be several attempts in improving the soil moisture and vegetation feedbacks and their impact is to be analyzed on the model sensitivities.

Increasing availability of palaeomonsoon records and their spatial and temporal coverage have to be documented. For instance the regions coming under the influence of Indian monsoon circulation may show different temporal evolution than those coming under north African monsoon. Within the Indian monsoon region, the palaeomonsoon data may show different temporal evolution pattern over different locations. Such evidences point towards major changes in monsoon dynamics and may be modelled with climate models. In particular a detailed analysis of palaeo-data during the transition from LGM to early Holocene and modelling with the help of known changes in boundary conditions needs to be attempted.

When the models become sufficiently realistic, a more direct comparison with palaeo-data using forward/inverse modelling techniques can be attempted.

Bibliography

- Berger, A., and M. F. Loutre, 1991: Insolation Values for the Last 10 Million Years. *Quat. Sci. Rev.*, 10, 297-317.
- Berger A. and Loutre M.F., 1994: Precession, Eccentricity, Obliquity, Insolation and Paleoclimates. *Long-Term Climatic Variations Data and Modelling*, Eds. J. -C. Duplessy and M. -C. Spyridakis, Springer-Verlag, pp 107-151.
- Bonan, G. B., 1994: Comparison of the land surface climatology of the National Center for Atmospheric Research community climate model 2 at R15 and T42 resolutions. *J. Geophys. Research.*, 99, 10357-10364.
- Briegleb, B. P., 1992: Delta-Eddington approximation for solar radiation in the National Centre for Atmospheric Research community climate model. *J. Geophys. Res.*, 97, 7603-7612.
- Broström A., Coe M., Harrison S. P., Gallimore R., Kutzbach J.E., Foley J., Prentice I. C., Behling P., 1998: Land surface feedbacks and palaeomonsoons in northern Africa. *Geophys. Res. Lett.*, 25, 3615-3618.
- Bryson, R. A., and A.M. Swain, 1981: Holocene variations of monsoon rainfall in Rajasthan. *Quat. Res.*, 16, 135-145.
- Bush A.B.G., 1999: Assessing the impact of Mid-Holocene insolation on the atmosphere-ocean system. *Geophys. Res. Lett.*, 26, 99-102.
- Charney J.G., 1975: Dynamics of deserts and droughts in the Sahel. *Quat. J. R. Met. Soc.*, 101, 193-202.

Chervin, R. M., 1986: Interannual variability and seasonal climate predictability. *J. Atmos. Sci*, 43, 233-251.

Claussen M., Kubatzki C., Brovkin V., Ganopolski A., Hoelzmann P., and Pachur H.-J., 1999: Simulation of an abrupt change in Saharan vegetation in the mid-Holocene. *Geophys. Res. Lett.*, 26, 2037-2040.

Clemens S., Prell W., Murray D., Shimmield G., and Weedon G., 1991: Forcing mechanisms of the Indian Ocean monsoon. *Nature*, 353, 720-725.

CLIMAP Project Members, 1981: Seasonal reconstruction of earth's surface at the last glacial maximum. *Geol.Soc.Am.Map.Chart.Ser.*, MC-36.

Crowley T.J., and North G.R., 1991: *Palaeoclimatology*, Oxford University Press Inc., 339 pp.

deNoblet N., Braconnot P., Joussaume S and Masson V., 1996: Sensitivity of simulated Asian and African summer monsoons to orbitally induced variations in insolation. *J. Geophys. Research.*, 98, 7265-7287.

DeVries, T. J., L. Ortlieb, A. Diaz, L. Wells, C. Hillaire-Marcel, 1997: Determining the early history of El Niño. *Science*, 276, 965-966, 1997.

Dütsch H.V., 1978: Vertical ozone distribution on a global scale. *Pure Appl. Geophys.*, 116, 511-529.

Dong, B., P.J. Valdes, and N.M.J. Hall, 1996: The changes of monsoonal climates due to earth's orbital perturbations and ice age boundary conditions. *Paleoclimates*, 1, 203-240.

- Gadgil S., and Asha G., 1992: Intraseasonal variation of the Indian summer monsoon. *J. Meteorol. Soc. Jpn*, 70, 517-527.
- Gadgil S., and S. Sajani, 1998: Monsoon precipitation in AMIP runs. To appear in *Clim. Dyn.*.
- Ganopolski, A., C. Kubatzki, M. Claussen, V. Brovkin, and V. Petoukhov, 1998: The influence of Vegetation-Atmosphere-Ocean Interaction on Climate During the Mid-Holocene. *Science*, 280, 1916-1919.
- Gates, W. L., 1976: The numerical simulation of ice-age climate with a general circulation model. *J. Atmos. Sci.*, 33, 1844-1873.
- Gates, W. L., 1992: The Validation of Atmospheric Models. *Program for Climate Model Diagnosis and Intercomparison(PCMDI) Report No. 1*, Lawrence Livermore National Laboratory, CA, USA.
- Goswami B. N., Krishnamurthy V., and Annamalai H., 1999: A broad scale circulation index for the interannual variability of the Indian summer monsoon. *Quart. J. Roy. Meteor. Soc.*, in press.
- Hack, J. J., 1994: Parameterization of moist convection in the National Center for Atmospheric Research Community Climate Model (CCM2). *J. Geophys. Res.*, 99, 5551-5568.
- Hack, J. J., B.A. Boville, B.P. Briegleb, J.T. Kiehl, P.J. Rasch, and D.L. Williamson, 1993: *Description of the NCAR community climate model (CCM2)*, NCAR Tech. Note, NCAR/TN-382+STR, 108pp., National Center for Atmospheric Research, Boulder, CO, USA.

Hays J. D., J. Imbrie, and N. J. Shackleton, 1976: Variations in the earth's orbit: Pacemaker of the ice ages. *Science*, 194, 1121-1132.

Holtslag, A.A.M., and B.A. Boville, 1993: Local versus nonlocal boundary-layer diffusion in a global climate model. *J. Climate*, 6, 1825-1842.

Hurrell J. W., J. J. Hack, and D. P. Baumhefner (1993) Comparison of NCAR Community Climate Model (CCM) Climates. *NCAR Technical Note, NCAR/TN-395+STR*, 335 pp., National Center for Atmospheric Research, Boulder, CO.

Imbrie J., J. D. Hays, D. G. Martinson, A. McIntyre, A. C. Mix, J. J. Morely, N. G. Pisias, W. L. Prell, and N. J. Shackleton, 1984: The orbital theory of Pleistocene climate: Support from a revised chronology of the marine $\delta^{18}\text{O}$ record. In: *Milankovitch and Climate*, A. L. Berger, J. Imbrie, J. Hays, G. Kukla, and B. Saltzman (Eds.) D. Reidel, Dordrecht, Netherlands, Part 1. pp. 269-305.

Jagadheesha D., R.S. Nanjundiah, and R. Ramesh, 1999: Orbital forcing of monsoonal climates in NCAR CCM2 with two horizontal resolutions. *Palaeoclimates*, 3, 279-301.

Joussaume, S., and K.E. Taylor, 1995: Status of Paleoclimate Modelling Intercomparison Project (PMIP). In *Proceedings of the First International AMIP Scientific Conference*, WCRP, 92, 425-430.

Joussaume, S., 35 others, 1999: Monsoonal changes for 6000 years ago: Results of 18 simulations from the Paleoclimate Modeling Intercomparison Project (PMIP). *Geophys. Res. Lett.*, 26, 859-862.

Ju J., and J. M. Slingo, 1995: The Asian summer monsoon and ENSO. *Quart. J. Roy. Met. Soc.*, 121, 1133-1168.

Kalnay, E., 20 others, 1996: The NCEP/NCAR 40-year Reanalysis Project. *Bulletin of the American Meteorological Society*, 77, 437-471.

Keshavamurthy, R. N., and M. Sankar Rao, 1992: *The Physics of Monsoons*, Allied Publishers Ltd., India, 199pp.

Kothavala Z., R. J. Oglesby, B. Saltzman, 1999: Sensitivity of Equilibrium Surface Temperature of CCM3 to Systematic Changes in Atmospheric CO₂. *Geophys. Res. Lett.*, 26, 209-212.

Krishna Kumar K., B. Rajagopalan, M. A. Cane, 1999: On the Weakening Relationship Between the Indian Monsoon and ENSO. *Science*, 284, 2156-2159.

Kutzbach, J. E., and B. L. Otto-Bleisner, 1982: The sensitivity of African Asian monsoon climate to orbital parameter changes for 9000 years B.P. in a low-resolution general circulation model. *J. Atmos. Sci*, 39, 1177-1188.

Kutzbach, J. E., G. Bonan, J. Foley, and S. Harrison, 1996: Vegetation and soil feedbacks on the response of the African monsoon to forcing in the early and middle Holocene. *Nature*, 384, 623-626.

Kutzbach J. E., and Z. Liu, 1997: Response of the African monsoon to orbital forcing and ocean feedbacks in the middle Holocene. *Science*, 278, 440-443.

Manabe S., 1969: Climate and ocean circulation, 1. The atmosphere circulation and the hydrology of the earth's surface. *Mon. Wea. Rev.*, 97, 739-773.

McIntyre A., W. F. Ruddiman, K. Karlin, and A. C. Mix 1989: Surface water response of the equatorial Atlantic ocean to orbital forcing. *Paleoceanography*, 4, 19-55.

Meehl, G., 1994: Coupled ocean-atmosphere-land processes and south Asian Monsoon variability. *Science*, 265, 263-267, 1994.

Nanjundiah R. S., J. Srinivasan, and S. Gadgil, 1992: Intraseasonal variation of the Indian summer monsoon, II, Theoretical aspects. *J. Meteorol. Soc. Jpn.*, 70, 529-549.

Overpeck J. T., D. M. Anderson, S. Trumbore, and W. L. Prell, 1996: The southwest Indian monsoon over the last 18000 years, *Clim. Dyn.*, 12, 213-225.

Otto-Bleisner B.L., 1999: El Niño/La Niña and Sahel precipitation during the middle Holocene. *Geophys. Res. Lett.*, 26, 87-90.

Pant, G. B., and K. Rupa Kumar, 1997: *Climates of South Asia*, John Wiley and Sons Ltd., 320 pp.

Parthasarathy, B., K. R. Kumar, and D. R. Kothawale, 1994: All-India monthly and summer rainfall indices: 1871-1993. *Theor. Appl. Climatol.*, 49, 219-224.

Pokras E. M., and A.C. Mix, 1985: Eolian evidence for spatial variability of late Quaternary climates in tropical Africa. *Quat. Res. NY*, 24, 137-149.

Prell, W. L., 1984: Monsoonal Climate of the Arabian sea during the late Quaternary: A response to changing solar radiation. *Milankovich and Climate*, Eds. Berger A. et al., Reidel, pp 349-366.

Prell, W. L., and J.E. Kutzbach, 1987: Monsoon variability over the past 150,000 years. *J. Geophys. Res.*, 92, 8411-8425.

Prell, W. L., and J.E. Kutzbach, 1992: Sensitivity of the Indian Monsoon to forcing parameters and implications for its evolution. *Nature*, 360, 640-652.

Qin B., S. P. Harrison, and J. E. Kutzbach, 1998: Evaluation of modelled regional water balance using lake status data: A comparison of 6 ka simulations with the NCAR CCM. *Quart. Sci. Rev.*, 17, 535-548.

Qin B., and G. Yu, 1998: Implications of lake level variations at 6 ka and 18 ka in mainland Asia. *Global and Planetary Change*, 18, 59-72.

Rind D., 1988: Dependence of warm and cold climate depiction on climate model resolution. *J. Clim.*, 1, 965-997.

Rollins H.B., J.B. Richardson III, D.H. Sandweiss, 1986: The birth of El Niño: Geoarcheological evidence and implications. *Geoarchaeology: An international journal*, 1, 3-15.

Ruddiman, W. F., and A. McIntyre, 1984: Ice-age thermal response and climatic role of the surface Atlantic Ocean. 40°N to 63°N. *Geol. Soc. Am. Bull.*, 95, 381-396.

Ruddiman, W. F., and A. C. Mix, 1993: The north and equatorial Atlantic at 9000 and 6000 yr BP. In *Global Climates Since the Last Glacial Maximum*, edited by H.E. Wright, Jr., et al., pp94-124, Univ. of Minn. Press., Minneapolis.

Sandweiss D.H., J.B. Richardson III, E.J. Reitz, H.B. Rollins, K.A. Maasch, 1996: Geoarcheological evidence from Peru for a 5000 years BP onset of El Niño". *Science*, 273, 1531-1533.

Sarkar A., R. Ramesh, S.K. Bhattacharya, and G. Rajagopalan, 1990: Oxygen isotopes evidence for a stronger winter monsoon current during the last glaciation. *Nature*, 343, 549-551.

Shea, D. J., K.E. Trenberth, R.W. Reynolds, 1990: *A Global Monthly Sea Surface Temperature Climatology*. NCAR Technical Note NCAR/TN-345+STR, Boulder, Colorado, 167 pp.

Shukla, J., 1987: Long-range forecasting of monsoons. in *Monsoons*, edited by J. S. Fein and P. L. Stephens, 523-548, John Wiley and Sons.

Shukla J., 1998: Predictability in the Midst of Chaos: A Scientific Basis for Climate Forecasting. *Science*, 282, 728-731.

Sikka, D. R., and S. Gadgil, 1980: On the maximum cloud zone and the ITCZ over India longitude during the southwest monsoon. *Mon. Wea. Rev.*, 108, 1840-1850.

Simmons, A. J., and R. Strüfing, 1981: An energy and angular-momentum conserving finite-difference scheme, hybrid coordinates and medium-range weather prediction. *ECMWF Technical Report No. 28*, 68pp.

Singh, G., R.D. Joshi, S.K. Chopra, and A.B. Singh, 1974: Late Quaternary history of vegetation and climate of the Rajasthan desert, India. *Philos. Trans. R. Soc. Lond.*, 267, 467-501.

Sirocko F., 1996a: Past and Present Subtropical Monsoons. *Science*, 274, 937-938.

Sirocko F., 1996b: The evolution of the monsoon climate over the Arabian Sea during the last 24,000 years. *Palaeoecology of Africa and the surrounding islands*, 24, 53-69.

Slingo, J.M., 1987: The development and verification of a cloud prediction scheme for the ECMWF model. *Quart. J. Roy. Meteor. Soc.*, 113, 899-927.

Soman M. K., J. M. Slingo, N. M. J. Hall, and P. J. Valdes, 1994: The simulation of the Indian monsoon in a seasonal integration of UGCM and its sensitivity to convective and land surface parameterizations. *U. K. Universities Global Atmospheric Modelling Programme technical report 36*.

Srinivasan, J., S. Gadgil, and P. J. Webster, 1993: Meridional propagation of large scale convective zones. *Meteorol. Atmos. Phys.*, 52, 15-36.

Stephenson, D. B., F. Chauvin, and J. -F. Royer, 1998: Simulation of the Asian Summer Monsoon and its Dependence on Model Horizontal Resolution. *J. Meteor. Soc. Japan.*, 76, 237-265.

Street-Perrott, F. A., D.S. Marchand, N. Roberts, and S.P. Harrison, 1989: Global Lake-Level Variations from 18000 to 0 Years Ago: a Paleoclimatic Analysis. *Technique Report of Department of Energy, USA*.

Sukumar R., Ramesh R., R. K. Pant, and G. Rajagopalan, 1993: A $\delta^{13}\text{C}$ record of late Quaternary climate change from tropical peats in southern India. *Nature*, 364, 703-706.

Texier D., N. deNoblet, and P. Braconnot, 2000: Sensitivity of the African and Asian monsoons to mid-Holocene insolation and data-inferred surface changes. *J. Clim.*, 13, 164-181.

Torrence, C., and P. J. Webster, 1998: The annual cycle of persistence in the El Niño-Southern Oscillation Statistics. *Q. J. R. Meteorol. Soc.*, in press.

Van Campo E., J. C. Duplessy, and M. Rossignol-Strick, 1982: Climatic conditions deduced from a 150-kyr oxygen isotope-pollen record from the Arabian sea. *Nature*, 296, 56-59.

- Wang, B., and Z. Fan, 1999: Choice of South Asian Summer Monsoon Indices. *Bull. Am. Meteor. Soc.*, 80, 629-638.
- Wasson, R. J., G. I. Smith, and D. P. Agarwal, 1984: Late Quaternary sediments, minerals, and inferred geochemical history of Didwana lake, Thar Desert, India. *Paleoeco. Paleoclim. Paleoeco.*, 46, 345-372.
- Webster, P. J., and L. Chou, 1980: Seasonal structure in a simple monsoon system. *J. Atmos. Sci.*, 37, 354-367.
- Webster P. J., Magaña V. O., Palmer T. N., Shukla J., Tomas R. A., Yanai M. and Yasunari T., 1998: Monsoons: Processes, Predictability, and the prospects for prediction. *J. Geophys. Res.*, 103, 14451-14510.
- Webster, P. J., and S. Yang, 1992: Monsoon and ENSO: Selectively interactive systems. *Quart. J. Roy. Meteor. Soc.*, 118, 877-926.
- Williamson D. L., and Rasch P. J., 1994: Water vapour transport in NCAR CCM2. *Tellus*, 46A, 34-51.
- Xie P., and P. A. Arkin, 1996: Analysis of global monthly precipitation using gauge observations, satellite estimates and numerical model predictions. *J. Climate*, 9, 840-858.
- Yu G., and S. P. Harrison, 1996: An evaluation of the simulated water balance of Eurasia and northern Africa at 6000 y BP using lake status data. *Clim. Dyn.*, 12, 723-735.

Zhang, G. J., 1994: Effects of Cumulus Convection on the Simulated Monsoon Circulation in a General Circulation Model. *Mon. Wea. Rev.*, 122, 2022-2038.